Spring 5-6-2017

Basal and Experience Dependent Ampar and Synapse Dynamics: Alterations in a Mouse Model of Fragile X Syndrome

Anand Suresh
University of Nebraska Medical Center

BASAL AND EXPERIENCE DEPENDENT AMPAR AND SYNAPSE DYNAMICS: ALTERATIONS IN A MOUSE MODEL OF FRAGILE X SYNDROME

By

Anand Suresh

A Dissertation

Presented to the Faculty of

The Graduate College in the University of Nebraska Medical Center

In partial Fulfillment of the Requirements

For the Degree of Doctor of Philosophy

Biochemistry and Molecular Biology

Under the supervision of Professor Anna Dunaevsky

University of Nebraska Medical Center

Omaha, Nebraska

December 2016

Acknowledgements

I would like to first thank my mentor, Dr. Anna Dunaevsky for her patience, support and guidance throughout my graduate studies. Her immense drive and passion towards biomedical research has been a constant source of inspiration for me and will remain so for the rest of my scientific career. I am also grateful for her endless investment in mine and other trainee's professional advancement. Her mentorship and constant discussions of scientific literature, experimental designs and data analysis were invaluable. It was through her encouragement that I applied and received the American Heart Association pre-doctoral fellowship which meant a lot to me. Anna has been also very generous in sponsoring conferences and workshops which have been crucial in broadening my scientific and professional horizons for which I am very grateful.

I would also like to thank the members of comprehensive exam committee: Dr. Parmender Mehta, Dr. Kaushik Patel and Dr. Dominic Cosgrove for their guidance and tutelage throughout my qualifying exams. I would take this opportunity to thank my supervisory committee: Dr. Hamid Band, Dr. Steve Caplan, Dr. Woo Yang Kim, Dr. Kaustubh Datta and Dr. Wallace Thoreson for their suggestion, guidance and immense support.

I would like to thank all present and past member of the Dunaevsky lab for their help during my stay in the lab and in creating an environment of curiosity and endeavor. I first want to warmly thank our lab manager Yoosun Jung for helping me in the breeding, cloning and tissue cultures which were integral for this thesis. She was my very first teacher in the lab and I learnt a variety of techniques under her tutelage. Next, a big thank you to Dr. Padmashri Ragunathan whom I collaborated with on more than a couple of projects. Her meticulous attention to detail and work ethics are both an inspiration and a role-model for a young researcher. I would like to thank Dr. Benjamin Reiner for his contributions to the motor learning deficits in the fmr1 KO mouse study and for enlightening me on American culture. I would like to thank Dr. Gurudutt Pendyala and James Buescher (of Dr. Howard

Fox's lab) for sharing the protocols in synaptosomal preparations and troubleshooting during the biochemical experiments. Additionally, I am grateful to other members of the Dunaevsky lab including Dr. Pierluca Coiro, Lara Bergdolt, Shreya Roy for creating a warm and collegial work environment.

Next, I want to thank members and labs within Munroe-Meyer Institute's Department of Developmental Neuroscience. A special thank you to Jerri Dayton, my go-to person for almost all administrative issues and a wizard in solving complex organizational nightmares! A grateful thank you to Dr. Shelly Smith and for her overall mentorship in leading a budding department and her lab for all their support over the years. I would also like to thank Dr. Channabasavaiah Gurumurthy and Rolen Macky Quadros for their cloning of the td-Tomato constructs which formed the foundations of the *in vivo* experiments and support during the long and frustrating cloning saga of the SEP-GluA1 construct. Finally, a big thank you to Dr. Eunju Seong and Li Yuan of the Arrikath lab for sharing their wonder, enthusiasm, passion for science. I am grateful to have witnessed their never-say-die attitude and this has served as an inspiration to me.

A very grateful thank you to Florent Maye, a developer from France who wrote the program for the neuronal analysis which saved me thousands of man hours and indirectly made possible this thesis.

I would also like to thank the faculty and staff of my parent department; Biochemistry and Molecular Biology for their support over the years.

Finally, a heartfelt thank you to Din, Gin, Biu and my parents for their unwavering support and constant encouragement that made this all possible.

Table of Contents:

Chapter 2. Relationship between AMPAR and Synapse dynamics in vivo; alterations in a mouse model of Fragile X syndrome

Table of Figures

BASAL AND EXPERIENCE DEPENDENT AMPAR AND SYNAPSE DYNAMICS: ALTERATIONS IN A MOUSE MODEL OF FRAGILE X SYNDROME

Anand Suresh

University of Nebraska Medical Center, 2016

Advisor: Anna Dunaevsky, Ph.D.

Dendritic spines are the principal sites of excitatory synapses in the neurons of mammalian central nervous system. Spine are plastic, undergoing structural and functional changes under basal and experience dependent conditions. Spine properties are altered in a number of neurodevelopmental disorders including the Fragile X syndrome (FXS) which is the most common inherited form of intellectual disability. The structural reorganization of dendritic spines is thought to be associated with synaptic plasticity mechanisms that are deficient in FXS. A number of synaptic plasticity mechanisms involve modulation of synaptic strength via insertion or removal of α-amino-3-hydroxy-5-methyl-4-isoxazolepropionic acid receptors (AMPAR). However, the link between synaptic behavior and AMPAR dynamics has not been previously studied *in vivo.*

To investigate the role of AMPAR in spine dynamics *in vivo* we expressed AMPAR subunit GluA2 tagged to superecliptic phluorin (SEP), a pH sensitive GFP variant, in layer 2/3 neurons of the primary motor cortex (M1). Dendritic spines and sGluA2 were imaged *in vivo* using two-photon light microscopy over a period of ten days in both wild type and the fmr1 knock out (KO) mice, a mouse model of FXS. Repeated *in vivo* imaging revealed that in the fmr1 KO mouse dendritic spines were denser, smaller, contained less sGluA2 and had higher turnover rates compared to littermate controls (WT). Our data confirmed the relationship between synaptic strength and synaptic stability, with greater AMPAR containing spines being more stable in both WT and the KO mice. Additionally, we observed that AMPAR levels were dynamic in most stable spines, fluctuating over 10 days with larger proportion of spines showing multiple dynamic events of AMPAR in the KO.

Directional changes in sGluA2 were also observed in subpopulation of spines, with new small spines gradually accumulating sGluA2. Moreover, sGluA2 levels dropped just prior to spine elimination with greater loss observed in the KO spines. To further investigate the role of AMPAR in experience dependent plasticity, we trained KO mice in a forelimb task and monitored behavioral learning and biochemically measured synaptic AMPAR levels. KO mice had mild motor deficits in a single forelimb reaching task compared to WT controls. Furthermore, after one day of motor skill training WT mice had a gradual increase in synaptic sGluA1 which was delayed in the KO. Thus we conclude that AMPAR levels within spines are continuously dynamic and are predictive of spine behavior. These dynamics are further modulated upon learning with impairments under basal and experience dependent conditions in the fmr1 KO mouse.

Chapter 1

1.1 Introduction

The central nervous system (CNS) consisting of the brain and spinal cord, controls every conscious and unconscious momentary function in the life of a living being. The central nervous system is complex and structured, consisting of millions of cells of which the principal components are neurons and glia. Neurons are electrically charged and highly polarized cells consisting of a cell body and two structurally and functionally distinct processes; dendrites and axons. The electrically excitable nature of a neuron allows it to transmit information through electrical and chemical signals across the cell. Classically, the flow of electrical signals across neurons is directional, with dendrites conducting impulses towards and axons conducting impulses away from the soma. Neurons are arrayed in complex interconnected networks and communicate with each other through transfer of electrical impulses across special junctions called synapses. Synapses are highly specialized compartments of neurons with thousands of proteins on both pre- and postsynaptic side working in a highly coordinated manner to maintain synaptic structure and to mediate synaptic transmission. At a chemical synapse, neurotransmitter released by the presynaptic axon terminal binds to a receptor on a dendrite of another neuron. At an excitatory synapse, synaptic transmission results in depolarization, which if strong enough can generate an action potential which propagates along its axons causing neurotransmitter release in subsequent synapses. Synaptic transmission within neuronal circuits forms the basis of information transfer in the CNS.

The flow of information through neuronal circuits can be modulated by multiple mechanisms including changing the synaptic properties of neurons. This process of synaptic plasticity occurs by either regulating the number of synapses (through formation or elimination of synapses) or through modification of the transmission at preexisting

synapses and are thought to be the fundamental process by which the brain stores and processes information. Impairments in the formation of neuronal circuits and synaptic structure and function are thought to underlie many neuropsychiatric disorders. Specifically, impairments in glutamatergic synapses, which form the vast majority of excitatory synapses and are located on specialized dendritic compartments called dendritic spines, have been implicated in many neurodevelopmental disorders. Understanding basic biological mechanisms of synaptic plasticity in shaping neuronal circuits involved in various behavioral and cognitive states will be critical for understanding the impairments underlying neurodevelopmental disorders such as ASD and the development of therapies for treatment of patients.

In my thesis, the main focus has been to monitor synaptic proteins as a measure of synaptic function and understand how functional changes shape synaptic fate both in normal and diseased conditions. Towards this end I focused on tracking α-amino-3-hydroxy-5-methyl-4-isoxazolepropionic acid receptor (AMPAR), a type of glutamate receptor in synapses *in vivo* and over time. I monitored AMPAR levels within synapses both under basal conditions and with learning in normal (wild type) and fmr1 KO mice, a mouse model for Fragile X syndrome. Fragile X syndrome is the most commonly inherited form of intellectual disability and is an extensively studied model of neurodevelopmental disorders. In the following introduction, I am going to briefly review the important aspects of synapses focusing on architecture, function and change of synapses under normal and in Fragile X syndrome.

1.2 Dendritic Spines

Dendritic spines (spines) are small (0.5-2 microns) membranous protrusions that project from the dendritic shaft. Spines were first described by Santiago Ramón y Cajal (Ramon y Cajal, 1888) in the late 19th century using golgi staining. Extensive research over decades have confirmed that spines form the postsynaptic compartment of an excitatory glutamatergic synapse (J. N. Bourne & Harris, 2008).Spines are known to be present in neurons across many organisms from annelids to primates (DeFelipe, Alonso-Nanclares, & Arellano, 2002). Spines are present on several cell types in the CNS including cerebellar Purkinje cells and pyramidal neurons(Nimchinsky, Oberlander, & Svoboda, 2001). Pyramidal neurons form the majority of neurons in the cortex and hippocampus and research focusing on synaptic properties in these neurons will be the primary focus in the following sections.

The unique architecture and prevalence of spines on dendrites have been postulated to confer many advantages to neuronal function (R Yuste & Denk, 1995). The distribution and arrangement of spines and axons in an almost helical manner upon a dendrite increases surface area hence optimizing neuronal connectivity (R. Yuste, 2011). This also increases the diversity of presynaptic partners thus making the neuronal circuitry more distributed which has advantages in terms of anatomical organization (R. Yuste, 2011) and computational function (Hopfield, 1982). Secondly, it is postulated that the narrow spine neck increases electrical and diffusional resistance between the dendrite and the spine thus isolating synaptic inputs (Tonnesen, Katona, Rozsa, & Nagerl, 2014; Tonnesen & Nagerl, 2016; R. Yuste, 2013; R. Yuste & Urban, 2004). This would avoid electric interference and shunting between neighboring spines and make input specific plasticity possible by restricting the diffusional flow of signaling molecules (Lee, Soares, & Beique, 2012; Tonnesen & Nagerl, 2016). Thus the unique structural geometry of a spine, confers

upon it distinct biophysical properties making a spine not just a reception site but the smallest processing unit of the brain (Bellot et al., 2014).

According to present theories of memory and learning, information is stored in the brain through modifications in neuronal connectivity (Malenka & Bear, 2004). Modification in synaptic strength is known as functional plasticity whereas elimination or formation and expansion or shrinkage of spines is called structural plasticity (Kasai, Matsuzaki, Noguchi, Yasumatsu, & Nakahara, 2003; Sala & Segal, 2014; R. Yuste & Bonhoeffer, 2001).The proper functioning of these unique attributes of the synaptic plasticity are critical for normal function and are targets for dysfunction in neurological disorders (Bellot et al., 2014; Fiala, Allwardt, & Harris, 2002; Penzes, Cahill, Jones, VanLeeuwen, & Woolfrey, 2011; Svitkina et al., 2010).Relevant to this thesis neurodevelopmental disorders such as Fragile X syndrome have documented dysfunction in synaptic properties(Contractor, Klyachko, & Portera-Cailliau, 2015; S.A. Irwin, Galvez, & Greenough, 2000) and thus provide unique windows into understanding basic synaptic behavior and identifying targets for therapy (Darnell & Klann, 2013; Krueger & Bear).

1.2a Structure of spines

Dendritic Spines as discussed earlier are uniquely specialized for synaptic transmission. Directly opposing the presynaptic bouton and crowning the surface of a spine are a varied array of membrane bound neurotransmitter receptors, adhesion, scaffolding and signaling proteins which are essential for synaptic function and plasticity (Nimchinsky, Sabatini, & Svoboda, 2002; Sala & Segal, 2014).. Holding these proteins in place is a large specialized electron rich structure called post synaptic density (PSD)(Sheng & Hoogenraad, 2007). PSD is attached to the postsynaptic plasma membrane and is held together by actin filaments. The PSD is dynamic with levels of PSD proteins directly correlated with synaptic strength (Cane, Maco, Knott, & Holtmaat, 2014; Gray, Weimer, Bureau, & Svoboda, 2006). Among the PSD protein, the most abundant are PSD-95 which binds to guanylate kinase-associated protein (GKAP) which in turn binds to SHANK and HOMER to form the scaffolding structure of the PSD. Mass spectroscopy analysis of purified PSD have identified nearly a thousand proteins associated with the PSD (J. Peng et al., 2004; Walikonis et al., 2000).

Apart for the PSD the spine is composed of a network of actin cytoskeleton and a number of organelles including smooth endoplasmic reticulum (SER) (Nimchinsky et al., 2002; Spacek, 1985), polyribosomes (Steward & Levy, 1982), proteasomes (Bingol & Schuman, 2006) and vesicular components . Smooth endoplasmic reticulum are membranous tubules which form a continuum of the nuclear membrane and involved in the synthesis of lipids, metabolism of nutrients, calcium homeostasis and detoxification (Phillips & Voeltz, 2016). SER are found in mature spines and play an important in calcium regulation and homeostasis during synaptic plasticity (Nimchinsky et al., 2002; Spacek & Harris, 1997) and synapse stabilization (Czarnecki, Haas, Bas Orth, Deller, & Frotscher, 2005; Vlachos et al., 2009). Unique to mature spines is a spine apparatus (SA) which is thought to be a

specialized continuum of the SER present in large synapses and important in protein delivery and calcium homeostasis (E. G. Gray, 1959; Segal, Vlachos, & Korkotian, 2010). Polyribosomes are found in almost all spines in the hippocampus(A. Peters & Kaiserman-Abramof, 1970) and are involved in local protein translation. During synaptic plasticity local translation is essential and unsurprisingly polyribosomes are actively recruited into a spine upon plasticity induction. (K. M. Harris, Fiala, & Ostroff, 2003; Ostroff, Fiala, Allwardt, & Harris, 2002). Finally, other organelles present in spines are proteasomes (Bingol & Sheng, 2011), which degrade proteins in situ, vesicular components including endosomes and clathrin-coated vesicles involved in protein trafficking, spine remodeling and spine growth (J. N. Bourne & Harris, 2008)

1.2b Glutamate receptors

Glutamate is a primary neurotransmitter in brain and in neurons binds to three families of ionotropic and metabotropic receptors. Ionotropic receptors are ligand gated ion channels and include N-methyl-D-aspartate receptor (NMDAR), α-amino-3-hydroxy-5-methyl-4-isoxazolepropionic acid receptor (AMPAR) and kianate receptor. AMPAR and NMDAR are the primary receptors involved in synaptic plasticity and will be further discussed later. Metabotropic glutamate receptors (mGluR) are G-protein coupled receptors (GPCR) and are slower acting exerting their effects indirectly due to gene repression or protein translation. There are three broad families of mGluR with distinct pharmacological and signal transduction properties. Group1 mGluRs (include mGluR1 & 5) are the best studied with Gq receptors acting through PLC-PKC pathway and playing a key role in induction of some forms of synaptic plasticity.

NMDAR: are voltage dependent glutamate-gated cation channels permeable to sodium, potassium and calcium. NMDAR are high affinity glutamate receptors which at normal resting potentials are blocked by the presence of Mg^{2+} within the channel pore. Under special conditions when there is both depolarization within the synapse and glutamate within the synaptic cleft the Mg^{2+} block is released leading to opening of NMDAR receptors. This allows the flow of Ca^{2+} which triggers a series signal transduction pathways important in functional plasticity as discussed later.

AMPAR: are the workhorses of a glutamatergic synapse and mediate the bulk of fast excitatory transmission within the CNS. Neurons shuttle AMPAR in and out of synapses in an activity dependent manner to modulate the strength of synapses. Changes in AMPAR numbers, composition, phosphorylation state, and accessory proteins can all regulate AMPAR dynamics and thus modify synaptic strength (Huganir & Nicoll, 2013; Malenka & Bear, 2004). Alterations in synaptic strength play crucial roles in memory and

learning (Matsuo, Reijmers, & Mayford, 2008; Rumpel, LeDoux, Zador, & Malinow, 2005; T. Takahashi, Svoboda, & Malinow, 2003).Furthermore, dysregulation of AMPAR plasticity has been implicated in various neurological conditions especially neurodevelopmental disorders (Penzes et al., 2011) and is an active area of biomedical research.

AMPARs are tetrameric, cation-permeable ionotropic glutamate receptors, and are expressed throughout the brain (Beneyto & Meador-Woodruff, 2004). AMPAR consist of four AMPAR subunits (GluA1–GluA4) are encoded by the genes GRIA1-GRIA4. The four subunits are highly homologous (70% homology) with conserved transmembrane and extracellular domains but variable c-terminus across the subunits (Shepherd & Huganir, 2007). These are assembled as dimers-of-dimers to form the hetero-tetrameric receptors (Hollmann & Heinemann, 1994; Traynelis et al., 2010), although homo-tetrameric receptors have been reported (W. Lu et al., 2009; Wenthold, Petralia, Blahos, & Niedzielski, 1996). Binding of glutamate opens the channel pore allowing influx of Na^+ ions (and K^+ efflux) leading to depolarization of the postsynaptic compartment. However, depending on sub unit composition and RNA editing, AMPAR can also permit entry of Ca^{2+} which could then trigger Ca^{2+} dependent signaling pathways which are important in synaptic plasticity. Most GluA2 units in adult brains undergo RNA editing whereby glutamine is replaced by arginine in the pore-region of GluA2 which prevents Ca^{2+} influx. Thus in the adult brain majority of GluA2 containing AMPAR's are Ca^{2+} impermeable with lower single channel conductance and longer decay times. GluA2 lacking AMPAR's are calcium permeable. These include GluA1-GluA3 heteromers and GluA1-GluA1 homomers. However, role of Ca^{2+} permeable AMPARs in LTP is hotly debated. (Adesnik & Nicoll, 2007)

AMPAR trafficking: AMPAR exocytosis is still unclear with multiple mechanisms suggested such as insertion directly into soma (Adesnik, Nicoll, & England, 2005), insertion into dendrites adjacent to spines (Makino & Malinow, 2009; M. A. Patterson, Szatmari, & Yasuda, 2010), or directly into spines (Ehlers, Heine, Groc, Lee, & Choquet, 2007). At present the consensus is that AMPAR receptors are inserted in a three step process (Opazo & Choquet, 2011) which is modulated by synaptic activity. The first step is insertion of fully functional AMPAR into the extrasynaptic regions on the dendrite. After this AMPARs diffuse into the spine and are then trapped by the PSD through interaction with TARP such as stargazin (Opazo & Choquet, 2011)

1.2c Synaptic plasticity

Synaptic plasticity describes number of pre or postsynaptic phenomenon affecting synaptic strength. Among the postsynaptic mechanisms described, majority involve the insertion or removal of AMPAR to modulate synaptic strength. Among the best described mechanisms are Long term potentiation (LTP), long term depression (LTD) and homeostatic plasticity.

Long Term Potentiation

LTP is an umbrella term to describe phenomenon whereby long lasting experience-dependent increase in synaptic transmission induced by a variety of electrical, pharmacological and behavioral paradigms. LTP was originally described in 1973 by Bliss and Lomo (Bliss and Lomo 1973) where they showed that repetitive stimulation of the perforant pathway caused potentiation of responses within the dentate gyrus in rabbits. This classical LTP was long lasting and stable for months (Bliss and Collingridge 1993) and presumably a similar mechanism is at work in humans. A key change in LTP is an increase in number of AMPAR at a subset of spines thereby increasing synaptic response to neurotransmitter release. Although presynaptic mechanisms (Kullmann, Erdemli et al. 1996) can be involved in this process, for the purpose of the thesis I will focus on post synaptic mechanisms in the following sections. LTP involves coincident depolarization of the postsynaptic structure and subsequent activation of NMDAR leading to influx of Ca2+ which sets off a cascade of phosphorylation events leading to potentiation of synaptic transmission (Nicoll, Kauer et al. 1988, Malenka and Nicoll 1999, Lynch 2004). LTP is an attractive model for memory due to several of its properties. LTP is (1) input specific whereby LTP does not spread to non-potentiated spines; (2) associative and cooperative whereby LTP on one synapse decreases the threshold for the induction of LTP on

adjacent synapses and (3) persistent as LTP is stable for prolonged periods of time (Lynch 2004).

At the molecular level, calcium influx into the post synaptic compartment binds to calcium binding messenger protein calmodulin (Stevens 1983) in a stoichiometry of 1:4 (Chin and Means 2000). Calmodulin serves as a calcium sensor (Faas, Raghavachari et al. 2011) which then transiently activates (about 1min) Ca2+/calmodulin-dependent protein kinase II (CAMKII) by autophosphorylating at T286A (Lee, Escobedo-Lozoya et al. 2009, Lisman, Yasuda et al. 2012). CAMKII is a serine threonine kinase which after activation, translocates into the spine (Shen and Meyer 1999, Otmakhov, Tao-Cheng et al. 2004) and binds to NMDAR subunit NR2B within the PSD. The bound CAMKII activates a number of signaling pathways including RAS-Extracellular regulated kinase (ERK) (Zhu, Qin et al. 2002, Patterson, Szatmari et al. 2010) and potentially targets small Rho-GTPases (Patterson and Yasuda 2011). Triggering of these pathways leads to phosphorylation of AMPAR subunit GluA1 at multiple sites such as Ser845 by Protein kinase A (Banke, Bowie et al. 2000), Ser831 by Protein Kinase C or CAMKII (Roche, O'Brien et al. 1996) and Ser818 by PKC (Boehm, Kang et al. 2006). These phosphorylation tags both increase single channel conductance (Barria, Muller et al. 1997, Kristensen, Jenkins et al. 2011) and AMPAR exocytosis into extrasynaptic membrane. Both these mechanisms need CAMKII activation. Phosphorylation at Ser831 is important for increased AMPAR conductance by increasing the transition of high conductance states by glutamate binding (Kristensen, Jenkins et al. 2011). For synaptic exocytosis, vesicles containing AMPAR are rapidly inserted into extrasynaptic plasma membrane (Makino and Malinow 2009, Patterson, Szatmari et al. 2010) providing a pool of AMPAR to be then inserted into the synapse. AMPAR binding onto the synapse requires AMPAR binding protein stargazin (Chen, Chetkovich et al. 2000). Stargazin is a transmembrane AMPAR regulatory protein (TARP) which upon phosphorylation (Tomita, Stein et al. 2005) interacts

with PSD95 and AMPAR (Opazo, Labrecque et al. 2010) and thus locks AMPAR to the synapse. Locking of AMPAR to the synapse, increases AMPAR content within the spines thereby increasing synaptic response to neurotransmitter release. Thus monitoring AMPAR content has been used as a means to track synaptic potentiation within spines (Makino and Malinow 2011, Padmashri, Reiner et al. 2013, Zhang, Cudmore et al. 2015).

Long Term Depression

LTD Is a long-lasting decrease in the synaptic response of neurons to stimulation of their afferents following a long patterned stimulus (Collingridge, Peineau, Howland, & Wang, 2010). LTD was first described in the Purkinje cells of the cerebellum and involves the coincident depolarization of parallel fibers and climbing fibers (Ito, Sakurai, & Tongroach, 1982). In the cerebellum the stimulation of climbing fibers leads to a large rise in intracellular calcium within Purkinje cells and activation of postsynaptic group 1 mGluR., which triggers a series of mechanisms which finally lead to AMPAR internalization and thus LTD.

However, research within other brain regions have led to identification of multiple routes of LTD induction which engage different mechanisms of AMPAR internalization. In the hippocampus two well studied models are NMDAR- and mGluR-dependent LTD mechanisms. A well-used model of NMDAR LTD involves the activation of calcium/calmodulin dependent phosphatase calcineuirn and protein phosphatase 1 (PP1) (Lisman, 1989). Calcineurin's affinity to calcium/calmodulin is very high and would be activated even with modest increases in calcium in contrast to CAMKII which requires much higher calcium concentrations (Lisman, 1989). Consistent with this, both calcineurin (Mulkey, Endo, Shenolikar, & Malenka, 1994) and PP1 (Mulkey, Herron, & Malenka, 1993) are known to be important for LTD (Carroll, Beattie, von Zastrow, & Malenka, 2001). Activation of phosphatases presumably dephosphorylates and internalizes AMPAR which

are then degraded via proteasomal and lysosomal pathways (Li et al., 2010; Luscher & Malenka, 2012).

Unlike NMDAR dependent LTD, mGluR dependent LTD is mechanistically different. mGluR LTD requires rapid translation of preexisting mRNA (Huber, Kayser, & Bear, 2000) and occurs even when dendrites are severed from the cell body. mGluR is also usually considered irreversible with loss of AMPAR from the post synaptic compartment and may prelude synapse elimination (Bastrikova, Gardner, Reece, Jeromin, & Dudek, 2008; Snyder et al., 2001). From a signaling standpoint, mGluR LTD in CA1 does not act through canonical mGluR Gq pathways. Instead CA1 LTD depends on tyrosine dephosphorylation and tyrosine phosphatase STEP (striatal-enriched tyrosine phosphatase) which dephosphorylates the AMPAR subunit sGluA2 (Cho et al., 2008; Moult et al., 2006; Moult, Schnabel, Kilpatrick, Bashir, & Collingridge, 2002; Zhang et al., 2008) acting via TNFα signaling pathway. Although general outlines of the process are being developed, what is clear is the complexity of the signaling cascades involved and the multiple mechanisms of LTD.

1.2d Structural plasticity of synapses

Plasticity in relation to the brain refers to either functional or structural changes that occur within the neuronal circuits adjusting to changes in external or internal environments (Luscher, Nicoll, Malenka, & Muller, 2000). So far in this introduction the focus has been on functional changes associated with stimuli. In more recent times, the role and emergence of structural changes has been extensively studied and appreciated (A. Holtmaat & Svoboda, 2009). Structural changes have been characterized during development, experience and pathological conditions (A. Holtmaat & Svoboda, 2009; Penzes et al., 2011). Spines are a heterogeneous population of structures with diverse shapes and behavior. Extensive electron microscopy studies have categorized dendritic spines based on the relative proportions of spine head and neck and into four main categories: mushroom, thin, stubby and filapodial spines (K.M. Harris, Jensen, & Tsao, 1992; A. Peters & Kaiserman-Abramhof, 1970). Filapodial, stubby and thin spines considered immature forms of spines as they have shorter lifespans, are more dynamic and more motile. With stimuli these spines are thought to mature into a mushroom shaped spine which are more stable. This has led some investigators to call thin spines as 'learning spines' and mushroom spines as "memory spines" (J. Bourne & Harris, 2007; Kasai et al., 2003). These morphological features of spines are shaped both during development and experience and will be discussed subsequently.

Structural dynamics during development: The morphology of dendritic spines is highly plastic in shape, numbers and fate which evolves dramatically during the life time of an organism (Penzes et al., 2011). Early in development in humans is a period of synaptogenesis where higher densities of spines are observed which then gradually decreases over time. Transgenic mice models expressing fluorescent protein in subsets of neurons have allowed investigators to track spines *in vivo* over long periods of time(G.

Feng et al., 2000). Similar to humans, mice also show a development evolution in spines dynamics. At birth dendrites are sparsely studded with spines followed by a period of synaptogenesis lasting between two to four weeks after birth with high density of immature looking spines having higher rates of formation and elimination (Coiro et al., 2015; Cruz-Martin, Crespo, & Portera-Cailliau, 2010; A. J. Holtmaat et al., 2005). Transition from adolescence to adulthood is a period of synaptic pruning with reduced spine formation, increased spine elimination and increase in spine stability. For example, at P16 in apical tufts of layer 5 neurons in the somatosensory cortex at P16 overall spine stability was 35% whereas at 6 months' stability was 73% over 8 days (A. J. Holtmaat et al., 2005). A point to note is that although spine properties are dependent of brain region and cell type studied (Cruz-Martin et al., 2010; A. J. Holtmaat et al., 2005; Trachtenberg et al., 2002; Zuo, Lin, Chang, & Gan, 2005) in general all brain region show a similar trajectory in spine behavior.

Experience dependent synaptic plasticity: Modulation of synapses structurally and functionally is believed to be the basis of learning and memory (Hayashi-Takagi et al., 2015). Over the years a number of studies have observed structural changes in animals with various behavioral protocols in various brain regions. In the motor cortex, which is the focus of this study, various motor training protocols have shown to affect structural plasticity of dendritic spines and across different populations of neurons. Rats trained on an acrobatic motor task when Golgi stained to visualize spines were shown to have increased synaptic density in layer 2/3 neurons in the motor cortex compared to untrained mice (Kleim, Lussnig, Schwarz, Comery, & Greenough, 1996). Later on it was demonstrated that rats trained on a single forelimb reaching task had a transient increase in dendritic spine size in the motor cortex suggesting synaptic strengthening accompanying learning (Harms, Rioult-Pedotti, Carter, & Dunaevsky, 2008). Recent in vivo studies have confirmed these earlier findings. The first report of such plasticity was in

2009, where Xu and others observed rapid (within 2 hours) formation of spines in layer 1 apical dendrites of layer 5 neurons in the motor cortex (Xu et al., 2009b). The same group later showed that these spines were not randomly occurring on the dendrite but formed in clusters (M. Fu & Zuo, 2011). Similar findings were observed using an accelerating rotorod assay with dendrites in both layer 2/3 and layer 5 showing increases in spines following the training (Ma et al., 2016; G. Yang, Pan, & Gan, 2009). Interestingly in these studies the newly formed spines were preferentially stabilized with elimination of preexisting structures thus maintaining normal dendritic density. These experiments illustrate the structural remodeling of dendrites during learning. Similar results were observed in mice trained in a lever press task (S. X. Chen, Kim, Peters, & Komiyama, 2015; A. J. Peters, Chen, & Komiyama, 2014) with increased spine formation in layer 2/3 neurons.

Apart from the motor cortex other brain regions have also been shown to undergo structural plasticity. These include the somatosensory cortex with studies performing sensory deprivation by whisker trimming or sensory task discrimination (A. Holtmaat, Wilbrecht, Knott, Welker, & Svoboda, 2006; Kuhlman, O'Connor, Fox, & Svoboda, 2014; Wilbrecht, Holtmaat, Wright, Fox, & Svoboda, 2010) visual cortex with binocular or monocular deprivation (Oray, Majewska, & Sur, 2004), prefrontal cortex with fear conditioning (Lai, Franke, & Gan, 2012) and auditory cortex during memory recall (Moczulska et al., 2013). These results have also been observed across species in zebra finch further strengthening the notion of a broadly conserved mechanism of learning and memory (Roberts, Tschida, Klein, & Mooney, 2010).

1.2e Relationship between structural and functional plasticity

Structure and organization of a dendritic spine is critical for synaptic function and in principle is the foundations of memory, learning and cognitive process. However, the importance of structure vs. function and their cross relationship with each other is not always clear. Over the years, a number of studies have tried to shed light on the impact of functional or structural plasticity on each other either in *in vitro* preparations or in behaving animals and these will be summarized here.

Functional plasticity in spine formation and elimination: Spine geometry and functional strength of a spine are positively correlated with large mushroom spines having large AMPAR content and immature spines having less to none (K.M. Harris & Stevens, 1989; Matsuzaki et al., 2001). These structure function correlations are preserved even during functional plasticity such as LTP where induction of LTP upon a spine induces almost instantaneous increase in spine size followed by a slightly delayed increase in AMPAR content (Buchs & Muller, 1996; Gustafsson & Wigstrom, 1990; Kopec, Li, Wei, Boehm, & Malinow, 2006; Matsuzaki, Honkura, Ellis-Davies, & Kasai, 2004). Along with morphological changes LTP induction has a lasting increase in synaptogenesis and basal turnover within dendrites (De Roo, Klauser, & Muller, 2008; Engert & Bonhoeffer, 1999b; Nagerl, Eberhorn, Cambridge, & Bonhoeffer, 2004) with elimination of inactive synapses and stabilization of active synapses (De Roo et al., 2008; Hill & Zito, 2013; Y. Yang, Wang, Frerking, & Zhou, 2008). In contrast to LTP, both NMDAR and mGluR dependent LTD are associated with spine retraction and elimination. These changes involve endocytosis of synaptic machinery through complex cellular mechanisms

Synaptic clustering: Apart from functional perturbations within a synapse affecting its behavior, there is a growing appreciation that that local micro-circuitry influences synaptic behavior. Given the complexity of a neuron a variety of factors ranging from geometrical

and biophysical morphology of a dendrite, to diffusible extracellular signaling molecules and local plasticity mechanisms have all been implicated in modulation of synapse behavior. To account for these complex mechanisms involved in memory storage, a clustered memory storage hypothesis has been proposed (Govindarajan, Kelleher, & Tonegawa, 2006). According to the model, groups of neighboring spines within a local cluster on a neuron encode related memories (Govindarajan et al., 2006). This model is in sharp contrast to previous distributed memory storage hypothesis (R. Yuste & Urban, 2004) where synapse relevant to a memory are distributed randomly across the dendrites of a neuron. The clustered storage model offers a number of functional, biochemical and computational advantages to neuronal function and synaptic transmission (Govindarajan et al., 2006; Kastellakis, Cai, Mednick, Silva, & Poirazi, 2015).

Functionally, a clustered arrangement would make it easier to reactivate memory engrams and allow the neuron to differentiate multiple patterns of activity compared to a distributed arrangement. This is because clustered spines depolarized by similar inputs would make it easier to achieve an action potential (AP) especially since depolarization of a single spine is not necessarily sufficient to trigger one (Govindarajan et al., 2006). This would also mean lesser synapses are needed for storage of a memory. Additionally, since the summation of relevant inputs in a clustered system is supralinear, this allows multiple clusters of spines to store separate units of memory and thus allowing a single neuron to recognize a larger repertoire of activity. Finally, since later stages off long term potentiation requires protein synthesis and translocation of synaptic material from the nucleus to the potentiated spines, transport of synaptic material would be biochemically more efficient in a clustered system as the cargo targets are close by (Redondo & Morris, 2011).

There is accumulating evidence for a clustered model of memory storage. Computational modelling of patterns of synaptic activity in biophysically detailed models show that

clustered synapses lead to supralinear responses as proposed (Poirazi, Brannon, & Mel, 2003a, 2003b). There is also experimental evidence for the model where appropriately timed and patterned activity leads to supralinear responses (Losonczy & Magee, 2006; Polsky, Mel, & Schiller, 2004).

Clustering at an anatomical level has been shown across multiple paradigms and model systems. The first evidence of clustering came from studies in barn owl where owls exposed to abnormal vision through a prismatic lens developed clustered synapses in the adaptive zone developed in response to the behavior (McBride, Rodriguez-Contreras, Trinh, Bailey, & Debello, 2008). Similarly, both in primates and rodents there is evidence for anatomical clusters. Yadav et. al. observed that spines within apical dendrites in the primate prefrontal cortical neurons were more likely to occur together than by chance (Yadav et al., 2012). In mice trained on a forelimb reaching task, Fu et. al. identified that newly formed spines developing in response to the behavior were more likely to occur close to each other (< 5 μm) and close to neighboring preexisting spine than control untrained conditions(M. Fu, Yu, Lu, & Zuo, 2012). Makino and Malinow, showed that with whisker stimulation, coordinated translocation of AMPAR subunit GluA1 occurred in neighboring spines within the dendritic tree in the somatosensory cortex. In sensory deprived (whisker trimmed mice) this clustering was not observed (Makino & Malinow, 2011). Clustering has also been observed during development where neurons in the CA1-CA3 hippocampus sharing similar times of neurogenesis were 5 times more likely to connect with each other than predicted by random clustering (Druckmann et al., 2014)).

Functional clustering of adjacent spines that are active together has also been reported. In hippocampal organotypic slices spines located close together had more correlated activity as measured by changes in [Ca^{2+}] indicating that synapses tended to activate in clusters (Kleindienst, Winnubst, Roth-Alpermann, Bonhoeffer, & Lohmann, 2011). In the barrel cortex of mice, functional mapping of active synapses found that active spines

formed functional clusters which were synchronized in activity and locally confined. These clusters consisted of 2-12 co-active spines within 10 μm of each other and tended to be innervated by locally convergent axons (N. Takahashi et al., 2012).

Mechanistically, the formation of these clusters could be a product of LTP like mechanisms. LTP induction triggers a cascade of signaling pathways which promote co-operatively of synaptic potentiation. One such pathway is the MAPK (mitogen-activated protein kinase) pathway which is known to be active several minutes after LTP (Wu, Deisseroth, & Tsien, 2001). Ras GTPase (Harvey, Yasuda, Zhong, & Svoboda, 2008) and Rho GTPase (Murakoshi, Wang, & Yasuda, 2011), members of this signaling cascade, has been shown diffuse within 10 micron stretches of a stimulated spine and invade neighboring spines and may be the molecular basis for reduced thresholds in LTP induction and selective stabilization of nearby synapses (De Roo et al., 2008; McNaughton, 2003; M. Patterson & Yasuda, 2011; Roggenhofer, Fidzinski, Shor, & Behr, 2013).

1.3 Fragile X Syndrome

1.3a Clinical classification and diagnosis

Fragile X syndrome (FXS) also known as Martin-Bell syndrome(J. P. Martin & Bell, 1943), is an X-linked condition caused by mutation of the fmr1 gene and is the leading cause of inherited intellectual disability (ID) (Penagarikano, Mulle, & Warren, 2007; Warren & Nelson, 1994). FXS affects 1 in 4000 male children and 1 in 8000 females. The fmr1 gene is located on the X chromosomes at the loci Xq27.3 (Hirst et al., 1993)and the gene product formed is Fragile X mental retardation protein (FMRP). FMR1 gene is characterized by a trinucleotide CGG repeat sequence in the 5' untranslated region (Y. H. Fu et al., 1991; Hirst et al., 1993). Under normal conditions the gene has 5-44 nucleotide (Y. H. Fu et al., 1991) repeats which under diseased conditions expands to more than 1000 repeats. According to the American College of Medical Genomics and Genomics classification, 45-54 repeats is a borderline, 54-200 is a permutation and greater 200 is a full mutation of the FMR1 gene (American.College.of.Medical.Genetics, 1994; Sherman, Pletcher, & Driscoll, 2005). Individuals with a borderline case exhibit no clinical symptoms and are not considered carriers for the disease. However, there is a small chance that the FMR1 gene maybe at unstable and may affect future progeny. Premutations affects an individual based on their sex. Premutation gene alleles are unstable and there is a possibility of the mother transmitting a full blown mutation which is dependent on number of repeats(Sherman et al., 2005). About 25% of women with premutations also suffer from Fragile X associated primary ovarian insufficiency characterized by ovarian dysfunction, irregular periods, early menopause, hot flushes and infertility(Sherman et al., 2005). Women are also at risk from depression (Lachiewicz et al., 2010; Rodriguez-Revenga, Madrigal, Alegret, Santos, & Mila, 2008) with reports of general anxiety and shyness. In a recent study, 70% of patients (both sexes) with a permutation met at least one criteria for

anxiety (Cordeiro, Abucayan, Hagerman, Tassone, & Hessl, 2015). Male permutation individuals are at further risk of FragileX tremors/ataxia syndrome (FXTAS) which is a neurodegenerative disorder associated with ataxia, tremors, numbness, loss of intellectual ability and Parkinsonism. Males with premutations act as carriers and pass on the mutation to their daughters(R. Hagerman & Hagerman, 2013).The full blown mutation is when there are anywhere between 200-1000 repeats and causes silencing of the gene product FMRP. The cause of the gene silencing is due to complex epigenetic mechanisms. In a normal allele the fmr1 promoter undergoes some methylation. However, in a FXS allele the expanded CGG repeats leads to hypermethylation upstream of the CGG repeats by a still unknown mechanism thus causing silencing to the gene product(R. Hagerman & Hagerman, 2013). Deacetylation and demethylation of histones at the fmr1 gene loci have also been reported which prevent binding of transcription factors leading to gene silencing (Tabolacci et al., 2008). Modern southern blot and PCR screening test are highly accurate and provide accurate diagnosis. Risk factors include familial history of FXS (parents are diagnosed carriers) or family history of autism and intellectual disability. However, for individuals with no risk factors, diagnosis is done symptomatically. Early diagnosis is made on children at about 3 years of age with behavioral deficits such as delayed motor milestones, hand flapping, poor eye contact, irritability, lack of muscle tone (hypotonia) and social and language disorders. These usually leads to a diagnosis of autism spectrum disorder (ASD) before the diagnosis of FXS. About 30% of FXS diagnosis meet the criteria for ASD(R. Hagerman & Hagerman, 2013). Usually, after a diagnosis of FXS, a subsequent testing of family members is performed to identify other potential affected relatives. Physically infants with FXS are not born with any characteristic physical features. However, after puberty children develop features typical to FXS such as narrow face, large head, large ears, hyper flexible joints, prominent forehead and macroorchidism (enlarged testes)(R. Hagerman & Hagerman, 2013; Sherman et al., 2005).

Adult males with complete methylation have an IQ between 40-85 which is considered moderate to mild mental retardation(Gross, Berry-Kravis, & Bassell, 2012; R. J. Hagerman et al., 2009). Interestingly, IQ in females with FXS is much less affected with borderline normal IQ(Gross et al., 2012). Patients also exhibit learning disabilities including language processing problems such as speech impairments, inability to understand nonverbal ques, reduced working and short-term memory, attention deficits and impaired mathematical and visuospatial ability(R. J. Hagerman et al., 2009). Behaviorally patients show sexual dysmorphism in symptoms with male FXS patients being hyperactive, impulsive, moody, attention deficits and with general phobias making them anxious. Patients also exhibit autistic behavior including repetitive behavior, shyness, avoiding eye contact and having perseverative choice of words, sentences and topics (R. Hagerman, Lauterborn, Au, & Berry-Kravis, 2012). Interestingly, FXS individuals although socially curious but are restricted by social anxiety. Females generally have only a subset of these symptoms including anxiety, social awkwardness, shyness and selective mutism. Patients also are bothered by bright lights and loud noises which may cause them to display inappropriate behavior and are susceptible to audiogenic seizures.

1.3b Structural human brain studies

Postmortem analysis of brains from human patients with FXS show no gross abnormalities in weight, morphology or number of neurons (Hinton, Brown, Wisniewski, & Rudelli, 1991; S. A. Irwin et al., 2001; Wisniewski et al., 1985). However, more recent functional and structural magnetic resonance imaging have revealed abnormalities in specific brain structures(Luo, Wu, & Duan, 2016). A consistent finding in these studies is a significantly enlarged caudate nuclei (CN) which is part of the basal ganglia and plays a key role in frontal subcortical circuits(Grahn, Parkinson, & Owen, 2008; Villablanca, 2010). CN along with the putamen form the input nuclei of the basal ganglia and is innervated from a range of frontal subcortical circuits and are important for maintaining and shifting attention, executive function, motor programming and oculomotor functions (Grahn et al., 2008), all of which are disrupted in FXS (R. J. Hagerman et al., 2009). Another consistent finding in both FXS patients of both sexes have smaller posterior cerebellar vermis, a structure that is important for processing sensory stimuli and performing sensorimotor integration.(Hoeft et al., 2010; S. H. Mostofsky et al., 1998; D. X. Peng et al., 2014). Moreover, size of the posterior vermis and caudate nuclei correlate with FMR1 expression (S.H. Mostofsky et al., 1998), suggesting that FMRP may cause the observed changes. Studies reporting reduced volumes of the insular nuclei, an important sensory integration region associated with anxiety may also be linked to prominent hyperarousal and gaze aversion in FXS patients (Cohen, Nichols, Brignone, Hall, & Reiss, 2011). In children with FXS, the hippocampus was found to be transiently enlarged with size recovering by adulthood (Kates, Abrams, Kaufmann, Breiter, & Reiss, 1997; Reiss, Lee, & Freund, 1994). Children with FXS have demonstrated increased ventricular cerebral spinal fluid volumes (Kaplan et al., 1997) and reductions in the size of the amygdala (Eliez, Blasey, Freund, Hastie, & Reiss, 2001). However, what is unclear with the human studies is whether the anatomical

changes are causative or the result of the neurological deficits seen in FXS patients(O'Donnell & Warren, 2002). Hence, the development of animal models for FXS are essential in delineating the cause-effect mechanisms in FXS. The earliest reports of synaptic deficits in FXS observed long, thin dendritic spines with prominent heads in the parieto-occipital cortex from one individual (Rudelli et al., 1985). Subsequent analysis reported similar results in layer 2/3 and layer 5 neurons in three other individuals with FXS(Hinton et al., 1991). A quantitative comparison with age matched controls from human postmortem studies identified increased density in layer 5 pyramidal neurons in visual and temporal cortex(S. A. Irwin et al., 2001). The study also confirmed the presence of long, thin spines as the mean length and proportion of spines with immature morphology was higher in FXS samples. Taken together this suggests that patients with FXS have deficits in dendritic spine morphology which could be causative cause of the behavioral deficits reported in these patients.

1.3c Molecular basis of Fragile X syndrome

Fragile X mental retardation protein (FMRP) FMRP was first identified and cloned in 1991(Verkerk et al., 1991). Over the last 25 years the role of FMRP in synaptic plasticity and function has been gradually uncovered. FMRP is localized at postsynaptic sites within dendritic spines and regulated synaptic plasticity and strength in a complex manner (Darnell & Klann, 2013). FMRP represses translation of select targeted mRNA which then leads to increased synthesis of other key synaptic proteins. A number of target protein involved in synaptic plasticity have been uncovered. However, the molecular mechanism that FMRP and signaling pathways involved in regulating FMRP function are still to be discovered.

FMRP expression in human's tissue starts very during development. The first expression of FMRP was observed as early as 3 weeks with broad expression in many fetal tissue including brain, liver, kidneys and lungs (Agulhon et al., 1999; Tamanini et al., 1997). However, later in adulthood expression is more restricted with high expression across various brain regions with small expression in other tissue (Agulhon et al., 1999; Tamanini et al., 1997). Early in development expression in neuronal cells is mainly cytoplasmic whereas in adulthood expression is much broader with strong expression in cytoplasm and within dendrites(Agulhon et al., 1999).

Similar to humans, in mice which are used as an animal model for FXS research, FMRP expression starts early in development with expression seen as early as embryonic age 10 although no expression was observed before this age(Hinds et al., 1993). Expression is hetrogenous with high expression in brain and testis but low expression in skeletal muscles, pancreas and liver. Interestingly, expression profiles in general wane during development(Hinds et al., 1993). At adulthood expression is high within the brain, testis,

spleen, ovaries and eye but not in heart, lungs, liver, pancreas and muscles(Hinds et al., 1993).

Multiple splice isoforms of FMRP exist in humans and mice and the isoforms may have difference in function (C. T. Ashley et al., 1993). The main isoform of FMRP is a 71 kDa protein(Santoro, Bray, & Warren, 2012) which has a number of functional domains. These include three RNA-binding motifs, a nuclear export signal (NES) and a nuclear localization signal (NLS). The three RNA binding motifs include two K homology domains, an arginine and glycine (RGG) box and two tandem Agenet domain at its N terminus (Santoro et al., 2012). The KH domain is critically important for FMRP function as clinically documented by a patient with a denovo single nucleotide 1304N mutation in within the KH motif expressed severe symptoms of FMRP(De Boulle et al., 1993). Agenet domains are known to interact with trimethylated histones (Adams-Cioaba et al., 2010)whereas methylation of arginines in the RGG box (Blackwell, Zhang, & Ceman, 2010) has been suggested to regulate FMRP's affinity for certain RNA's. Although FMRP is cytoplasmic it can shuttle in and out of the nucleus as expected by presence of NLS and NES domains (Y. Feng et al., 1997). It is believed that FMRP binds to mRNA targets which both facilitate FMRP export and FMRP serves as a mRNA chaperone (Eberhart, Malter, Feng, & Warren, 1996; M. Kim, Bellini, & Ceman, 2009).

More recently, a novel role of FMRP in DNA stability during replication was identified. Alpatov et.al identified that cells lacking FMRP when exposed to treatment which induced single strand breaks, fail to initiate DNA damage repair mechanisms (Alpatov et al., 2014). This was due to a failure in phosphorylation of γH2A.X and recruitment of BRCA1 to the damaged DNA in a chromatin dependent manner most likely due to binding to methylated histone H3 (Alpatov et al., 2014). These findings are in line with other reports of a protective role of FMRP to cellular damage(Jeon et al., 2012; Jeon et al., 2011) and these

protective mechanisms are thought to be independent of mRNA translation(Santoro et al., 2012).

FMRP was initially characterized as a polysome-associated protein (Eberhart et al., 1996; Khandjian, Corbin, Woerly, & Rousseau, 1996) and is a selective RNA-binding protein binding to about 4% of the mRNA in the mammalian brain (Ashley, Wilkinson, Reines, & Warren, 1993). Screening studies for putative FMPR mRNA targets have identified anywhere between 400 to 842 targets (Dolzhanskaya, Sung, Conti, Currie, & Denman, 2003; Miyashiro et al., 2003; Zou et al., 2008). A more recent screening using a High-throughput sequencing of RNA isolated by crosslinking immunoprecipitation (HITs-CLIP) approach identified 842 targets of which 32% were PSD associated proteins, 34% were proteins in the NMDAR proteome and 62% of the metabotropic glutamate receptor proteome. A substantial number of targets were also presynaptic proteins. This suggests a broad spectrum of synaptic and synaptic associated protein regulated by FMRP. An ingenuity analysis on FMRP targets identified by the study linked FMRP to a number of synaptic signaling pathways involving: synaptic long term potentiation, glutamate receptor signaling, neuropathic pain signaling, GABA receptor signaling, synaptic LTD, and CREB signaling.(Darnell et al., 2011). Interestingly, the study also identified a number of autism and intellectual disability related protein being regulated by FMPR suggesting conserved mechanism across wide spectrum of neurodevelopmental disorders (Darnell et al., 2011).

1.3d Mouse models of Fragile X syndrome

Since the first identification of the fmr1 gene in 1991 several attempts have been made to generate mouse models for the fmr1 expansion mutation since humans and mice share 95% to 97% homology between nucleotide and amino acid sequence identity (C. T. Ashley, Jr. et al., 1993). Apart from sequence homology, both timing and tissue specificity of FMRP expression is similar between mice and humans (Hinds et al., 1993). However, no naturally occurring repeat expansion in the 5' UTR in mice has ever been observed. Two main approaches in design of the model has been to a) knock out of the fmr1 gene b) recapitulate the expanded repeat sequence.

The first attempts at generating a FXS mouse was to knock out the fmr1 gene using a targeted deletion of exon 5 in the mouse fmr1 gene(Consortium, 1994). This mouse model, the fmr1 KO (KO) mouse, has been extensively studied over the years (Contractor et al., 2015; C. X. He & Portera-Cailliau, 2013) and is the model used in this thesis. The mouse does recapitulate behavioral, physiological and cellular abnormalities seen in humans and will be reviewed in the next section.

More recently to recapitulate the expanded repeat sequences two separate mice line have been generated. The first of the mice lines expressed an expanded human 98 CGG repeat sequence replacing the endogenous 8 CGG repeat mouse sequence in the fmr1 promoter (Bontekoe et al., 2001). This mouse showed only moderate instability of the gene both by female and male transmission with both expansion and contraction of the fmr1 gene (Bontekoe et al., 2001). These transgenic mice have been bred over multiple generations to express over 300 repeats within the fmr1 loci. Although this length is within the range of full human mutations, no abnormal methylation was seen. However, these mice do show increased fmr1 mRNA, decreased FMRP protein and motor and spatial deficits (Berman & Willemsen, 2009; Bontekoe et al., 2001).

A more recent line generated at National Institute of Health (NIH) using a different cloning strategy as the above mouse had an expanded 118 CGG repeats (Entezam, Biacsi et al. 2007,Hoffman, Le et al. 2012). The mouse retains the translational TAA stop codon just upstream of the CGG118 repeat that is present in the endogenous murine gene but not the human gene. This mouse also shows elevated fmr1 mRNA levels, decreased FMRP levels, moderate intergenerational expansions and no methylation (even when repeat numbers were >300) (Entezam et al., 2007).

Surprisingly, neither model reliably shows large expansions in the CGG repeat tract seen with maternal transmission in FXS and neither has methylation or silencing of fmr1 gene. More research is ongoing in characterizing these expanded repeat models of FXS and may provide new avenues in FXS research (Berman et al., 2014).

Behavioral deficits in the fmr1 KO mice As mentioned earlier the most widely studied animal model in FXS research is the fmr1 KO (KO) mouse where the gene is knocked out by deletion of exon 1(Consortium, 1994) . Over the years a number of behavioral deficits have been reported in the KO mice from hyperactivity and anxiety behavior, social interaction deficits, sensory perception, motor deficits and seizures (Santos, Kanellopoulos, & Bagni, 2014).

Individuals with FXS are hyperaroused and anxious (Berry-Kravis 2014). A numbers of studies have tested for hyperactivity and anxiety in the KO and have reported mixed results. Mice tested in an open field test had increased hyperactivity (Olmos-Serrano, Corbin, & Burns, 2011; Peier et al., 2000; Restivo et al., 2005) and increased anxiety (Restivo et al., 2005). Further support for hyper anxiety in the KO was in a mirrored chamber test where KO mice had increased anxiety to their own reflection(Spencer, Alekseyenko, Serysheva, Yuva-Paylor, & Paylor, 2005). However, in contrast to this, KO mice tested on a two chambered box reported lower anxiety behaviors (Peier et al., 2000;

Veeraragavan et al., 2012). Similarly, in an elevated plus maze, the KO mouse was seen to be less anxious with less time spent in the open arm (Yuskaitis et al., 2010). These contradicting results may partly be due to age and strain of mice used and may also inherently reflect the difficulty in quantifying anxiety in mice due to confounding variables during behavior.

Social interaction in the FXS mouse was tested using a classical three chambered apparatus where in phase 1 the test mouse is given a choice between an empty box and a novel mouse. In the second phase the empty box is replaced by a new mouse and the test mouse is allowed to interact with either the stranger or now familiar mouse. The numbers of approaches and the time spent in proximity with each is scored during both phases (Moy et al., 2004). The KO mice exhibited no difference in social preference (phase 1) but did score low in novel social discrimination (Bhattacharya et al., 2012; Mines, Yuskaitis, King, Beurel, & Jope, 2010). Similarly, the KO mouse spent less time with a novel female mouse (Mineur, Huynh, & Crusio, 2006) as well as impaired social dominance with a novel male mouse (Spencer et al., 2005). These results could either be a consequence of increased anxiety or lack of novelty seeking (Bhattacharya et al., 2012; Busquets-Garcia et al., 2013; Ventura, Pascucci, Catania, Musumeci, & Puglisi-Allegra, 2004).

Since problems in communication and speech are symptomatic of FXS (Bagni, Tassone, Neri, & Hagerman, 2012; R. Hagerman et al., 2012) KO mice tested for patterns of ultrasonic vocalization (USV) to stimuli had significantly altered vocalization patterns (Santos et al., 2014). After maternal separation, the types and duration of USV in 8 day old pups were different from controls(Roy, Watkins, & Heck, 2012). A similar communicational deficit was observed when male KO mice were paired with females with reduced USV's per second in response to the female (Rotschafer, Trujillo, Dansie, Ethell, & Razak, 2012).

Learning deficits Studies of spatial learning using a Morris water maze task, wherein a mouse is placed in a darkened pool and has to remember to find its way to a hidden platform, the KO mouse performed as well as the controls. Memory retrieval and consolidation were also not affected as the time spent in the quadrant with the platform was similar (Bakker & Oostra, 2003; Kooy et al., 1996; Paradee et al., 1999). However, when the KO mice were tested on the Barnes maze where the mouse has to learn to find an escape hole given environmental cues to find the hole, the KO mice displayed significant deficits in retrieval and memory consolidation compared to controls (Yan, Rammal, Tranfaglia, & Bauchwitz, 2005). Similarly, in a radial arm maze, the KO performed worse indicating that deletion of FMRP affected spatial and memory recall (Guo et al., 2012).

Studies of associative learning in the fmr1 KO mouse have also produced mixed results. In a passive avoidance task wherein the mouse has to avoid a location where they received a noxious stimulus, the KO performed normally (Baker et al., 2010; Dolen et al., 2007). However, when tested for a associative learning in a five-choice serial reaction time task the KO had a deficit in performance (Krueger, Osterweil, Chen, Tye, & Bear, 2011). Additionally, the KO had deficits in freezing behavior during cued and contextual fear learning (Guo et al., 2012; Olmos-Serrano et al., 2011; Paradee et al., 1999).

To test for sensory perception, the acoustic startle task which measures a mouse's sensory processing ability, reported mixed results with some reports showing a deficit (Baker et al., 2010; Frankland et al., 2004; Olmos-Serrano et al., 2011; Veeraragavan et al., 2012) and others reporting no difference (Peier et al., 2000; Yan, Asafo-Adjei, Arnold, Brown, & Bauchwitz, 2004). However, the KO mouse did show a consistent propensity to audiogenic seizures reminiscent of humans FXS patients (Baker et al., 2010; Peier et al., 2000; Veeraragavan et al., 2012; Yan et al., 2004)

Patients with FXS have both delays in motor development and deficits in fine motor movement (Sabaratnam, Murthy, Wijeratne, Buckingham, & Payne, 2003; Zingerevich et al., 2009). The KO mice did not show any gross defects in motor function in a rotorod task (Wang et al., 2008). However, in an associative motor learning task on an Erasmus ladder the KO mouse showed deficits in motor learning (Vinueza Veloz et al., 2012).However, whether any deficit in motor learning during development is still unknown.

Dendritic spine deficit in the fmr1 KO mice Early studies in the fmr1 KO using Golgi staining identified increased density in layer 5 pyramidal neurons of the visual and somatosensory cortex in adult mice (Comery et al., 1997; Galvez & Greenough, 2005; McKinney, Grossman, Elisseou, & Greenough, 2005). Similar results were reported in layer 2/3 pyramidal neurons in adult mice (Dolen et al., 2007; Hayashi et al., 2007; Liu, Chuang, & Smith, 2011). Golgi stained sections also showed a developmental increase in spine density from the somatosensory cortex across 1 to 8 weeks of age (Su et al., 2011). Apart from increased density, human FXS studies also indicate that dendritic spines in FXS are immature looking with spines being longer and having narrower spine heads(S. A. Irwin et al., 2001). Studies in the KO have had brain specific alterations with increased length of spines in the prefrontal cortex (Liu et al., 2011; Meredith, Holmgren, Weidum, Burnashev, & Mansvelder, 2007) but not in the temporal cortex(Hayashi et al., 2007).
Majority of live imaging studies of spines either in vivo with two-photon light scanning microscopy (2PLSM) or in vitro have failed to pick up differences in density of spines (Cruz-Martin et al., 2010; Meredith et al., 2007; Padmashri, Reiner, Suresh, Spartz, & Dunaevsky, 2013; Pan, Aldridge, Greenough, & Gan, 2010) although increased density was seen in older mice (Jennifer L. Hodges, 2016).Additionally, length of spines was also not different in the KO mice in number of in vivo studies (Cruz-Martin et al., 2010; Jennifer L. Hodges, 2016; Pan et al., 2010). However, almost all in vivo studies have picked up

increased basal turnover in spines across multiple layers. Cruz-Martin and group found a developmental delay in turnover rates in layer 2/3 neurons during the first two postnatal days in the somatosensory cortex (Cruz-Martin et al., 2010). This increased turnover was also observed over days to weeks in apical dendrites of layer 5 neurons in the somatosensory cortex in older mice (Pan et al., 2010). Interestingly, the same group observed that the spines in the KO were insensitive to sensory modulations by whisker trimming. Unlike normal WT controls where whisker trimming increased spine turnover rates, the KO mice were insensitive to modulations and did not show the corresponding increasing turnover. This suggests that deletion of FMRP although increases synaptic dynamics it adversely makes synapses insensitive to modulation (Pan et al., 2010). This is with consistent another study wherein synapses in the KO needed more stimulation to show similar levels of plasticity as controls and maybe a general underlying theme in FXS research (Meredith et al., 2007).

1.3e Synaptic plasticity in the fmr1 KO mouse

LTP in the fmr1 KO have been varied and region specific. Early LTP studies in the KO were unable to identify any changes in the hippocampus, which the most well studied system in LTP studies. (Godfraind et al., 1996; Paradee et al., 1999; Zhang et al., 2012). However, a more recent study using a different chemical LTP protocol did pick up deficits (Shang et al., 2009). Interestingly, this chemical LTP was partially rescued by use of a mGluR antagonist DL-AP3 suggesting FMRP only plays a role in mGluR-LTP (Shang et al., 2009).

However, unlike the hippocampus, deficits in LTP have been reported in other brain regions. In the amygdala, the brain region associated with emotions, deficits in LTP and decrease in surface AMPAR in the fmr1 KO have been observed (Suvrathan, Hoeffer, Wong, Klann, & Chattarji, 2010) along with presynaptic deficits including decrease in the frequency of spontaneous miniature excitatory postsynaptic currents (mEPSCs) and increased paired-pulse ratio. Although the postsynaptic deficits were not rescued by a mGluR antagonist the presynaptic deficits were(Suvrathan et al., 2010).

Anterior cingulate cortex (ACC), a brain region associated with higher-level behavior such as reward anticipation, decision making and emotions (Stevens, Hurley, & Taber, 2011) had deficits in late-LTP. Late LTP is dependent on protein synthesis and this effect was rescued by a mGluR antagonist (T. Chen et al., 2014; Koga et al., 2015). Similarly, in the somatosensory cortex, the main receptive site of sensory information in the brain deficits in LTP have also been observed which were linked with aberrant RAS, a small GTPase important in signal transduction (Hu et al., 2008).

Apart from the above mentioned brain regions, deficits in LTP have been reported in the auditory cortex (H. Kim, Gibboni, Kirkhart, & Bao, 2013; S. Yang, Yang, Park, Kirkwood, & Bao, 2014), prefrontal cortex (H. G. Martin, Lassalle, Brown, & Manzoni, 2016; Wang et al., 2008) and piriform cortex (Gocel & Larson, 2012) in the FMR1 KO. Along with deficits

in LTP, deficient maturation of synapses including delayed GABA switch have been identified (Q. He, Nomura, Xu, & Contractor, 2014). The consistent rescue of the LTP using mGluR antagonist led to the famous mGluR hypothesis to treat both deficient LTP and exaggerate LTD as will described in the next section (Bear, Huber, & Warren, 2004). LTD as described earlier is a form of synaptic plasticity involving reduction of synaptic strength by decreasing synaptic AMPAR content. In the hippocampus there are two distinct forms of LTD, classical NMDAR dependent LTD and mGluR dependent LTD (Oliet, Malenka, & Nicoll, 1997) of which mGluR LTD is specifically exaggerated in the fmr1 KO mouse (Huber, Gallagher, Warren, & Bear, 2002). mGluR LTD is most commonly triggered by activating mGluR receptors using either a paired pulse low frequency stimulation (Huber et al., 2000) or using a selective agonist (S)-3,5 dihydrophenoxyglycine (DHPG) and is mechanistically distinct from NMDAR LTD (Huber, Roder, & Bear, 2001; Palmer, Irving, Seabrook, Jane, & Collingridge, 1997). This form of LTD is protein synthesis dependent and interestingly a number of proteins translated during LTD are also regulated by FMRP including PSD 95 (Todd, Mack, & Malter, 2003; Tsai et al., 2012), Amyloid precursor protein (APP) (Westmark & Malter, 2007), microtubule associated protein 1B (MAP1B) (Hou et al., 2006) and activity regulated cytoskeleton protein (ARC) (Park et al., 2008). Based on these results FMRP is thought of as a repressor of proteins involved in LTD. In fmr1 KO mice where FMRP is lacking, these LTD proteins are already readily available and hence bypassing the need for protein translation during LTD (Hou et al., 2006; Ronesi & Huber, 2008). It is interesting to note however, that the mere presence of increased LTD protein does not cause increased AMPAR internalization, but the process must be triggered by LTD induction (Waung, Pfeiffer, Nosyreva, Ronesi, & Huber, 2008). This has led to the hypothesis that FMRP through still unknown LTD proteins acts by regulating AMPAR endocytosis upon LTD induction (Guo et al., 2015; Waung & Huber, 2009).

A few potential candidates for LTD proteins include ARC, STEP (striatal enriched protein tyrosine phosphatase) and MAP1B. ARC protein is an activity induced early gene which is transcribed upon activity and it's mRNA transported into the dendrite where the protein accumulates within active spines (Link et al., 1995; Lyford et al., 1995) and causes internalization of AMPAR through its interaction with endophilin 2/3 and dynamin (Chowdhury et al., 2006). These results prompted the idea that local translation of Arc at synapses may mediate LTD. This was supported by the reports that mGluR activation triggered rapid translation of ARC in dendrites and ARC-knock out mice had no mGluR LTD and internalization of AMPAR (Waung et al., 2008). Furthermore, in the fmr1 KO neurons, basal and dendritic Arc protein levels are increased along with enhanced mGluR-LTD but mGluR-triggered Arc synthesis was found absent (Waung et al., 2008). Rescue by wild-type FMRP in fmr1 KO neurons suppresses basal dendritic Arc levels and mGluR-LTD, and restores rapid mGluR-triggered Arc synthesis. These effects were dependent on dephosphorylation of FMRP and suggested a model whereby phosphorylated FMRP functions to suppress steady-state translation of Arc and LTD. Upon mGluR activation FMRP is rapidly dephosphorylated, which contributes to rapid new synthesis of Arc and mGluR-LTD (Niere, Wilkerson, & Huber, 2012).

Another protein identified to regulate mGluR-driven AMPAR endocytosis is STEP. STEP levels increases in hippocampal synaptoneurosomes within minutes after DHPG treatment and this required protein translation. Deletion of STEP increases AMPAR surface expression and blocks mGluR LTD dependent AMPAR endocytosis (Zhang et al., 2008). Further experiments to establish whether STEP mRNA is found in dendrites and interacts with FMRP are needed.

A third candidate 'LTD protein' is microtubule-associated protein 1B (MAP1B). MAP1B mRNA is a known FMRP target and plays a role in mGluR mediated LTD wherein DHPG treatment increases MAP1B levels in dendrites and knockdown of MAP1B prevents DHPG

LTD (Davidkova & Carroll, 2007; R. Lu et al., 2004). One potential mechanism for MAP1B internalization could be through MAP1B's interaction with GRIP1. GRIP1 stabilizes AMPAR and MAP1B may sequester GRIP1 causing AMPAR internalization (Seog, 2004). These data suggest that mGluRs stimulate a coordinated synthesis of multiple proteins that together mediate persistent decreases in surfaces AMPARs and LTD. Further research into mechanisms and signaling pathways regulating these process and how these mechanisms affect behavioral and synaptic level changes in FXS are still needed (Waung & Huber, 2009).

1.4 Organization of the motor system

In chapter 3 we studied the effects of motor learning using a single forelimb-reaching task on AMPAR dynamics in primary motor cortex (M1). This motor training task has been shown previously to induce specific plasticity with trained hemisphere contralateral to the trained forelimb and not in the untrained hemisphere which is ipsilateral to the trained forelimb. This training paradigm has been used to study learning induced synaptic plasticity *in vivo* (Harms et al., 2008; Rioult-Pedotti, Friedman, & Donoghue, 2000; Rioult-Pedotti, Friedman, Hess, & Donoghue, 1998; Xu et al., 2009a).

The motor cortex in humans is located directly adjacent to the rostral portion of the central sulcus and is made up of three brain regions including primary motor cortex (M1), supplementary motor cortex and premotor cortex (Purves, 2008). The primary motor cortex is the principal site for the control of voluntary and involuntary movement and corresponds to Brodmann's area 4. Experiments in the late 30's identified that the M1 cortex is somatotopically organized and electrical stimulation of the cortex elicits movement is the contralateral side of the body (Penfield, 1937). Electrical stimulation of the M1 elicits responses from different body parts and moving medial to lateral, stimulation elicits responses from the torso, arm, hand and face. Additionally, the representations of brain regions that perform delicate movements are disproportionally large compared to representation that perform coarse movements like the trunk and legs (Purves, 2008).

The motor cortex receives three primary inputs including inputs from the premotor cortical areas, the somatosensory cortex and the thalamus. These inputs converge upon the motor cortex which is able to integrate and act upon it (Purves, 2008). The premotor cortical areas include the supplementary motor cortex and premotor cortex. The supplementary motor cortex is located on the medial surface of Brodmann area 6 and

receives input from the basal ganglia and thalamus. The premotor cortex is located on the lateral portion of Brodmann area 6 and its primary input is from the cerebellum and thalamus and is thought to be important for movements directed by sensory stimulations including vision. Projections from the somatosensory cortex allow for direct integration of sensory information whereas the inputs from the thalamus provide relay information from the ascending tracts into the motor cortex. These also provide sites for the cerebellum and basal ganglia to modulate motor information.

In terms of efferents, the motor cortex exerts influence over muscles by a variety of descending tracts. The primary motor output from layer 5 pyramidal neurons of the M1 is direct cortical innervation of alpha motor neurons via the corticospinal tract (Purves, 2008). Apart from the corticospinal tract the motor cortex modulates other motor pathways. These include the corticorubral, corticotectal and rubrospinal tracts. The corticorubral tract allows the cortex to modulate the rubrospinal tract which is a projection from the red nuclei to the spinal cord and is responsible for voluntary movements. Next, the corticotectal tract allows M1 cortex to modulate the tectospinal tract which is a projection from the midbrain tectum to the spinal cord and modulates hand and eye movement. Finally, the last motor tract regulated by the primary cortex is the reticulospinal tract. The reticulospinnal tract descends from the reticular formation and acts on the motor neurons supplying trunk and proximal limb muscles and is involved in locomotion and postural control (Purves, 2008).
A similar cortical motor organization is also evident in mice with well characterized organizational maps available. We used the stereotaxic coordinates of the forelimb representation as described by Tennent et.al in the thesis (Tennant et al., 2011).

1.5 Goals of the study

Although there is much interest in synaptic AMPAR as a determinant of synaptic strength, it is not known how dynamic AMPAR are in synapses and how their dynamic properties relate to structural synaptic plasticity. The goal of the study is to understand the relationship between AMPAR and synaptic dynamics *in vivo* and determine if this relationship was altered in Fragile X syndrome. To do this we developed a surgical and imaging approach to visualize AMPAR and spines *in vivo* in normal and in the fmr1 KO mouse, a mouse model for FXS. Using this approach we were successfully able to visualize AMPAR and dendritic spines and repeatedly image these structures over multiple days. Using this approach in chapter 2, under basal conditions, we elucidated the relationship between AMPAR and synaptic behavior in WT mice and further identified altered AMPAR, spine dynamics in the fmr1 KO mouse in the motor cortex. To better understand these relationships under experience dependent conditions, in chapter 3, we trained normal and fmr1 KO mice on a motor forelimb reaching task and biochemically measured synaptic AMPAR content. We identified that with motor training there is a transient increase in AMPAR subunit GluA1 upon training. In the fmr1 KO mouse, which has a deficit in motor learning, this increase in synaptic AMPAR content is delayed. Since levels of AMPAR correspond to functional strength of a synapse our results identify an altered structure-function relationship of synapses of the motor cortex in the fmr1 KO mouse.

Chapter 2 Relationship between AMPAR and Synapse dynamics in vivo; alterations in a mouse model of Fragile X syndrome.

2.1 Introduction

Dendritic spines are the principal sites of excitatory synapses in the neurons of mammalian central nervous system (Cajal, 1888; E.G. Gray, 1959). Spines are plastic and undergo structural and functional changes under basal and experience dependent conditions (M. Fu & Zuo, 2011; A. Holtmaat & Svoboda, 2009). Structural dynamics involves spine formation, elimination as well as change in size of the spine (Alvarez & Sabatini, 2007; Bosch & Hayashi, 2012; Dunaevsky, Tashiro, Majewska, Mason, & Yuste, 1999; Trachtenberg et al., 2002). The structural reorganization of dendritic spines is thought to be associated with synaptic plasticity mechanisms that involve modulation of synaptic strength via insertion or removal of α-amino-3-hydroxy-5-methyl-4-isoxazolepropionic acid receptor (AMPAR) (Malenka & Bear, 2004; Turrigiano, 2012). Indeed, under in vitro conditions both long term potentiation (LTP) (Engert & Bonhoeffer, 1999a) and long term depression (LTD) (Hasegawa, Sakuragi, Tominaga-Yoshino, & Ogura, 2015), paradigms of synaptic plasticity, have shown to induce spine formation and elimination respectively. These changes are thought to bring about functional reorganization of the neuronal circuits and are critical for learning and memory (Hayashi-Takagi et al., 2015; Hofer & Bonhoeffer, 2010). However, the link between synaptic stabilization and AMPAR insertion has not been previously studied *in vivo.*

Dendritic spines are altered in number of neurodevelopmental disorders (Penzes et al., 2011) including the Fragile X syndrome (FXS) which is the most common inherited form of intellectual disability (Penagarikano et al., 2007). Moreover, in a mouse model of FXS, there is impaired structural and functional plasticity with increased spine turnover, reduced

LTP and impaired experience dependent plasticity of spines (Contractor et al., 2015; Cruz-Martin et al., 2010; Padmashri et al., 2013; Pan et al., 2010). Here we therefore also investigated the relationship between AMPAR insertion and dendritic spine dynamics in an FXS mouse model.

To investigate the role of AMPAR in spine fate and dynamics *in vivo* we expressed AMPAR subunit GluA2 tagged to superecliptic phluorin (SEP), a pH sensitive GFP variant (Miesenbock, De Angelis, & Rothman, 1998), in layer 2/3 neurons of the primary motor cortex (M1). Since the majority of AMPAR contain the GluA2 subunit (W. Lu et al., 2009) we used SEP-GluA2 (sGluA2) levels in spines as a proxy for synaptic AMPAR. Dendritic spines and sGluA2 were imaged *in vivo* using two-photon microscopy over a period of ten days in wild type mice and in the FXS mouse model, the fmr1 knock out (KO) mice. Repeated *in vivo* imaging revealed that in the fmr1 KO mouse dendritic spines were denser, smaller, contained less sGluA2 and had higher turnover rates compared to littermate controls (WT). Our data confirmed the relationship between synaptic strength and synaptic stability, with greater AMPAR containing spines being more stable in both WT and the KO mice. Additionally, we observed that AMPAR levels were dynamic in most stable spines, fluctuating over 10 days with larger proportion of spines showing multiple dynamic events of AMPAR in the KO. Directional changes in sGluA2 were also observed in subpopulation of spines, with new small spines gradually accumulating sGluA2. Finally, sGluA2 levels dropped just prior to spine elimination with greater loss observed in the KO spines. Thus we conclude that AMPAR levels within spines are continuously dynamic but are also predictive of spine behavior, with impairments observed in the fmr1 KO mice.

2.2 Materials and Methods

2.2a *Mice*

Mice were cared for in accordance with NIH guidelines for laboratory animal welfare. All experiments were approved by the University of Nebraska Medical Center Institutional Animal Care and Use Committee. Female C57BL/6 fmr1 heterozygous (HET) mice were crossed with male C57BL/6 fmr1 KO mice and used for in utero electroporation. Because FXS is more common among boys, male WT littermates and fmr1 KO pups were used for all experiments.

2.2b *DNA Constructs*

We used a FUGW pUB-SEP-GluA2-WPRE and pCAG-tdTom constructs for our experiments. FUGW pUB-SEP-GluA2-WPRE was a generous gift from the lab of Noam Ziv (Zeidan & Ziv, 2012). First, Superecliptic phluorin (SEP), a pH sensitive GFP variant (Miesenbock et al., 1998) was tagged to the 5' UTR of GluA2 and the SEP-GluA2 (sGluA2) was cloned under the ubiquitin promoter in a FUGW lentiviral construct. For the morphological tracer, we used pCAG-tdTomato construct where the td-Tomato (tdTom) was cloned under a CAG promoter.

2.2c *In utero electroporation*

Timed pregnant female C57BL/6 fmr1 HET mice were in-utero electroporated as described previously (Saito & Nakatsuji, 2001)(Figure 1a). Briefly, embryonic (E) 15.5 timed pregnant C57BL/6 fmr1 HET mice were anaesthetized using an isoflurane-oxygen mixture (induction: 5% Isoflurane/2 liter/min O2, maintenance: 2% isoflurane/2 liter/min O2). A small incision was made within the abdominal walls and uterine horns were exposed. 0.5 µl of 4µg/µl DNA solution of pCAG-tdTomato and pUb-SEP-GluA2-

WPRE was injected into the cerebral ventricles of E15.5 mouse embryo using Parker Picospritzer III microinjection system. The head was then placed between tweezer electrodes so as to target the motor cortex. Electroporation was achieved using 5 square pulses (duration 5 millisecond frequency = 1 Hz, 35 mV). Embryos were returned back into the abdominal cavity and dams were revived and allowed to deliver normally.

2.2d *Tissue preparation and immunohistochemistry*

Mice were perfused with 4% paraformaldehyde at postnatal day 30 and brain sections (100 microns) containing the motor cortex were selected for analysis. Sections were incubated in 10% normal goat serum (NGS) and 0.3% Triton X-100 for 3 min, then washed three times with PBS 1×, pre-incubated 1 h in 5% NGS and then immunostained with primary antibodies against GluA2 (polyclonal 1:500, Millipore) overnight at 4 °C. The secondary antibodies were Alexa 647 coupled anti-guinea pig (1:500 Invitrogen), in 1% NGS and 0.3% Triton X-100, for 90 min at RT.

2.2e *Cranial window*

At postnatal day 28-30 mice were anesthetized with Tribromoethanol (Avertin®) (0.25 mg/g body weight). A 5 mm cranial windows were implanted over the motor cortex (Figure 1c. Briefly, half an hour before the surgery, dexamethasone (~2 µg/g body weight) and carpofen (5 µg/g body weight) was injected intraperitoneally to reduce cerebral edema and inflammation during the craniotomy. A 5mm craniotomy centered on bregma, was made across the sutures, above the primary motor cortex. After the craniotomy, the exposed surgery site was rinsed with an enrofloxacin antibiotic solution (0.5 µg/ml) and covered with a 5-mm-diameter cover glass, which was permanently glued to the skull using dental acrylic cement. The dura remained intact in this procedure. Mice were treated with antibiotic enrofloxacin (5 µg/ml) twice daily for 6 days after surgery to prevent bacterial

infection. Mice were also injected daily with carpofen (5µg/ml) for three weeks following surgery to reduce inflammation. Mice were allowed three weeks to recover from the surgery.

2.2f *Imaging*

All imaging was performed with a multiphoton microscope (Moving Objective Microscope, MOM; Sutter), using a Ti:Sapphire laser (Chameleon Vision II, Coherent) tuned to 925 nm. Mice were anaesthetized with a ketamine/dexdormitor mixture (100 mg/ml and 0.5 mg/ml respectively, 2.5 ml/Kg). Images were collected with a Nikon water-immersion objective (60X, 1.0 NA). Excitation power measured at the back aperture of the objective was typically ~20 mW and was adjusted to achieve near identical levels of fluorescence for each imaged region using a Pockels cell. Two-channel imaging was achieved by using a 565 nm dichroic mirror and two external photomultiplier tubes. A 535/50 bandpass filter was used to detect sGluA2 emission and a 610/75 bandpass filter was used to detect tdTom. For imaging, we used ScanImage software written in MATLAB (MathWorks) (Pologruto, Sabatini, & Svoboda, 2003). During an imaging session, six to ten regions of interest (ROIs) per animal were selected along the dendritic tufts of tdTom and sGluA2 expressing layer 2/3 pyramidal neurons (Figure 1d). All imaged dendrites were in layer 1 (within the first 100 µm below the dura matter) within the forelimb M1, as determined by stereotaxic measurements (between 750µm-2000µm lateral to the midline and between 1000µm rostral and 250µm caudal from bregma) (Tennant et al., 2011). Each ROI consisted of a stack of images (20–80 optical sections, separated axially by 1 µm). The coordinates of each ROI were recorded using the XYZ motor on the MOM for subsequent imaging days. After imaging, mice were revived from anesthesia with Antisedan (atipamezole hydrochloride 5.0 mg/ml).

2.2g *Image analysis*

Spine identification: All images were corrected for tdTom bleed-through into sGluA2 (green) channel by quantifying percent bleed-through on a tdTom only expressing mouse and subsequently subtracting out the bleed-through from images of the sGluA2 (green) channel images. A custom written imaging program written in python was used to track dendritic spines and sGluA2 levels over imaging sessions. Dendritic segments of 30-80 microns were chosen in three dimensional stacks and dendritic spines were identified and marked in tdTom image channel on 0 hour images (Figure S1a). Unless mentioned, 0 hour images were considered as baseline for all analysis. For spine dynamics, images were compared to baseline images and categorized as stable if they were present in both images, eliminated if they appeared in the previous image but not in the image being analyzed and newly formed when they appeared in the image being analyzed but not in the baseline image. Spine formation and elimination was calculated as a percentage of new or eliminated spines of the total number of spines at baseline. Turnover rates were calculated as ratio of sum of spines formed and eliminated to twice the total number at baseline (A. J. Holtmaat et al., 2005).

sGluA2 and spine intensity measurement: To mark a spine, a region of interest (ROI) was placed manually over the spine with care being taken not to include the dendrite (Figure S1a). To correct for background, a similar sized ROI was placed adjacent to the spine but away from the dendrite. To normalize across imaging sessions, we used tdTom dendrite intensity values as these were stable across sessions (Figure S1b). For normalization two 16 pixel rectangular ROI were marked on either side of the spine and average dendritic shaft tdTom value was measured and a normalization factor derived by comparing to baseline tdTom dendrite values. Care was taken to place the dendrite ROI on a stretch of dendrite that did not have a spine protruding in the z plane. To quantify sGluA2 and spine intensity, the sum of total integrated pixel intensity within the spine ROI across the three

brightest optical frames of the spine was calculated for each channel, individually corrected for background and normalized. Since spine brightness is correlated with spine volume, we used spine intensity as a measure of spine size. Additionally, care was taken to make sure that no protruding structures contaminated the readings. Spines were re-identified on subsequent sessions and intensity values measured as above. For new spines appearing during imaging sessions, spines were marked and sGluA2 and spine intensity were quantified and normalized to time of identification. For presentation purposes, all images were de-speckled and smoothened. Crisscrossing axons traversing the field of view were removed from some frames and 3-5 frames were maximally projected. All analysis was done blinded to mouse genotype on unprocessed images except for the bleed through correction described above.

2.2h *Spine grouping*

Percentile spine grouping: sGluA2 intensity for all spines within a dendrite (50-100 microns) at baseline, were arranged in an ascending order and percentile rank for every spine calculated. Spines were divided into four percentile groups (bin width of 25) with progressively increasing levels of sGluA2. Within each mouse the fraction of stabile spines (Fig 4b) and sGluA2 percentage changes (Figure 5d) were quantified. For the k-means cluster analysis we used two-partition k-means on MATLAB to separate out High and Low GluA2 containing spines per dendrite. Fraction of stable spines per group and proportion of clusters per genotype were calculated (Figure S3). Unless indicated otherwise the averages were calculated per mouse.

Local dendrite ranking: Similar sGluA2 containing spines (“target spines”, minimally 10 microns apart) with opposing fates were identified on a baseline image. sGluA2 within spines in 5 micron stretches on either side of the target spine (cluster) were quantified and arranged in an ascending order. These were then ranked in steps calculated by 10/ (total

number of spines in a cluster – 1) with the smallest spine given a rank of zero, the next spine a rank of zero + step size and with the largest a rank of 10. To calculate dendrite rank, total number of spines within the entire dendrite was used to calculate step sizes and a similar procedure as above was followed.

New spines grouping: For both genotypes, spines within dendrites imaged at 40 and 64 hours were pooled based on sGluA2 levels as described above. Group proportion and fraction of stable spines of all newly formed spines within these sessions were calculated per mouse and compared across groups and genotypes.

sGluA2 spine dynamic grouping: sGluA2 dynamics was quantified as percentage change of sGluA2 at all time points compared to baseline. We defined change as ± 2 standard deviation of 24 hour percentage change in WT which set a threshold of ± 30% (Zhang, Cudmore, Lin, Linden, & Huganir, 2015). Spines were classified as “no change” if sGluA2 intensity did not cross the threshold on any day, “persistent” if it crossed only once and did not return to baseline, “transient” if it crossed the threshold and returned back to baseline or “recurrent change” if it crossed the threshold multiple times. Group proportions were calculated per mouse and compared within groups and across genotypes.

2.2h *Statistics*

Analysis was done either on GraphPad prism or Proc GLIMMIX from SAS/STAT Software and error bars represent Standard error means (SEM). To test for statistical significance an unpaired student t.test (Figure 2a, 2e, 4d-g), multiple t.test with Bonferroni correction (Figures 2b-d), one-way ANOVA with post hoc Bonferroni correction (Figures 5c, 5e), two-way ANOVA with post hoc Bonferroni correction (Figures 5d, 6c, 7d), Kolmogorov-Smirnov test (Figure 3a-b) and a generalized linear mixed models for the percent eliminated data. Multiple comparisons of differences in means were adjusted with the

simulation technique, the recommended approach for random effect models (Peter Westfall, 2011) (Figures 4b).

2.3 Results

2.3a *Repeated in vivo imaging of dendritic spines and SEP-GluA2*

To track spine and AMPAR dynamics in layer 2/3 pyramidal neurons of M1 cortex, E15.5 mouse embryos were in utero electroporated with AMPAR subunit GluA2 tagged to superecliptic phluorin (sGluA2) and morphological tracer td-Tomato (tdTom) (Figure 1). For repeated in vivo imaging, a cranial window (A. Holtmaat et al., 2009) was implanted over the primary motor cortex using previously published coordinates (Figure 1c)(Tennant et al., 2011). Following recovery, mice were imaged and dendrites expressing bright signal across both channels were chosen for imaging (Figure 1d). Stable images were obtained over a ten-day period with no evidence of photo-bleaching (Figure 1e and Figure S1b). While tdTom had uniform expression throughout the cells, sGluA2 had a more punctate appearance with relatively low expression in the dendritic shaft and negligible expression within axons, as would be expected from a postsynaptic protein (Figure 1e, S2a)(Zhang et al., 2015). Moreover, sGluA2 expression was detected even within immature filopodia-like structures (Zito, Scheuss, Knott, Hill, & Svoboda, 2009) giving us further confidence in our ability to track AMPAR *in vivo* (Figure S2b). The use of sGluA2 tagged to superecliptic pHluorin, allowed to track only the surface bound GluA2 which are the functionally relevant pools of GluA2 (Kopec et al., 2006). Immunostaining of sections from transfected mouse brains with an antibody against GluA2 indicated about a 50% overexpression of sGluA2 at postnatal day 30 (Figure S1c). To test whether sGluA2 overexpression affected spine morphogenesis and dynamics, we compared spine density in layer 1 apical dendrites of layer 2/3 neurons of WT mice transfected with sGluA2/tdTom

to mice transfected with tdTom alone (Figure S1d). We observed no difference in spine density between the groups (WTsGluA2/tdTom: 0.69±0.01spines/micron n=5mice, WT tdTom: 0.68±0.02 spines/micron n=3 mice $p>0.05$). Similarly, spine dynamics was also not altered with overexpression of sGluA2 compared to previous reports (Percentage formation and elimination-6% over 24 hours) day) (Ma et al., 2016) (Figure 2b-d). Thus with the in utero electroporation and cranial window strategy, we were able to repeatedly image and track both dendritic spines and spine AMPAR in apical dendrites of layer 2/3 pyramidal neurons of the motor cortex over multiple days.

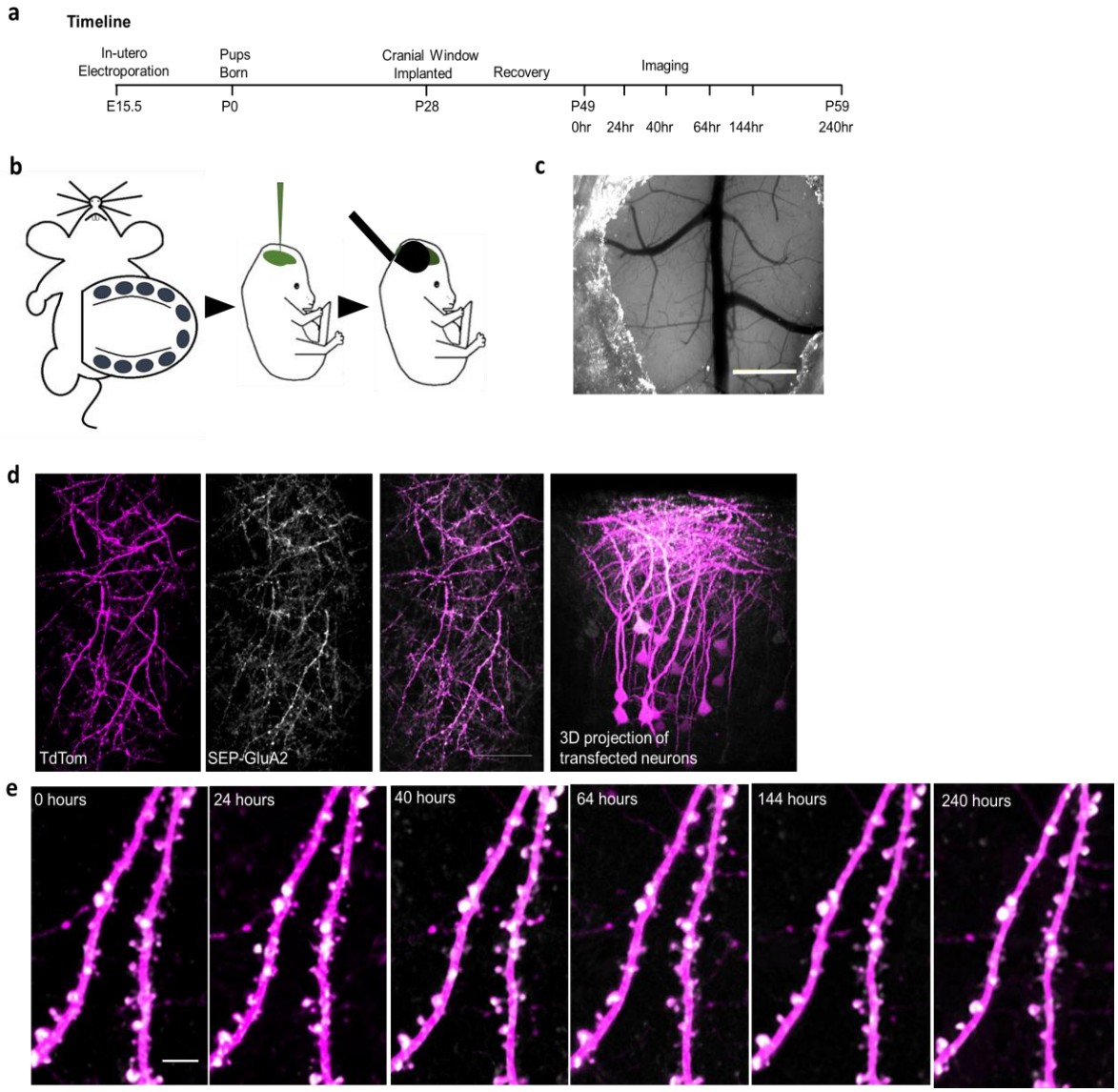

Figure 1: Repeated in vivo imaging of doubly transfected layer 2/3 neurons of M1 cortex. **(a)** Experimental time course. **(b)** Embryos from E15.5 timed pregnant C57Bl6 fmr1 Het mice were injected with a mixture of pUB-SEP-GluA2-WPRE and pCAG-tdTom DNA constructs into the lateral ventricles and neurons were transfected using an electrode tweezer. **(c)** A cranial glass window over the motor cortex. Scale bar: 1 mm. **(d)** 2PLSM in vivo images of transfected region of cortex showing overlap of tdTom (magenta) and sGluA2 (white) along with 3D projection of a Z of the same region. Scale bar: 100 microns. **(e)** Repeated *in vivo* images of apical dendrites of layer 2/3 neurons in M1 cortex showing stable expression of tdTom and sGluA2 over the experimental duration. Scale bar: 5 microns.

2.3b *Altered spine density, size, and dynamics in the primary motor cortex of fmr1 KO mice*

Reports of altered dendritic spine density and dynamics in the KO mice have been variable with spine properties depending on brain region, age and layer of neurons investigated (C. X. He & Portera-Cailliau, 2013). As no previous studies had investigated spine properties in layer 2/3 in the motor cortex at 8 weeks of age, we first investigated spine density in the M1 cortex (figure 2a). Unlike in layer 5 neurons (Padmashri et al., 2013), we observed an 11% increase in dendritic spine density of layer 2/3 pyramidal neurons in the KO mice as compared to tdTom/sGluA2 expressing WT mice (Figure 2a, $p=0.017$). To investigate spine dynamics in layer 2/3 neurons, we quantified spine formation and elimination over short (24 hours), intermediate (60 hours) and long (240 hours) durations and compared WT and KO mice. We observed higher rates of formation at all intervals (Figure 2b, $p<0.02$ for all comparisons) but increased elimination only at intermediate and longer time points (Figure 2c, 64hrs: $p=0.049$, 240hrs: $p=0.03$). This increased formation and elimination also translated to higher turnover rates (TOR) calculated at all intervals (Figure 2d, 24hrs: $p=0.01$, 64hrs: $p=0.006$ and 240hrs: $p=0.001$). The high rates of formation resulted in a trend towards an increase in total number of spines over 10 days in the fmr1 KO (Figure 2e, $p=0.08$). Thus our data suggest that at two months KO mice have increased spine densities and higher rates of spine dynamics in apical dendrites of layer 2/3 neurons in the M1 cortex.

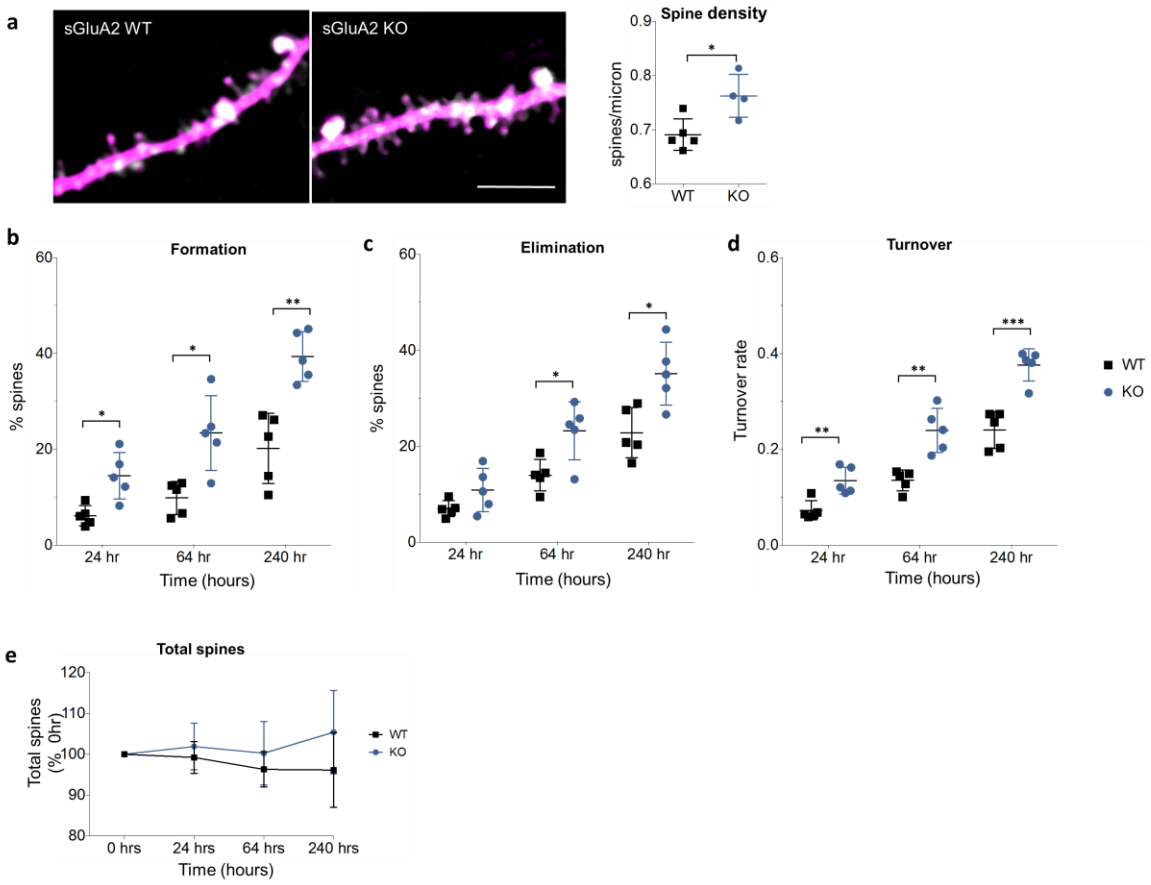

Figure 2: Altered dendritic spine properties in the fmr1 KO mice. (a) Representative images of dendrites from layer 2/3 pyramidal neurons expressing tdTomato and SGluA2 in WT and KO mice. **(b)** Spine densities were significantly higher in the KO mice compared to WT mice (WT: 0.69 ± 0.01 spines/micron, KO: 0.76 ± 0.02 spines/micron, n=4 mice, n=5, t.test, p=0.017) Scale bar: 10 microns. **(b)** KO mice had increased spine formation compared to WT over short (24 hr: WT 6.121± 0.5%, KO 14.5 ± 2.17%, p = 0.02), intermediate (64 hr: WT 9.834 ± 1.53%, KO: 23.41 ± 3.5%, p=0.02) and long time intervals (240 hr: WT 20.16 ± 3.3%, KO: 39.38 ± 2.3%, p=0.004, n=5 mice, multiple t.test with Bonferroni-Sidak correction). **(c)** KO mice had increased spine elimination compared to WT over intermediate (64hr: WT 13.96 ± 1.46%, KO 23.22 ± 2.71%,p=0.049) and long time intervals (240 hr: WT 22.81 ± 2.35%, KO 35.15± 3.9%, p= 0.03) but not over short intervals (24hr: WT 6.99 ± 0.75%, KO 10.9 ± 2.03%, p 0.29, n=5 mice, multiple t.test with Bonferroni-Sidak correction). **(d)** Turnover rates (TOR) were elevated in the fmr1 KO mice (24 hours: WT 0.07 ± 0.01, KO 0.14 ± 0.01, p=0.01, 64hr: WT 0.135 ± 0.01, KO 0.24 ± 0.02, p= 0.006, 240hrs: WT 0.24 ± 0.02, KO 0.38 ± 0.01, p=0.001, n=5 mice, multiple t.test with Bonferroni-Sidak correction respectively). **(e)** In the KO there was a trend toward increase in total number of spines over 10 days (Total spines 240 hours: WT: 96.14 ± 4.098 %, KO: 107 ± 3.484 %, n=5 mice, unpaired t.test, p=0.08). Data represented as Mean ± SEM.

Reports from humans with FXS (Hinton et al., 1991; S. A. Irwin et al., 2001) and fmr1 KO mice (C. X. He & Portera-Cailliau, 2013) have described preponderance of small immature looking spines. We observed a significant shift in the distribution of both sGluA2 intensity and spine intensity ($p<0.001$), which is an approximation of spine volume (A. J. Holtmaat et al., 2005), suggesting smaller spines in layer 2/3 neurons in the KO (Figure 3a, b). This was also evident in a frequency distribution for sGluA2 with increased fraction of spines with lower levels of sGluA2 in the KO (Figure 3c). Spine size and AMPAR levels are known to be strongly correlated (Zhang et al., 2015) (Noguchi et al., 2011) and we observed the same in the WT (Pearson $r=0.75$, $p< 0.001$). Although these correlations were similar in the KO (Pearson $r=0.78$, $p <0.001$) surprisingly the slope of sGluA2 vs. spine intensity linear regression line was smaller compared to the WT (Figure 3d, $p<0.0001$). This suggests altered structure function relationship in the KO with less sGluA2 per spine. Altogether, our results suggest a larger pool of small spines in layer 2/3 pyramidal neurons and altered AMPAR-spine size correlation in the M1 cortex of the fmr1 KO mice.

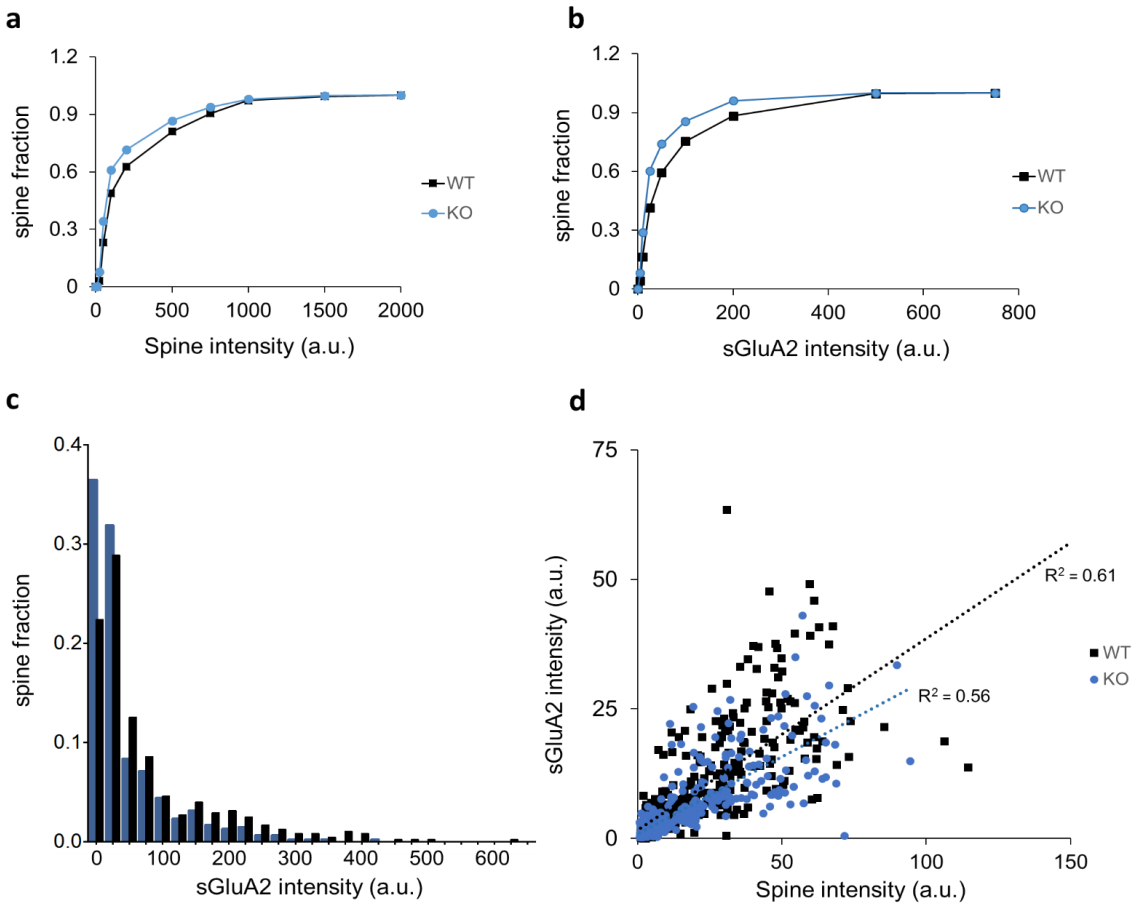

Figure 3: Altered spine size and GluA2 content in the fmr1 KO mice. (a, b) Cumulative frequency plots of spine intensity and sGluA2 intensity at 0 hours. Spine and sGluA2 intensities were smaller in the fmr1 KO mice compared to WT mice (WT: n=480 spines, KO: n=478 spines, Kolmogorov-Smirnov test, p <0.001 for both spine intensity and sGluA2 intensity). **(c)** Frequency histogram of sGluA2 intensity at 0 hours shows that fmr1 KO mice had a larger fraction of spines with low sGluA2. **(d)** Linear correlation between spine intensity and sGluA2 in WT and KO mice (WT: R=0.75, n=480 spines, p<0.001, KO: R=0.78, n=470 spines, p<0.001). The slope of the KO linear regression was significantly lower (WT slope: 3.74 ± 0.12, n=480 spines, KO slope: 3.03 ± 0.14, n=478 spines, Fixed effect regression analysis, p=0.0001).

2.3c *Spine fates and AMPAR levels*

Strength of synaptic tranmission at an excitatory synapse is mediated by the levels of AMPA receptors within the synapse (Matsuzaki et al., 2004). Large synapses have been shown to have stronger synaptic tranmission and to be more stable (A. J. Holtmaat et al.; Matsuzaki et al., 2004). Yet the direct relationship between levels of AMPAR and spine stability has not been investigated *in vivo*. We therefore next investigated whether sGluA2 levels within a spine correlated with spine fates and whether this relationship was altered in the KO mice. A total of 640 and 680 spines were quantified from 19 and 20 dendrites from 4 mice in WT and KO respectively over a period of 10 days measuring synaptic sGluA2 levels, spine intensity levels and noting spine fate. We ranked spines based on sGluA2 levels at Day 0 and divided them into 4 equal sized groups with increasing levels of sGluA2 (Figure 4a). Proportion of stable vs eliminated spines per group was then determined for every mouse and compared across genotypes.

We found that in the WT mice the stability of dendritic spines increased progressively with increasing levels of sGluA2 (Figure 4b). Thus, the spines with lowest amounts of sGluA2 (group 1) had average stability of 36% wheras spines with the highest amount of sGluA2 (group 4) were almost all stable. The remaining spines in groups 2 and 3 had intermediary spine stability of 75% and 92% respectively. Although the trend of increased spine stability with higher sGluA2 levels was maintained in the KO, this relationship was altered with approximately 20% and 26% reduction in stability within groups 2 and 3 respectively (WT vs. KO $p=0.002$ and $p<0.001$ respectively) but no difference in the groups with the lowest and highest sGluA2 levels. Similar results were obtained when the data were clustered into High and Low sGluA2 groups, using a k means partition analysis (Fig S3a). Spines of the High sGluA2 group were highly stable while spines of the Low sGluA2 had decreased stability. Interestingly, in the KO the propotion of spines with high levels of sGluA2 was

significantly smaller which is consistent with the finding of a larger population of smaller spines in the KO (Figure S3b).

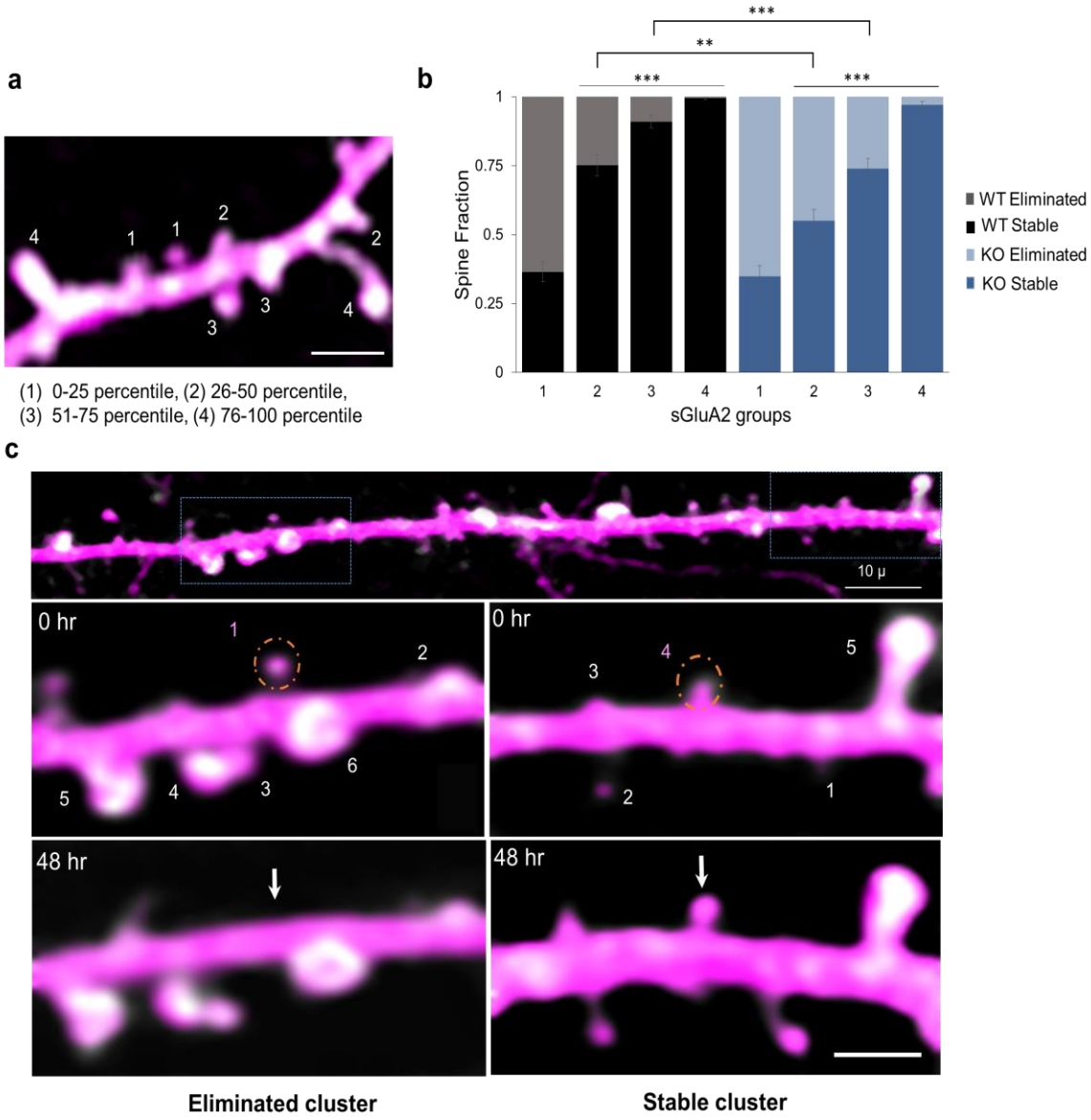

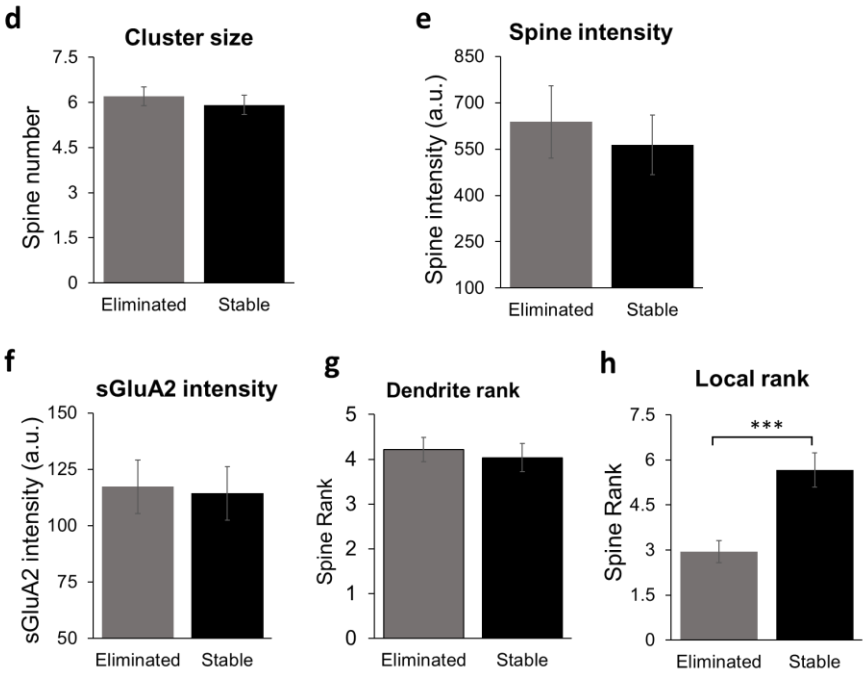

Figure 4: sGluA2 levels predict spine fate. (a) A representative image of a dendritic branch with spines assigned to one of 4 groups based on increasing percentile rank of sGluA2 intensity. scale: 2.5 microns. **(b)** The fraction of stable spines (dark bars) and eliminated spines (light bars) was plotted per sGluA2 level groups in the WT and KO mice. A random effect ANOVA was used to compare within groups and across genotypes. There was a main effect of group, $F(3, 1296)$, $p<0.001$ and genotype, $F(1, 6)$, $p<0.0189$ along with significant interaction, $F(3,1296)$, $p <0.007$. For stable WT spines, 1: 0.36 ± 0.04, 2: 0.75 ± 0.038, 3: 0.92 ± 0.02 and 4: 99.5 ± 00.5, n=5 mice. For stable KO spines, 1: 0.34 ± 0.04, 2: 0.55 ± 0.042, 3: 0.74 ± 0.04, and 4: 0.97 ± 0.01, n=4 mice. Post hoc analysis suggested significantly reduced stability in the KO within groups 2 ($p=0.002$) and 3 ($p<0.001$). **(c)** sGluA2 spine rank within a local cluster determines spine fate. Top: A dendrite containing two clusters centered around similarly sized spines with opposing fate. Scale bar: 10 microns. Below: Magnified images of boxed areas. Numbers represent ranking of spines within a cluster, a 10 micron stretch centered around the target spine (dotted orange circle). The target spines had similar sGluA2 intensity but opposing fates. Note that their local ranking was different with the higher rank spine (right) persisting 48 hr later while the spine with the lower rank (left) disappearing. Scale bar: 2.5 microns. **(d-g)** The properties of clusters of eliminated and persisting target spines were similar. No difference was observed in number of spines per cluster (eliminated: 5.9 ± 0.32 spines, stable: 6.2 ± 0.31 spines, $p>0.05$), target spine intensity intensity (eliminated: 637±116.5 a.u., stable: 562± 96.5 a.u., $p>0.5$), target spine sGluA2 intensity (eliminated: 117.2±11.91 a.u., stable: 114.3±11.92 a.u., $p>0.5$), or in target dendrite rank (eliminated: 4.216±0.27rank, stable: 4.06±0.31 rank, $p>0.5$). **(h)** Mean cluster rank of similar sGluA2 containing spines was significantly higher in stable spines (stable: 5.66±0.57, eliminated: 2.95±0.36, $p<0.001$). Eliminated target spines (or clusters) n=30, Stable target spines (or clusters) n=34. unpaired t.tests, All data represented as Mean ± SEM**.**

Although spines with more sGluA2 were generally more stable we observed many spines with very similar levels of sGluA2 showing opposite fates. Since spines are not uniformly distributed along the dendrite and local synaptic activity (Oh, Parajuli, & Zito, 2015) and synaptic competition (Fonseca, Nagerl, & Bonhoeffer, 2006) for resources are linked to shaping structural changes we hypothesized that the local ranking of a spine within its immediate vicinity would be a stronger determinant of spine fate than global dendrite ranking. To test this hypothesis, we identified spines of similar sGluA2 levels but opposing fates which were at least 10 microns apart (Figure 4c). We then computed the rank of the target spine within the 10 micron dendrite stretch surrounding it. We quantified 64 spines from 12 dendrites and identified 34 stable and 30 eliminated spines. The properties of clusters of eliminated and persisting target spines were similar; no difference was observed in number of spines per cluster, in target spine intensity, target spine sGluA2 intensity or its overall dendrite rank (Figure 4d-f). Yet, the average local rank of stable spines was 93% higher than those of the eliminated spines (Figure 4h, $p<0.001$). This relationship was however siginficant only within spines of intermediate sizes ($p<0.001$) and not true for the smallest spines (bottom 25% of spines) which are generally unstable (Figure S3c). Our results suggest that local sGluA2 level rank and thus relative strength of synapses within their local environment influences spine stability.

2.3d *sGluA2 dynamics within stable spines*

Synaptic transmission at dendritic spines is mediated through AMPAR. Although, synapses in the brain are continuously modified by experience, the dynamic properties of synaptic AMPAR levels over days *in vivo* are not known. To determine AMPAR dynamics we identified stable spines (350 spines per genotype) and quantified sGluA2 and spine intensity. We observed that although total synaptic sGluA2 content within a dendrite did not vary over days (Figure S4a), sGluA2 levels within individual stable spines fluctuated from one imaging day to another in both WT and KO mice (Figure 5a). We categorized spines based on sGluA2 intensity changes over days (Figure 5b). In both WT and KO spines only 10% of spines showed no change (defined as change of <30%) (WT and KO: $p<0.05$ for all comparision) over 10 days (Figure 5c). In the WT majority of spines had a change in sGluA2 with almost equal proportion of spines showing persistent, transient or recurrent changes (Figure 5c). On average, stable WT spines had a gradual accumuation of sGluA2 of 20% by 240 hours (Figure 5d, $p=0.015$). Interestingly, in the KO the percentage of both transient and recurrent spines was larger than persistent spines (persistent vs. recurrent $p=0.008$, persistent vs. transient $p=0.002$) suggesting more dynamic sGluA2 in spines. Similar to the WT, stable spines in the KO had an increase of sGluA2 of 20% in 240 hours (Figure 5d, KO: $p=0.01$). Next, to determine if a specific population of spines drove the increases in sGluA2, we grouped spines based on levels of sGluA2 (Figure 5e). We found that most of the increases within the stable population of spines in both WT and KO were driven by small spines that contained the lowest levels of sGluA2, which grew over time (Figure 5e, WT and KO $p<0.05$ all comparisons). Unlike sGluA2 changes, average spine intensity changes were smaller over 240 hours and were not significantly different from baseline (Figure S4b). Thus, we observed that majority of spines had dynamic AMPAR levels with the KO having a higher percentage of spines with

more sGluA2 dynamic events over days. On average, wheras average spine intensity levels did not change over time, both genotypes had a modest increase in sGluA2 levels in the persistent popluation of spines over 10 days which was mainly driven by small spines growing larger.

a

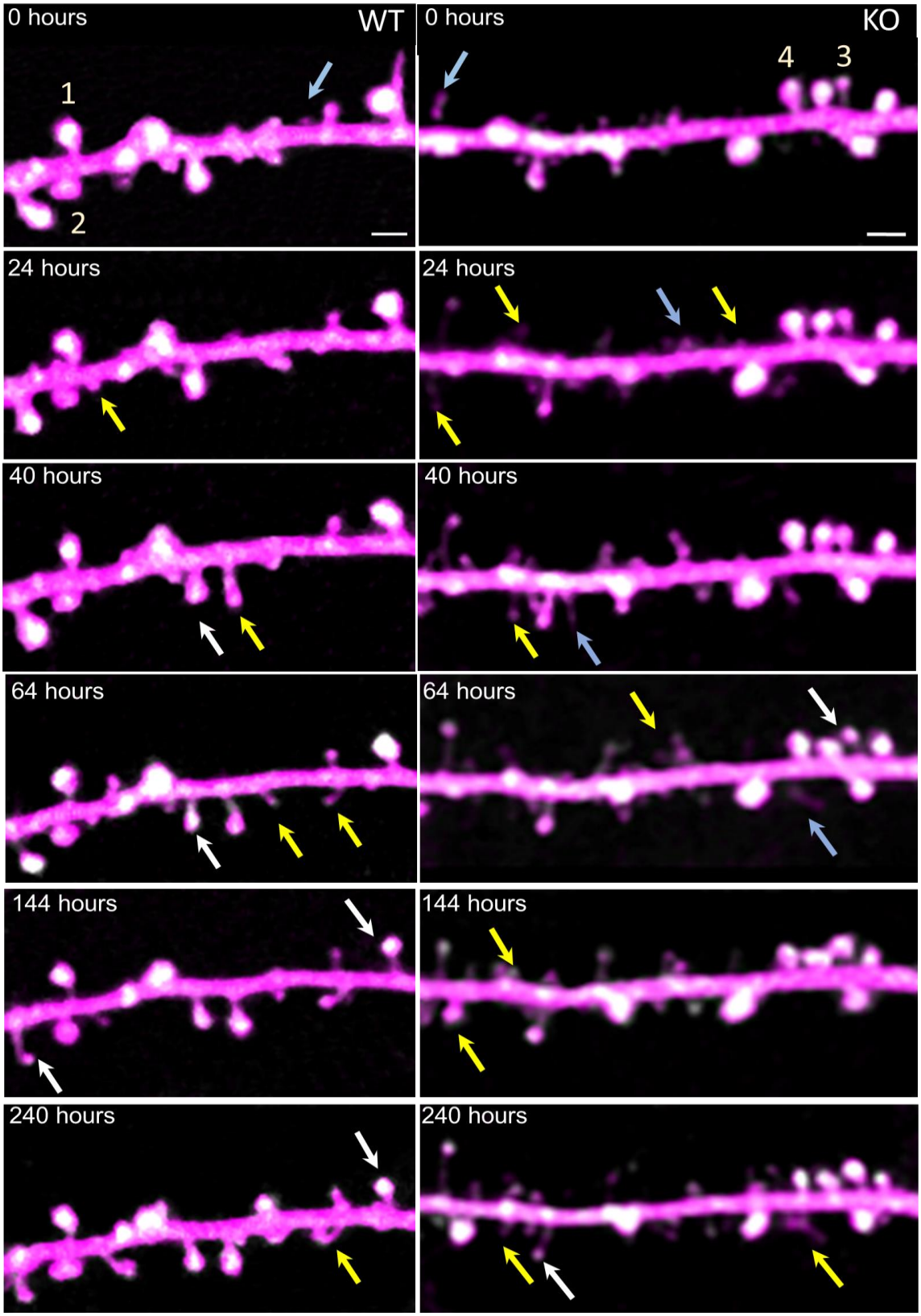
0 hours
WT
1
2
0 hours
KO
4
3
24 hours
24 hours
40 hours
40 hours
64 hours
64 hours
144 hours
144 hours
240 hours
240 hours

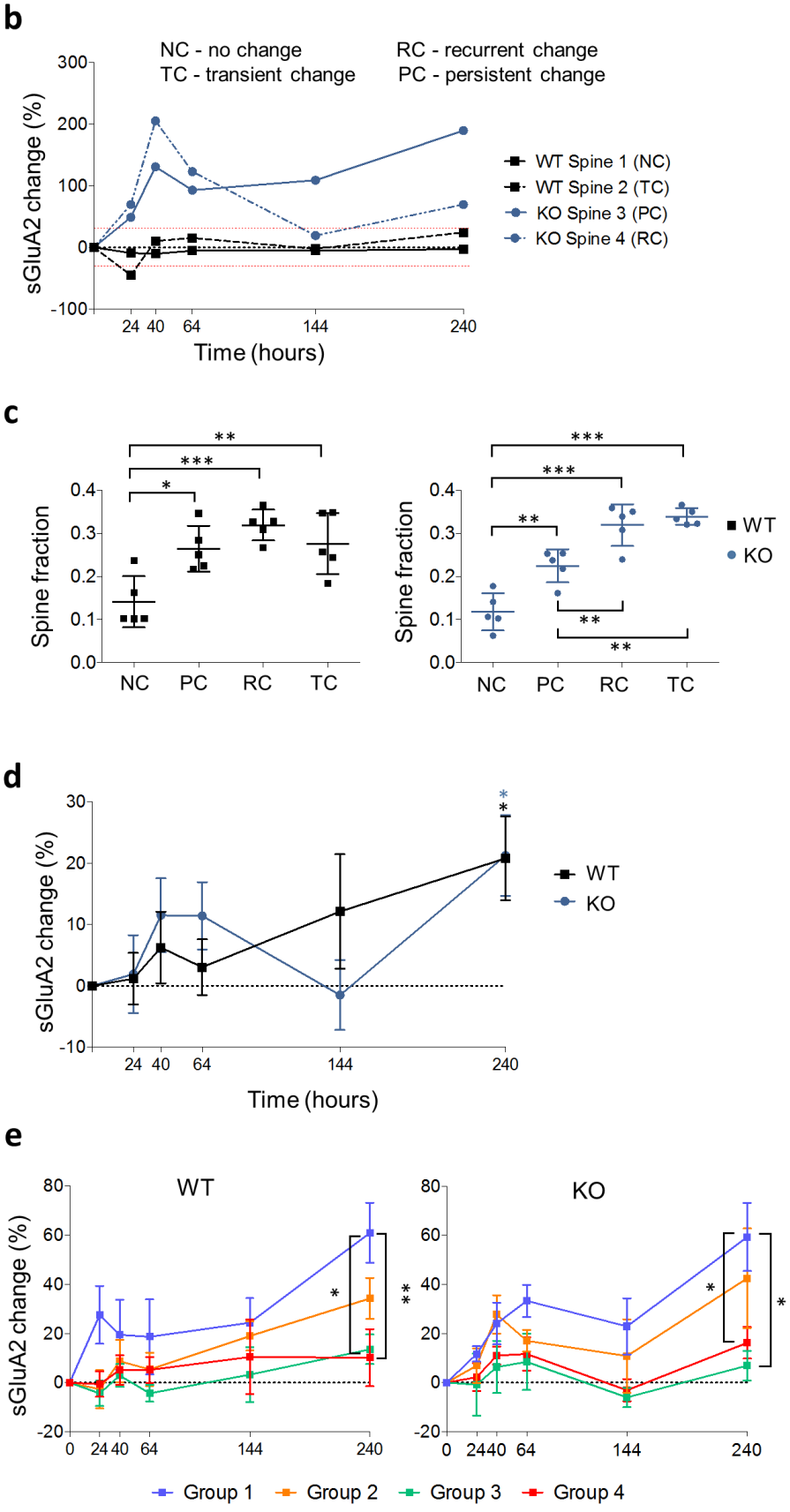
b
NC - no change
TC - transient change
RC - recurrent change
PC - persistent change
sGluA2 change (%)
Time (hours)
WT Spine 1 (NC)
WT Spine 2 (TC)
KO Spine 3 (PC)
KO Spine 4 (RC)
c
Spine fraction
NC
PC
RC
TC
WT
KO
d
sGluA2 change (%)
Time (hours)
WT
KO
e
WT
KO
sGluA2 change (%)
Group 1
Group 2
Group 3
Group 4

Figure 5: sGluA2 is dynamic within stable spines. (a) Representative time-lapse *in vivo* 2PLSM images of apical dendrites of layer 2/3 pyramidal neurons from WT and KO mice. Note the increased spine formation (yellow arrows) spine elimination (blue arrows) in the KO. White arrows point to spines which show fluctuations in sGluA2. Examples of spines exhibiting different types of sGluA2 dynamics are marked (1-no change, 2-transeint change, 3- persistent change and 4-recurrent change (scale bar: 2 microns). **(b)** Traces of percentage change in sGluA2 intensity of spines 1-4 representing different sGluA2 dynamic groups. Red dotted lines indicate cut offs used for grouping (±30%). **(c)** Fraction of spines belonging to the four sGluA2 dynamic groups (NC- no change, PR-persistent change, RC- recurrent change, TC- Transient change) from WT (black) and KO (blue) mice were plotted. A one way ANOVA was performed to compare percentage of groups within WT and KO mice separately with Bonferroni method for post hoc multiple comparisons. In WT mice the fraction of No change was significantly lesser than Persistent, Recurrent or Transient change groups (No change: 0.14±0.02, Persistent: 0.26±0.02, Recurrent: 0.31±0.02, Transient: 0.27±0.03, n=5 mice, One way ANOVA, No change vs. Persistent p=0.019, No change vs. Recurrent p=0.008, No change vs. Transient p=0.009). There was no difference between Persistent, Recurrent and Transient change spines. In KO mice No change and Persistent spines were also significantly lesser than Recurrent or Transient change groups (No change: 0.12±0.02, Persistent change: 0.26±0.024, Recurrent change: 0.32±0.016, Transient change: 0.27±0.03, n=5 mice, Oneway ANOVA. No change vs. Persistent p=0.0031, No change vs. Recurrent p<0.0001, No change vs. Transient p<0.0001). Howerver in the KO the Persistent group was smaller than both Recurrent and Tranasient spines (Persistent vs. Recurrent p=0.008, Persistent vs. Transient p=0.0017). Data presented as Mean±SEM. **(d)** Percent change of GluA2 and spine intensity (WT- Black lines, KO- Blue lines) for every time point was calculated by comparing intensity to 0 hour intensity and plotted. A two way repeated measure ANOVA was used to compare percentage change within the time points and across genotypes for both sGluA2 and spine intensity. For sGluA2 there was a main effect for time $F(5,40)=5.224$, $p=0.0009$ but not for genotype $F(1,8)=0.0015$,$p>0.05$ and no interaction $F(5,40)=1.32$, $p>0.05$. Post hoc analysis with Bonferroni comparison identified significant increases in sGluA2 intensity at 240 hours in the WT (20.2±5.3%, n=5 mice, p=0.014) and in the KO (20.2±5.2%, n=5 mice, p=0.012). **(e)** Mean percentage change of sGluA2 intensity for each sGluA2 intensity group (group 4- red lines, group 3- green lines, group 2-orange lines, group 1-blue lines). A one way ANOVA comparing group 4 percentage change at day 10 to all other groups for both WT and KO mice with Bonferroni method for post hoc multiple comparisons was performed. In both WT and KO mice group 4 percentage change was significantly different from group 1 and 2. (WT: Group 1: 10.1± 11.7%, Group 2: 13.5±6.03%, Group 3: 34.3±8.36%, Group 4: 61±12.3%, n =5 mice, One way ANOVA, p= 0.0068 for Group 4 vs Group 1, p = 0.013 Group 4 vs Group 2, KO: Group 1: 8.47± 4.3%, Group 2: 4.98± 6.5%, Group 3: 36.74± 21.6%, Group 4- 59.3± 13.87%, n = 5 mice, One way ANOVA, p<0.05 for Group 4 vs Group 1 and Group 2. Data presented as Mean ± S.E.M

2.3e *sGluA2 in newly formed and eliminated spines*

Finally we characterized AMPAR and spine relationship in newly formed and eliminated spine populations in the WT and KO mice. First to characterize newly formed spines, we followed spines formed within the first 40 hours of the experiment (Figure 6). Although the fmr1 KO has increased rate of new spine formation (Figure 2b), the overall stability of the newly formed strucutures was similar between the WT and the KO (Figure S5a). As expected soon after formation, the majority of newly formed spines were small and occupied the lowest ranks within their dendrites in both WT and KO (Figure S5b). Unlike in the preexising spine population (Figure 4b), spine stability of newly formed spines did not change with increasing initial levels of sGluA2 in either genotype (Figure S5c), suggesting that a certain threshold level of sGluA2 has to be reached for it to be a determinant of spine stabilization. Within 16-24 hours after formation, sGluA2 levels increased by 49% and 43% in WT and KO respectively and continued to increase to 109% in WT ($p=0.02$) and 91% in KO ($p=0.04$) by 200 hours post formation. We didn't observe a difference between the genotypes in sGluA2 accumulation in newly formed spines (Figure 6a-c). Although the size of the spines also increased by about 40% in both WT and KO after 200 hours, these changes did not reach significance (Figure 6c). Thus newly formed spines are small and have low levels of sGluA2 soon after formation. Additionally, there is a gradual increase of AMPAR in both WT and KO with sGluA2 increases outpacing the spine size changes.

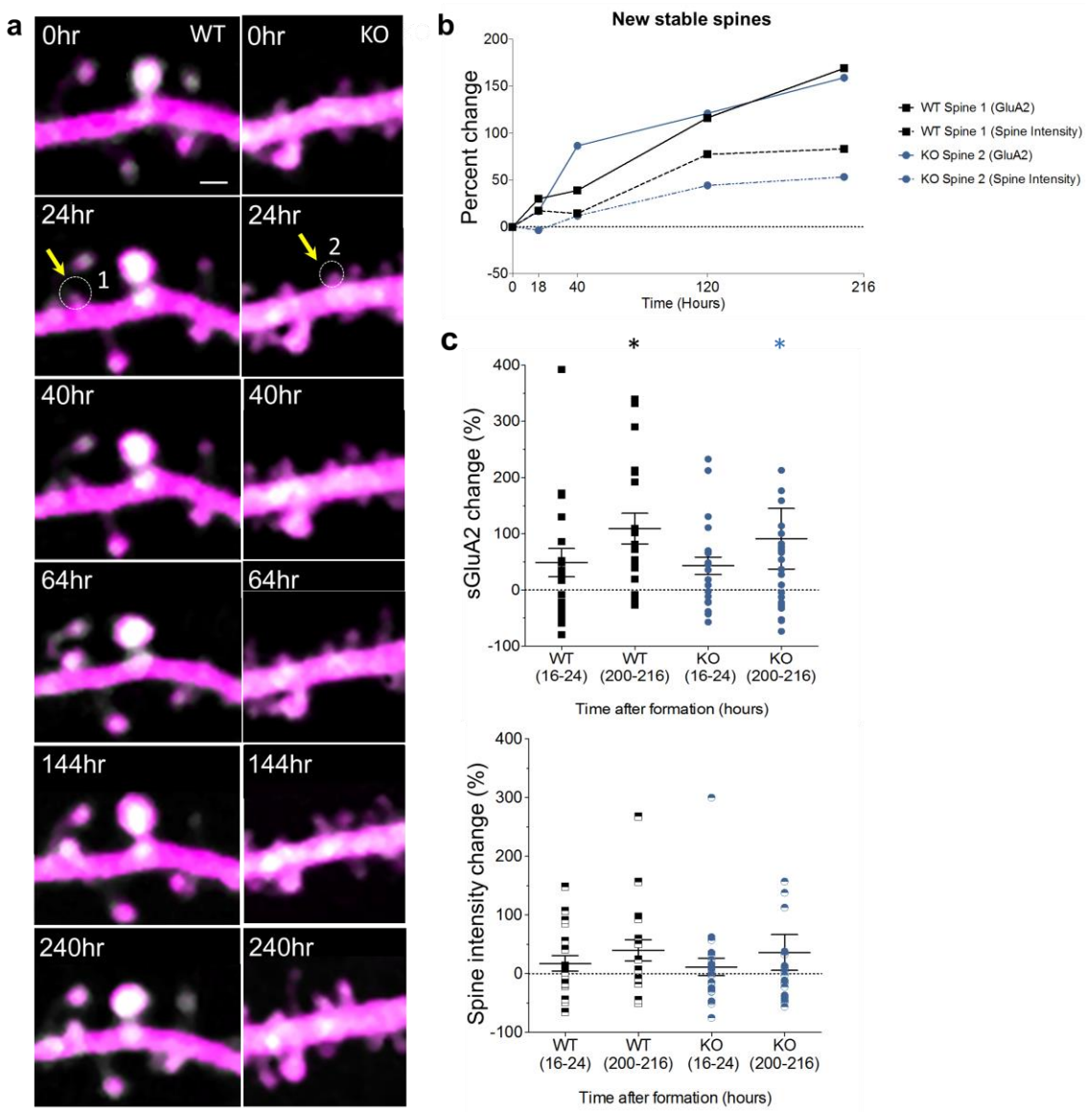

Figure 6: Newly formed spines gradually accumulated sGluA2 over time. (a) Representative time-lapse 2PLSM images of apical dendrites from WT and KO mice showing formation of new spine (marked in white dotted circle) in WT (spine 1) and KO (spine 2) with corresponding sGluA2 and spine intensity traces shown in (**b)**. Note the gradual accumulation of sGluA2 within these spines. Scale Bar: 1 micron **(c)** Percentage change of sGluA2 and spine intensity in stable new spines stable. A two-way repeated measure ANOVA was used to compare percentage change within the time points and across genotypes for both sGluA2 and spine intensity separately. For sGluA2 there was a main effect of time ($F(2, 76)=6.08$, $p=0.004$) but not of genotype ($F(1, 38)=0.1264$, $p=0.72$) and no interaction ($F(2, 76)=0.0399$, $p=0.96$). Post hoc analysis with Bonferroni correction identified increased sGluA2 at 200-216 hours in both WT and KO (WT sGluA2: 16-24 hrs 48.71±25.21%, $p=0.4$, 200-2016 hrs 109±27.31%, $p=0.02$, $n=19$ spines, KO sGluA2: 16-24 hrs 43.19±15.58, $p=0.53$, 200-2016 hrs 91.23±53.81 $p=0.04$, $n=22$ spines). Percentage change in spine intensity showed no effect for time $F(2,80)=2.66$ $p=0.07$,

genotype $F(1,40)=0.045$ $p=0.83$ and no interaction $F(2, 80)=0.0167$, $p=0.98$. Data presented as Mean % ± SEM

Lastly, to study eliminated spines, we pooled changes in sGluA2 and spine intensity of structures eliminated between 40 and 64 hours of the experiment (Figure 7a-d). We observed a significant decrease (Figure 7b,d) in sGluA2 (-28%, $p<0.001$) and spine intensity (-17, $p<0.001$ in WT mice in the imaging session prior to elimination (16-24 hours) that was not observed in the stable spines of the same dendrites (Figure 7c). Interestingly, in the KO for both sGluA2 (-38%, $p<0.001$) and spine intensity (-38.4%, $p<0.001$) the decreases were significantly sharper in the KO ($p=0.02$, $p<0.001$ respectively) suggesting that the spine complex was being disassembled more rapidly in the KO. Thus we conclude that in both WT and KO spines shrink and loose AMPAR before elimination and this decrease is steeper in the fmr1 KO spines.

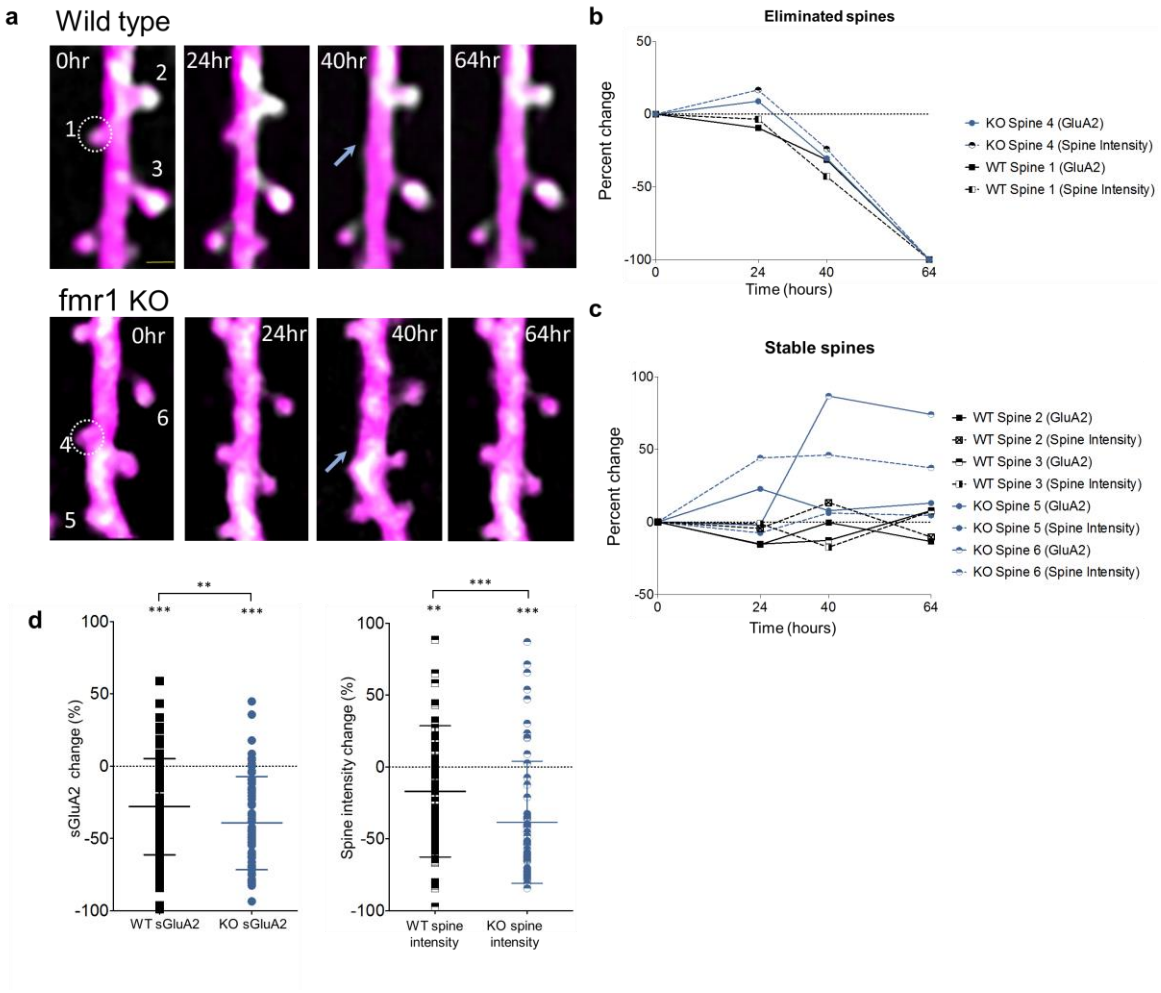

Figure 7: Eliminated spines have decrease in sGluA2 immediately before elimination. (a) Representative images of eliminated spines (1 and 4, circled) in WT and KO mice. **(b)** Individual traces of sGluA2 and spine intensity of eliminated spines 1 and 4. Note the gradual loss of sGluA2 and spine size before elimination in both genotypes. **(c)** Spines 2, 3 and 5 show relatively little change in sGluA2 or spine intensity while spine 6 shows an increase in both sGluA2 and spine intensity. **(d)** Percent change of sGluA2 and spine intensity of eliminated spines 16-24 hours prior to elimination was plotted for both KO and WT. A two way ANOVA was used to compare percentage change between the last two time points before elimination and across genotype for sGluA2 and spine intensity separately. There was a main effect of time, genotype and significant interaction for both sGluA2 (Time: $F(1,331)= 2973$ $p <0.0001$, Genotype: $F(1,331)=5.387$, $p=0.021$, Interaction $F(1.331)=5387$, $p=0.021$, 2 way ANOVA, n=91 spines) and spine intensity (Time: $F(1,331)=1479$, $p=0.001$, Genotype $F(1,331)=10.48$, $p<0.001$, Interaction $F(1,331)=10.48$, 2way ANOVA, n=91 spines). Post hoc analysis with Bonferroni correction identified significant decreases in both sGluA2 and spine intensity in KO mice (sGluA2: WT -28.01 ± 3.46%, KO: sGluA2 -39.1 ± 4.19% (WT vs. KO) $p=0.013$, Spine intensity: WT -16.94± 4.6%, KO -38.44± 5.53% (WT vs. KO) $p<0.001$, n=91 spines). Data presented as Mean % ± SEM

2.4 Discussion

Here we report the first *in vivo* study that quantified changes in AMPAR in dendritic spines over multiple days. Using this approach, we characterized the relationship between AMPAR and spine stability in layer 2/3 pyramidal neurons in both WT and fmr1 KO mice. We found that sGluA2 levels within spines correlated with synaptic fate, with the largest spines being extremely stable (Figure 4a,b). Consistent with this correlation, before elimination spines both shrunk in size and lost sGluA2 (Figure 7a-d) wheras stable new spines gradually accumulated sGluA2 (Figure 6a-c). sGluA2 content within persistent spines was dynamic (Figure 5a-c) with majority of spines showing at least one dynamic event during the 10 day imaging period. Imaging of sGluA2 in spines of the fmr1 KO mice revealed several deficits. Dendritic spines in the KO were smaller (Figure 3a), denser (Figure 2a) and more dynamic (Figure 2b-d) as well as had reduced sGluA2 to spine size correlation (Figure 3d). In the KO, a greater proportion of spines exhibited the most dynamic behaviors (Figure 5c). Finally, before elimination, spines in the KO shrunk and lost sGluA2 faster as compared to the WT (Figure 7d). In summary, we find that while levels of AMPAR within spines are dynamic, they are predicitve of spine fates. Moreover, loss of FMRP impacts sGluA2 content in spines, thus affecting their dynamics.

2.4a *AMPAR and spine dynamics*

AMPAR are glutamate-gated cation channels that regulate majority of fast synaptic transmission in the brain (Anggono & Huganir, 2012). AMPAR's are heteromeric tetramers composed of multiple subunits GluA1-4 (Anggono & Huganir, 2012). Since majority of AMPAR are of GluA1-GluA2 heteromers (W. Lu et al., 2009), sGluA2 within spines is a good measure of functional synaptic AMPAR content (Makino & Malinow, 2011; Zhang et al., 2015). As long-term dynamic correlation between AMPAR and spine behavior has not been previously investigated *in vivo*, this was the primary goal of the study. Overexpression of sGluA2 construct *in vivo* did not alter synaptic properties such as

density and turnover rates (Ma et al., 2016) in apical dendrites of Layer 2/3 pyramidal neurons (Figure S2d, Figure 2b-d). Similarly, as expected from a postsynpatic protein sGluA2 expression was punctate and expressed primarily in dendrites with substantial localization in dendritic spines and no expression in axonal boutons (Figure S2a). Lack of aberant expression of sGluA2, suggests that synaptic incorporation of AMPAR is a tightly regulated process (Kessels, Kopec, Klein, & Malinow, 2009). All spines imaged in the study, including thin filopodial looking spines expressed some amount of sGluA2 (Figure S2b), suggesting that silent synapses may not be present at this stage. Levels of synaptic AMPAR determine the strength of a synapse (Matsuzaki et al., 2001) and have been associated with synaptic stability (Grutzendler, Kasthuri, & Gan, 2002; A. J. Holtmaat et al., 2005; Trachtenberg et al., 2002). Consistent with this, we observe progressive stability of spines with increasing AMPAR levels (Figure 4b). Large spines with highest levels of AMPAR were almost always persistent over 10 days wheras spines with least AMPAR had only 35% stability (Figure 4b). Morover, we observed that the relative AMPAR levels within the local dendritic synaptic cluster correlated with synaptic stability. Similar sGluA2 containing spines were more likely to be stabilized when surrounded by lower vs. higher sGluA2 containing spines (Figure 4c, h). Unlike previous *in vitro* studies that linked neigbouring synapse activity with synaptic fate (Fonseca, Nagerl, Morris, & Bonhoeffer, 2004; Oh et al., 2015), here we observed how local rank based on synaptic AMPAR content alone correlates with spine fate. This suggests a potential competition between synapses for local stabilizing factors and likely involves similar biochemical signalling molecules and pathways regulating spatial organiztion of local dendritic microcircuits (Nishiyama & Yasuda, 2015). We also observed spines hours prior to elimination to both lose AMPAR and shrink (Figure 7a-d). This is consistent with results of activity dependent structural plasticity where induction of LTD in slices resulted in shrinkage and even elimination of spines (Bastrikova et al., 2008; Fonseca et al., 2004; Zhou, Homma, & Poo,

2004). In contrast new spines which survived over many days, gradually accumulated AMPAR to about 100% over 200 hours (Figure 6). Surprisingly, spine size did not keep up with AMPAR changes and only increased by 40% (Figure 6). This breakdown in AMPAR and spine size correlation was also seen in persistent spines which accumulated AMPAR over time but did not have a similar increase in spine size. The increase in AMPAR in the persistent spines was mainly driven by small spines growing over time. The small spines could have been recently formed spines which then had similar profiles as newly formed spines suggesting that functional changes precede the structural change in growing spines. Supporting this notion in a recent *in vivo* study using whisker stimulation to stimulate spines, there was a similar increase in sGluA1 but not spine size (Zhang et al., 2015). This is inconsistent with *in vitro* studies where spine size usually precedes AMPAR increases (Kopec, Real, Kessels, & Malinow, 2007) suggesting a different spine behavior *in vivo*. Lastly, we also observed AMPAR levels to be dynamic over days (Figure 5c). Almost 90% of spines showed a 30% increase or decrease of AMPAR over time with nearly a third of spines showing multiple events (Figure 5c). Although surprising since decreases in synaptic strength is thought to be detrimental to spine fate, this result is consistent with more recent in vivo studies where variable synaptic properties were observed even in stable spine populations (Cane et al., 2014; Villa et al., 2016). Also since many persistent spines show large decreases in sGluA2 (Figure 5a) but still do not get eliminated, it might suggest that it's not the percentage decrease that determines spine fate but rather a threshold level beneath which a spine is eliminated.

2.4b *Fragile X spine and AMPAR dynamics*

Synaptic deficits in patients with FXS have been described with presence of dense dendrites and long immature spines ((S.A. Irwin et al., 2000). Spine deficits in Fmr1 KO mice, an animal model of FXS, have varied depending on brain region, age and population

of neurons investigated (C. X. He & Portera-Cailliau, 2013). In this study we observed in layer 2/3 neurons of the motor cortex higher turnover rates (Figures 2b-d), increased spine density (Figures 2a) and smaller spines (Figure 3a) in the KO. High turnover rates in the KO have been described previously in several *in vivo* studies (Cruz-Martin et al., 2010; Nagaoka et al., 2016; Padmashri et al., 2013; Pan et al., 2010) at different ages and population of neurons and our results are consistent with these findings. Reports of higher spine densities in the KO (Dolen et al., 2007; S. A. Irwin et al., 2001) however, are more variable. In this study we find a small (11%) but significant increase in spine density (Figure 2a). Morover, since spine formation is higher than elimination in these population of neurons (Formation 40% vs Elimination 37% over 10 days) it would be expected to observe higher density. We also observed a significant population of small spines in the KO mice (Figure 3a-c). Smaller spines in the KO are reminescent of the human studies (Hinton et al., 1991; S. A. Irwin et al., 2001; Rudelli et al., 1985) and thought to represent a more immature phenotype of spines. Smaller spines are also more dynamic (Figure 4b) and this supports our data of higher turnover rate in the KO. Unexpectidly, spine-AMPAR correlation was altered in the KO with less AMPAR per spine (Figure 3d). Previous studies in the KO have not identified deficits in synaptic AMPAR content or function under basal conditions in the cortex (Gocel & Larson, 2012; H. G. Martin et al., 2016; Padmashri et al., 2013), although reduced AMPAR have been observed in the amygdala (Suvrathan et al., 2010). Since, our study focused on specific subpopulation of synapses in apical dendrities of layer 2/3 neurons, these may represent a previously unappreciated defict in the KO mouse and further studies are required.

Similar to the WT, spine stability increased with higher sGluA2 content in the KO (Figure 4b) with the spines with the least and the most sGluA2 having similar stability to the WT. However, consistent with altered distribution of spine sizes, the interemediate percentile groups of spines had reduced stability in the KO (Figure 4b). Interestingly, the KO mice

had exaggerated decreases in both AMPAR and spine sizes before elimination (Figure 7d). Exaggerated internalization of AMPAR through elevated LTD (Bear et al., 2004; Huber et al., 2002) has been described in the KO and since LTD has been linked to synapse elimination (Bastrikova et al., 2008; Nagerl et al., 2004) it may explain the enhanced elimination in the KO. It is important to point out that, most elimination events described *in vitro* were on the time scale of minutes wheras in this study changes over hours are observed suggesting protracted AMPAR decreases before elimination *in vivo*. Unlike elimination, newly formed spines had similar stability, as well as AMPAR and spine changes (Figure 6a-d) as the WT , suggesting loss of FMRP does not affect growth and stabilization of synapses. This is consistent with previous studies that demonstrate that stability of new spines formed following experience is unaffected in the KO (Pan et al., 2010; Reiner & Dunaevsky, 2015). Interestingly, a larger percentage of KO spines showed more dynamic events over days suggesting less stable synaptic strength in KO which further could impact the function of neuronal circuits in FXS.

2.5 Supplementary figures

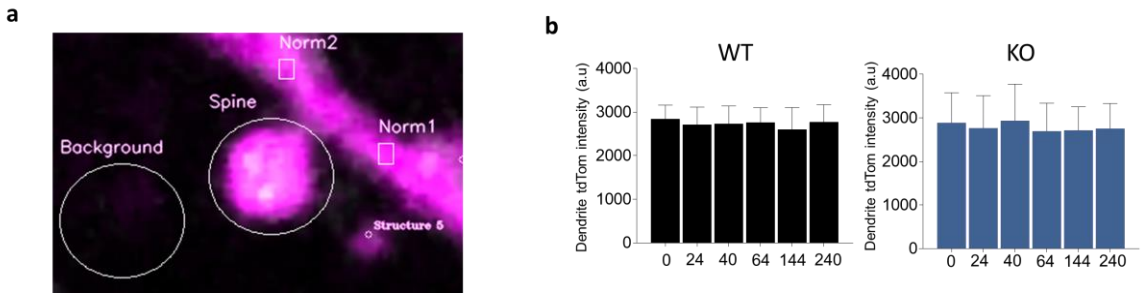

Figure S1: Experimental approach to measure sGluA2 and spine intensity.
(a) Images were stable over the entire experimental duration with no evidence of bleaching. **(b)** tdTom intensity values were calculated for all dendrites (WT=29 dendrites, KO = 27 dendrites). One way ANOVA was performed comparing total intensity across time points to 0 hours within WT and KO mice separately with Bonferroni method for post hoc multiple comparisons. In both WT and KO, there was no significant difference across all time points (WT: 0hr 2839±144,24hr 2713±178,40hr 2730±182,64hr 2599±226,240hr 2768±180,n=5mice, Oneway ANOVA, p >0.05 for all comparisons, KO: 0hr 2899±308,24hr 2762±334,40hr 2930±377,64hr 2693±288,144hr 2713±241,240hr 2752±259)

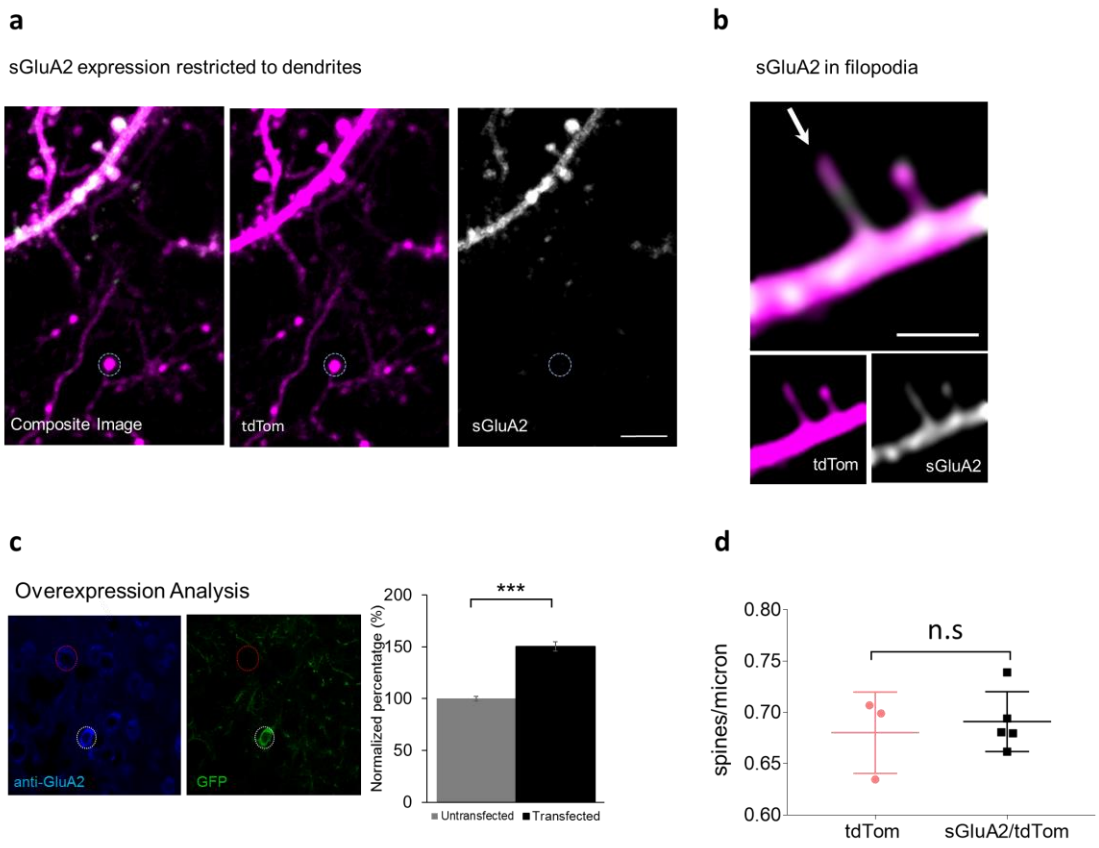

Figure S2: sGluA2 overexpression does not alter spine density or GluA2 expression profile. (a) GluA2 is overexpressed by about 50% in transfected neurons. Coronal sections of electroporated wild type animals were immunostained for GluA2 and transfected cells (White circle right panel) were identified by presence of GFP within the cell body. Levels of GluA2 was measured by applying an ROI over the cell body and measuring signal intensity which was then compared between transfected and non-transfected cells (red circles). Mean intensity is represented as a percent intensity of non-transfected cells. Untransfected cells 100 ± 0% , n= 53 cells; Transfected cell intensity 150 ± 4.46%, n = 53 cells, t.test,$p < 0.001$.**(b)** sGluA2 overexpression did not cause aberrant localization of sGluA2. sGluA2 was restricted to dendrites and no expression was seen in axonal boutons. Note the axonal bouton marked by a circle with no expression of sGluA2. Scale bar: 5 microns **(c)** sGluA2 expression is seen even in thin immature filapodia like structures (arrow). Scale bar: 2 microns **(d)** sGluA2 overexpression did not alter spine density. Dendrites of sGluA2\tdTom transfected WT mice had similar spine density when compared with WT mice transfected with only tdTom (tdTom: 0.68±0.022 spine/micron n = 3 mice; tdTom/GluA2 0.69 ± 0.013 spines/micron, n = 5 mice, unpaired t.test p = 0.67, scale bar: 10 microns)

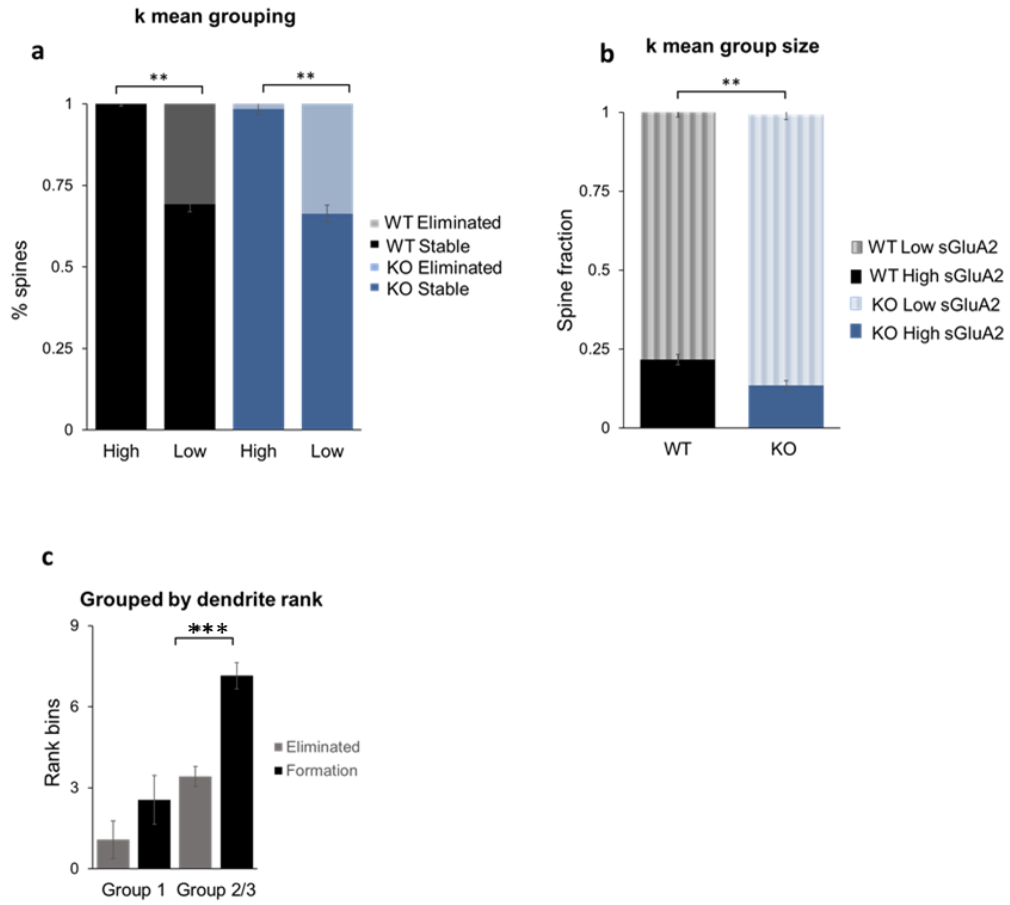

Figure S3: sGluA2 content predicts spine fate in k-means analysis and local rank predicts fate for all but the smallest spines. (a) Spines were clustered using the k-means test into the ”High sGluA2” or “Low sGluA2” groups and fraction of stable (dark bars) and eliminated spines (light bars) were calculated for each group. A random effect ANOVA was used to compare fraction stable spines within groups and across genotypes. There was a main effect of groups $F(1,1307 = 37.34$, $p<0.001$) but not of genotype $F(1, 6)=2.44$, $p=0.17$ and no interaction $F(1,1307)=0.75$, $p=0.39$ (WT: High sGluA2 99.3±0.01 %, Low GluA2 0.69± 0.02 spines, KO: High sGluA2 0.97±0.023 spines, Low sGluA2 0.60±0.02 spines, n=4 mice per group). **(b)** Significantly smaller fraction of spines classified as High sGluA2 were found in the KO (WT: High 0.21± 0.074, Low 0.79±0.074, KO: High 0.14 ± 0.07, Low 0.85±0.07, n=4 mice per group, unpaired t.test, $p=0.002$)**. (c)** Similar sGluA2 level spines were further grouped into two groups with Group 1 containing spines which ranked at bottom quarter of their respective dendrite and the remaining spines of intermediate size ranked into group 2/3. A similar rank comparison was performed as Figure 4F. The main effect of enhanced rank in stable spines was mainly seen in spines of Group 2-3 and not for Group 1 (Group 1: eliminated spines 10.76 ± 7 rank, n=7 spines, stable spines 25.54±9 rank, n=11 spines, Group 2/3: eliminated spines 34.19±3.67 rank, n=23 spines, stable spines 71.48±5 rank, n=23 spines, multiple t.test, group 1 eliminated vs. stable $p>0.05$, group 2/3 eliminated vs. stable $p<0.001$)

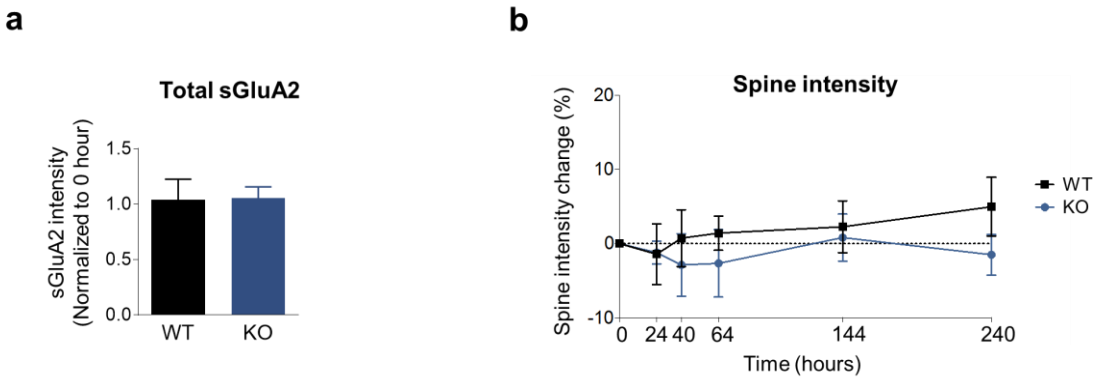

Figure S4: total sGluA2 levels and mean spine intensity do not change over time. **(a)**Total GluA2 content with spines in a dendrite are not different between 0 and 240 hours and across genotypes (WT: 240hr 1.03±0.083, multiple t.test, $p > 0.05$, $n = 5$ mice, KO: 240hr: 1.05±0.045, multiple t.test $p > 0.05$, $n = 5$ mice) **(b)** Percent change of spine intensity (WT- Black lines, KO- Blue lines) for every time point was calculated by comparing intensity to 0hour intensity and plotted. A two way repeated measure ANOVA comparing percentage change within time points and across genotypes had no effect of time $F(5,20)=0.54$, $p = 0.7$ and genotype $F(1,4)$, $p =0.49$. Data presented as Mean±SEM.

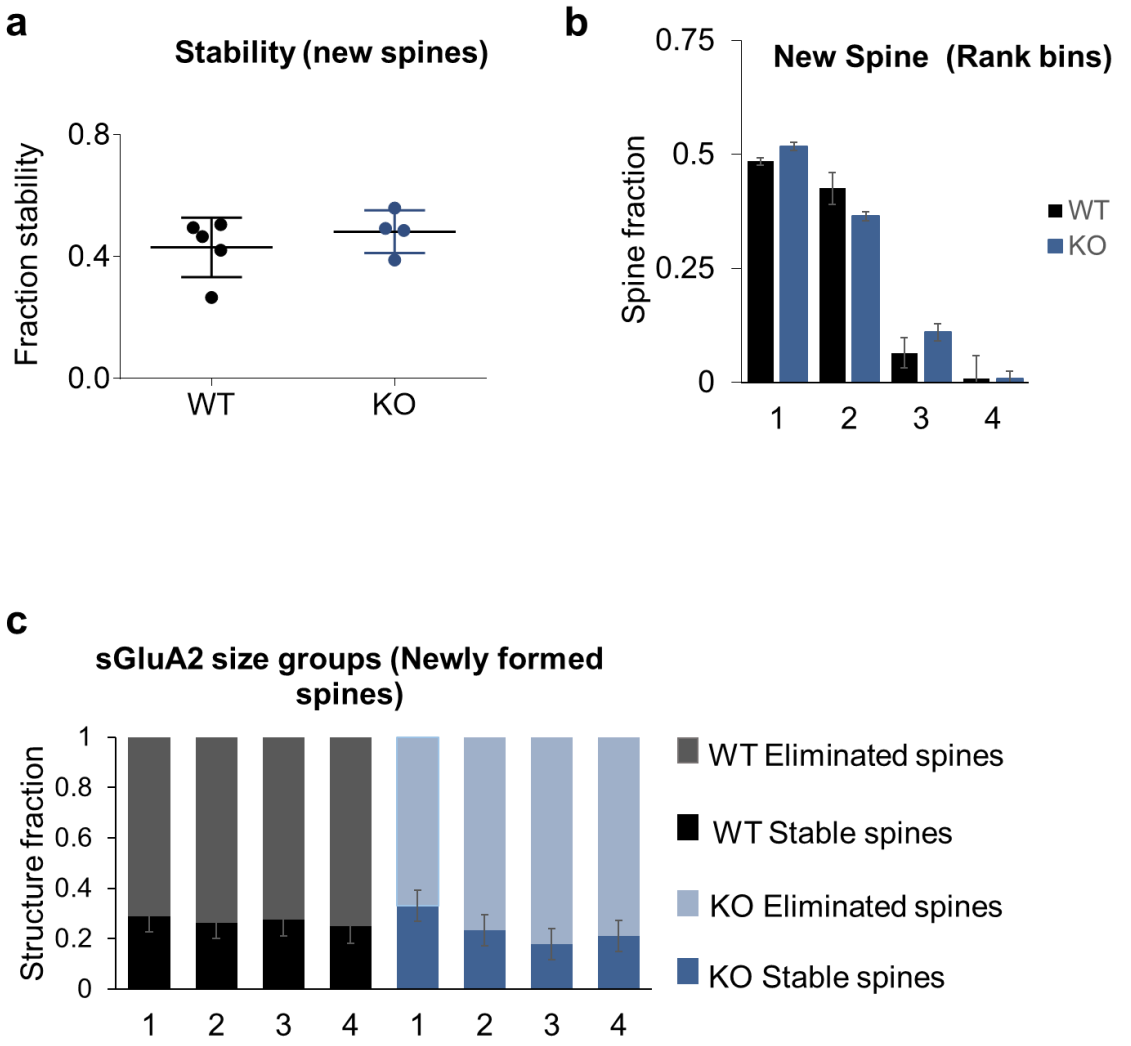

Figure S5 New spines are small and initial sGluA2 content does not predict spine fate with no difference across genotypes. (**a**) Overall stability of newly formed spines between WT and KO was not different (WT: 0.4314 ± 0.04369, n=5 mice ,KO: 0.4824 ± 0.0351, n=4 mice, t.test, p >0.05) **(b)** Majority of newly formed spines are small and appear at the lower end of the dendrite ranks (90% of spines occur in rank 1 and 2) in both WT and KO. Ranks were calculated on newly spines formed at 24 and 40 hours irrespective of future fate. (1: WT Group 1: 0.27±0.074, Group 2: 0.14, Group 3, Group 4 and KO: Group 1: 0.33±0.08, Group 2: 0.267±0.07, Group 3: 0.323±0.07, Group 4: 0.24±0.07, n = 5 mice) **(c)** Newly formed spines were arranged in an ascending order of sGluA2 content and were grouped into 4 groups with the highest group containing most sGluA2. To test within groups and across genotypes we performed a random effect ANOVA for fraction stability. There was no main effect of groups $F(3,309) = 0.97$, $p > 0.5$ or genotype $F(1, 8) = 1.71$, $p > 0.5$ and no interaction $F(3,309)=0.44$, $p=0.7$. (WT group 1: 28.8±0.67 %, WT group 2: 26.15±0.4%, WT group 3: 27.42±0.83%, WT group 4: 23±0.62%, n =5 mice, KO group 1: 32.9±0.49, KO group 23.7±0.42%, KO group 3: 17.71±0.5, KO group 4: 21.1±0.205, n= 5 mice, random effect ANOVA)

Chapter 3 Altered functional plasticity of synaptic GluA1 with motor learning in the Fragile X mouse.

3.1 Introduction

Fragile X syndrome (FXS) is the most common inherited form of an intellectual disability with a prevalence rate of >1:4000. FXS results from a mutation that causes silencing of the FMR1 gene, which encodes the fragile X mental retardation protein (FMRP). FMRP is an RNA-binding protein that is involved in regulating the translation of neuronal proteins and is thought to be important for some forms of synaptic plasticity (Darnell et al., 2011; Pfeiffer & Huber, 2009). Patients with FXS exhibit a range of neurological deficits, including cognitive impairments, social anxiety, seizures, sleep disorders, and motor skill deficits (Koekkoek et al., 2005; Van der Molen et al., 2010; Zingerevich et al., 2009). Although less attention has been given to studying these motor impairments, motor skills are integral to exploration, imitation (Vanvuchelen, Roeyers, & De Weerdt, 2007), communication (Gernsbacher, Sauer, Geye, Schweigert, & Hill Goldsmith, 2008), and other skills with which children with FXS struggle. Therefore, interventions targeted at motor impairments may be important in addressing the core areas of impairment in this neurodevelopmental disorder.

Motor skill learning requires the involvement of multiple brain regions, such as the cerebellum, basal ganglia, and the motor cortex (Shmuelof & Krakauer, 2011). Synaptic plasticity in the primary motor cortex (M1) has been shown to be particularly important. Previous experiments support this by demonstrating that motor skill learning: (1) enhances the synaptic responses of intracortical connections in the M1 (Rioult-Pedotti et al., 1998), (Hodgson et al., 2005)); (2) occludes long-term potentiation (LTP) in these connections (Hodgson et al., 2005; Rioult-Pedotti, Donoghue, & Dunaevsky, 2007; Rioult-Pedotti et al.,

2000) a leading candidate mechanism for persistent changes in synaptic strength; and (3) induces structural modification of M1 dendritic spines, sites of excitatory synaptic input (M. Fu & Zuo, 2011; Harms et al., 2008; Xu et al., 2009b)

The *fmr1* knock-out (KO) mouse recapitulates several behavioral and physical characteristics observed in FXS (Comery et al., 1997; Consortium, 1994; Koekkoek et al., 2005; Vinueza Veloz et al., 2012), including deficits in associative motor learning (Vinueza Veloz et al., 2012), yet the accompanying synaptic changes have not yet been analyzed in this mouse. To gain a better understanding of how FMRP contributes to regulation of synaptic plasticity in the M1, we trained *fmr1* KO mice and wild-type (WT) littermate control mice on a single forelimb reaching motor task and analyzed structural and functional synaptic plasticity. We report that the *fmr1* KO mice display a motor skill learning deficit. Although motor skill training induces a transient increase of synaptic AMPA-type glutamate receptor subunit 1 (GluA1), in the trained hemisphere of WT mice, in the *fmr1* KO mice there is a temporal dysregulation of synaptic GluA1 translocation with training.

3.2 Materials and methods

3.2a *Mice*

Mice were cared for in accordance with NIH guidelines for laboratory animal welfare. All experiments were approved by the University of Nebraska Medical Center Institutional Animal Care and Use Committee. Male C57BL/6 *fmr1* KO and littermate control mice were used for behavioral and biochemical experiments. Animals were housed in the animal facility at UNMC and raised on a 12 hours light/dark cycle and were given food and water ad libitum (except where noted otherwise).

3.2b *Motor skill training*

Apparatus: A custom made training box was used for motor sill training on a single forelimb reaching task. The training box measured 9.2 cm wide, 22.1 cm long and 20.8 cm long (Figure 8a). A small slit in the cage allowed the mouse to reach out and retrieve small pellets of food (#F0163, Bioserv). Pellets were placed on the interchangeable platforms in the front of the box. Two platforms were used for this behavior- a paw determination platform and a training platform as seen in the image. (Figure 8B and 8C)

Training- 5 to 6-week-old mice were food-restricted (85% of their free-feeding weight). Training was divided into two sessions 1) paw determination and 2) training. On the 1st day of training (Day 0) paw preference for mice was determined. Mice were placed in the cage with platform for paw determination. This platform had no gap between slit and pellet. Mice could use either of their paws for food retrieval. Mice were allowed about 10 attempts to retrieve the pellet. The paw with most retrieves was considered preferred and recorded for subsequent training.

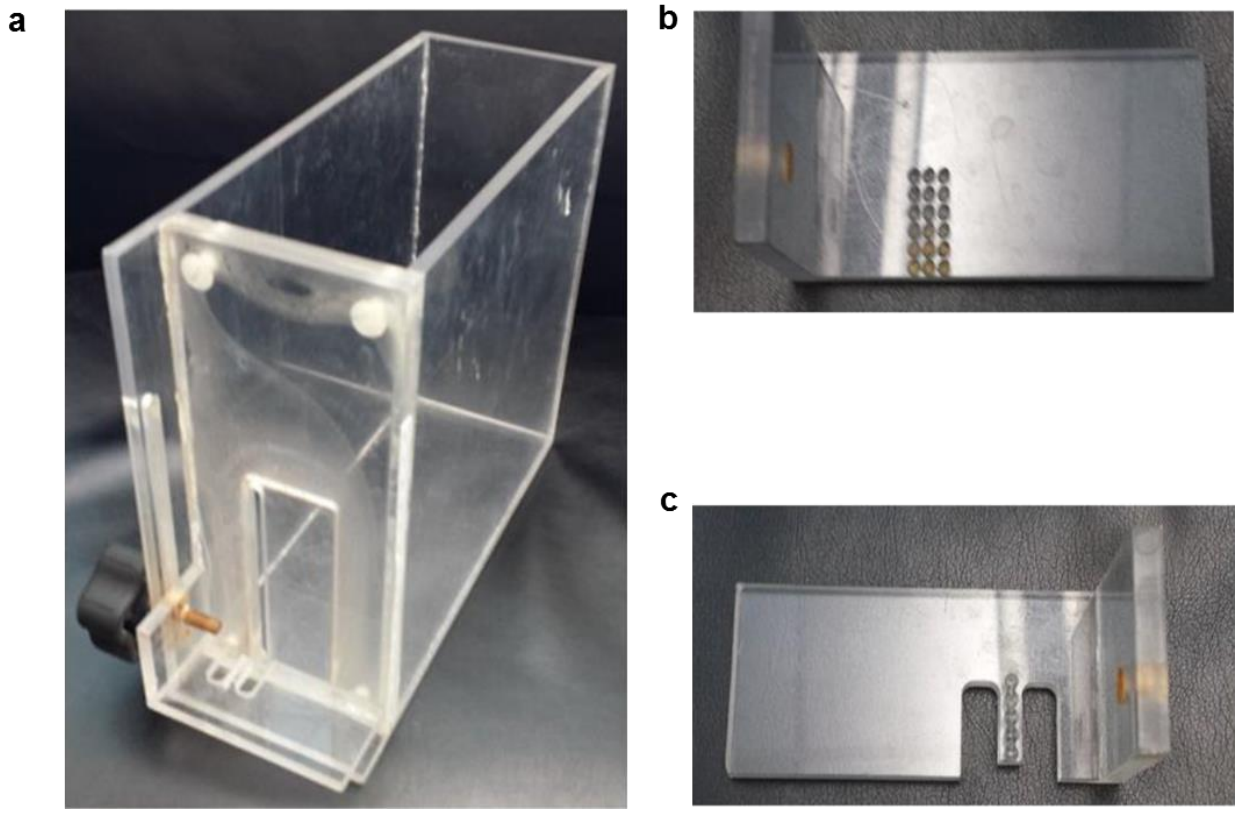

Figure 8: Motor skill training apparatus.
(a) Image of a custom mouse training box for the single forelimb reaching task. **b)** Image of platform used for forelimb preference determination. **c)** Image of training platform.

For training, mice were placed in the cage and trained with the training platform. The training platform was designed so as to be accessible only to the preferred paw. A 4 mm gap between the pellet and the slit ensured that the mouse had to grasp the pellet to retrieve it and could not slide it in. Mice had one training session per day over a period 5 days. Each session lasted 30 min or 100 reaches. Motor skill performance was quantified by the success rate (percentage of successful retrievals). The trained hemisphere (tr) is contralateral to the trained forelimb and the untrained hemisphere (utr), acts as an internal control.

Mice were always allowed access to ad libitum water. After Day 0 mice were fed about 0.8 to 1.2 grams of food pellet to maintain weight ad prevent catastrophic weight loss. The exact weight of food provided varied depending on the weight of the mouse on the day of training so as to maintain weight within the desired range. Mice were monitored twice every day and drastic weight loss or lethargy were considered terminal end points. Additionally, for the biochemistry experiments, mice were sacrificed 18hrs after the last session of training.

3.2c *Preparation of Synaptosomes from the Motor Cortex* (Suresh & Dunaevsky, 2015)

Materials and Reagents

1. C57BL6 mouse (Mus musculus)
2. Isoflurane (Isothesia) (Butler animal supplies)
3. Sodium chloride (NaCl) (Thermo Fisher Scientific, catalog number: S-271)
4. Potassium chloride (KCl) (Thermo Fisher Scientific, catalog number: P217-500)
5. Sodium bicarbonate ($NaHCO_3$) (Thermo Fisher Scientific, catalog number: S233-500)
6. Monosodium phosphate (NaH_2PO_4) (Thermo Fisher Scientific, catalog number: S369-500)
7. Magnesium sulphate heptahydrate ($MgSO_4 \cdot 7H_2O$) (Thermo Fisher Scientific, catalog number: MG63-500)

8. Calcium chloride ($CaCl_2$) (Thermo Fisher Scientific, catalog number: C79-500)
9. Dextrose (Thermo Fisher Scientific, catalog number: D16-500)
10. Sucrose (Thermo Fisher Scientific, catalog number: S5-3)
11. Radio immunoprecipitation assay (RIPA) lysis buffer (see Recipes)
12. Roche cOmplete protease inhibitor cocktail pellets (Roche Diagnostics, catalog number: 11697498 001)
13. Protease inhibitor (Sigma-Aldrich, catalog number: p8340)
14. Phosphatase inhibitor (Sigma-Aldrich, catalog number: 3 p0044)
15. Krazy glue
16. Millipore anti GluA1 antibody(Millipore, catalog number: ab1504)
17. Cell signaling anti-rabbit HRP antibody (Cell Signaling Technology, catalog number: 7074S)
18. Agar powder (Alfa Aesar, catalog number: A10752)
19. Artificial cerebrospinal fluid (ASCF) (see Recipes)
20. High magnesium ACSF (see Recipes)
21. Agar block (see Recipes)
22. Sucrose media (see Recipes)

Equipment

1) Leica vibratome S1000
2) Scissors (one large and one small)
3) Forceps
4) Sharp blade
5) Vibratome injector blade (Leica)
6) 1.5 ml Eppendorf tube
7) Pellet pestle motor hand held homogenizer (Kontes, catalog number: 749540-0000)
8) 4 ºC table top centrifuge
9) Ruler
10) Aerobic air mixture (Lindweld Alloy, model: MAA140)
11) Square petri dish with Grid- (Thermo Fisher Scientific FB0875711A)
12) Sonicator (Thermo Fisher Scientific)

Procedure

A. Synaptosome preparation

1. Prepare fresh artificial cerebrospinal fluid (1x ACSF) and bubble with aerobic air mixture at room temperature for at least 15 min.
2. Prepare a 4 mM $MgSO_4$ ACSF (high Mg^{2+} ACSF) and keep in an ice bath with constant bubbling.
3. Anesthetize the animal using isoflurane gas and euthanize by decapitation.
4. Make a sharp incision through the skin on top of the skull. Separate the skin from the bone.
5. Make a straight incision from the Foramen Magna to the top of the skull. Separate out the two sections of the skull to expose the brain.
6. Wash the brain with about 1 ml cold High Mg^{2+} ACSF.
7. Isolate the brain and lay out transversely (Figure 9C). Cut off the cerebellum and the olfactory bulb (Figure 9D). Stand the brain on the caudal side and cut out the ventral portion of the brain (Figure 9E).
8. Glue the caudal portion of the brain on the vibratome plate using a rectangle piece of agar as support (Figure 9F). Make sure the brain is submerged under ice cold High Mg^{2+} ACSF during slicing (Figure 9G). High Mg^{2+} ACSF is used as this prevents excitotoxicty to neurons by blocking N-methyl-D-aspartate receptor (NMDAR).
9. Make thin coronal sections until the corpus callosum from the two hemispheres join (Fig. 9H). Then make two 750 micrometer coronal sections which now contain the primary motor cortex M1 (1 mm anterior and 0.5 mm posterior to the bregma and 0.75 to 2.5 mm lateral).
10. Incubate the slices in a submersion chamber in ACSF at room temperature for 1 h with constant bubbling.
11. After incubation, place the brain slice on a petri dish under ASCF and constant bubbling at room temperature. Use a blade to isolate the forelimb region of primary

motor cortex by making cuts 0.75 and 2.5 mm lateral to the midline and a ventral cut to remove deeper non cortical structures (Figure 9I).

12. Place the brain tissue into a 1.5 ml Eppendorf tube containing 300 µl of 0.32M sucrose media 1 (see Recipes) containing protease inhibitor (1 tablet in 50 ml of media).
13. Homogenize with a hand held homogenizer for one minute with up and down movements.
14. Spin down the homogenized sample at 1,500 rpm for 10 min at 4 ºC. The pellet obtained contains nuclear and cellular debris and is discarded
15. Collect the supernatant which contains suspended synaptosomes and spin at 13,500 rpm at 4 °C for 20 min.
16. The pellet obtained is the required synaptosomal preparation.

    Note: The preparation obtained is an approximately 70% enriched preparation of synaptosomes. The preparation has contamination with mitochondria and debris from endoplasmic reticulum organelles. To prepare a more purified form of synaptosomes this preparation will have to be passed through a sucrose or percoll gradient and has not been described in this protocol.

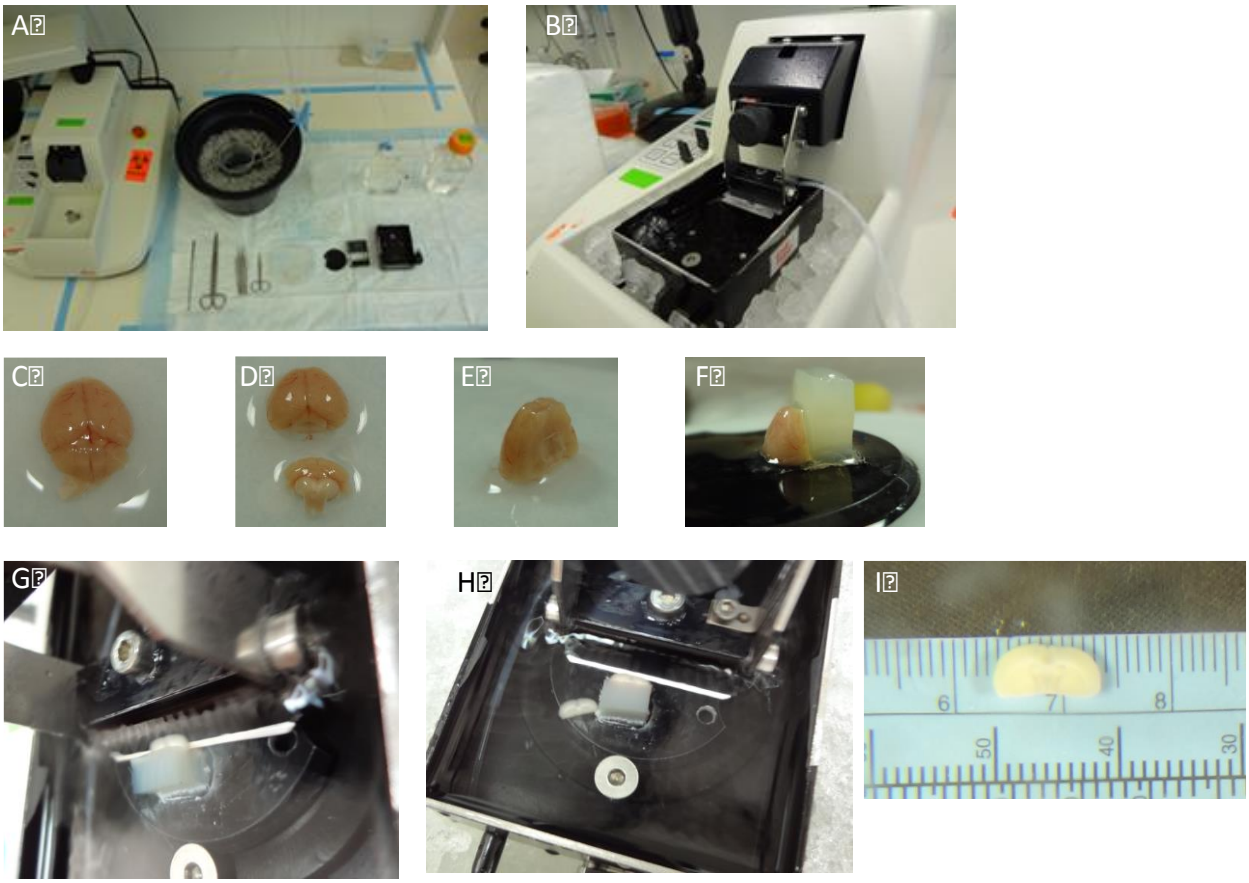

Figure 9. Preparation of brain slices on a vibratome.

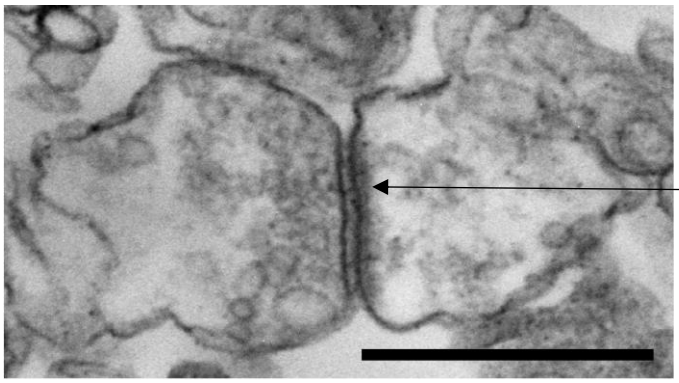

Figure 10: **Electron microscopy image of a synaptosome with pre and postsynaptic component**. Image obtained from the protocol described (scale bar 1 micrometer)

To evaluate synaptic GluA1 changes

17. Aspirate out the supernatant from step A14.

18. Re-suspend the pellet in 200 µl of RIPA lysis buffer.

19. Lyse the preparation by sonication on ice. (no post lysis spin required as the cellular debris is insignificant)
20. Estimate the protein levels by relevant protein estimation protocols (BCA assay from Pierce).
21. Run the protein lysates using a standard western blotting technique. We have run 20 microgram of protein for our experiments.
22. To immunoblot use Millipore anti GluA1 at 1:1,500 dilution as primary antibody and Cell signaling anti-rabbit HRP as secondary antibody at 1:5,000 dilution.

Note: We have evaluated other proteins such as mTOR, ERK, PSD-95, GLuA2, MAP2 from these preparations.

Recipes

1. Artificial cerebrospinal fluid (ASCF)
   Ingredients: Sodium chloride (NaCl) 126mM, Potassium chloride (KCl) 3mM, Monosodium phosphate (NaH2PO4) 1.25mM, Sodium bicarbonate ($NaHCO_3$) 26mM
   Magnesium sulphate heptahydrate (MgSO4.7H2O) 1mM, Calcium chloride dihydrate
   (CaCl2.2H2O) 2mM, Dextrose 10mM, Water
   pH 7.4
   Tonicity 300 mmoles/kg
   Note: We prepare a 10x stock of ACSF excluding $MgSO_4$, $CaCl_2$ and dextrose and store at 4 °C. Before the experiment a 1x ACSF is prepared and Dextrose, magnesium and calcium salts are added. Both $MgSO_4$ and $CaCl_2$ are prepared and stored as 1 M stocks which are then added in required volume to the 1x ACSF. A point to note is that 1x ACSF is vigorously bubbled for at least 15 min prior to adding the $CaCl_2$ to prevent calcium precipitation. Another alternative is to add the $CaCl_2$ in small volumes with vigorous stirring on a stir plate.
2. High magnesium ACSF
   ACSF 1X solution, Magnesium sulphate heptahydrate ($MgSO_4 \cdot 7H_2O$) 4mM

Note: High Magnesium ACSF is used to block NMDA receptors channels and prevent cell death due to excitotoxicty. The Mg^{2+} is prepared as a 1 M stock and 0.15ml of 1 M $MgSO_4$ stock is added to 50 ml of previously prepared 1x ACSF to obtain a final concentration of 4mM of Mg^{2+}.

3. Agar block
   Agar powder 33.2g, Sodium chloride 9g, water 1L
   Disperse the NaCl and Agar powder in water. Heat in a microwave oven until all the agar dissolves and a clear solution is obtained. Pour into a square petri dish and allow to cool to get agar blocks. Make small rectangles from the block and stick the breadth of the rectangle on the vibratome plate.
4. Sucrose media 1
   2.5 M sucrose
   0.5 M HEPES (pH 7.5)
   0.5 M EDTA (pH 8.0)
   Sucrose media is stored at -20 °C. Roche Protease inhibitor cocktail tablet is added to the media before use. (1 tablet in 50 ml)
5. RIPA lysis buffer Tris.HCl 0.3 g, Sodium chloride 0.44 g, Sodium dodecylsulphate 0.05 g, Sodium deoxycholate 0.125 g,Triton X 100 0.1 ml,0.5 M EDTA 0.05 ml, Water Make up to 50 ml,pH 7.4

3.2d *Surface biotinylation assay*

Surface protein expression in synaptosomal samples was detected through a biotinylation assay, followed by a Western blot analysis with antibodies directed against GluA1. Synaptosomal preparations were washed and incubated in Sulfo-NHS-SS biotin (0.5 mg/ml in ACSF, Pierce) for 1 h at 4°C. Surface biotinylation was stopped by removing the solution, followed by quenching of unbound biotin with cold 100 mM glycine in ACSF for 5 min, three times. Synaptosomes were lysed in RIPA buffer (50 mM Tris.HCl, 25 mM NaCl, 0.1% SDS, 0.5% Na deoxycholate, 1% Triton X-100, and 0.5 M EDTA). Biotinylated proteins (400 µg) were precipitated with 200 µl of neutravidin beads (Pierce) overnight at 4°C. The beads were washed (3×) and bound protein was eluted by boiling in Lammeli

buffer for 10 min. The eluate was separated on 4–15% Biorad Mini-Protean TGX Precast SDS-PAGE gels, and transferred to polyvinyl difluoride membranes. The membranes were probed with anti-GluA1 (1:1500, Millipore) and anti-GAPDH (1:4000, Cell Signaling Technology). The membranes were incubated with horseradish peroxidase-conjugated secondary antibodies (anti-rabbit 1:5000), and bands were visualized using a Cell Biosciences FluroChem HD2 system. Because we used a crude synaptosomal preparation, GAPDH was abundant in the biotinylated samples. Hence, we used GAPDH as a loading control

3.2e *Statistics*

Data are reported as mean ± SEM. Normal distribution was tested using Kolmogorov–Smirnov test and variance was compared. Analysis was done either using two-sided unpaired Student's *t*test or with one- or two-way ANOVA with the Bonferonni method for *post hoc* multiple comparisons. Data were analyzed using the GraphPad Prism.

3.3 Results

3.3a *fmr1 KO mice have a motor learning deficit in a single forelimb reaching task*

Five-week-old male fmr1 KO (*n* = 38) and littermate WT mice (*n* = 36) were trained to reach through a small slit and grasp a food pellet using their preferred forelimb (Figure 11*a*). Although the success rate, defined as proportion of successful retrieves from total reaches, of both the KO and WT mice increased over subsequent days of training, the KO mice achieved a lower success rate (Figure 11b).

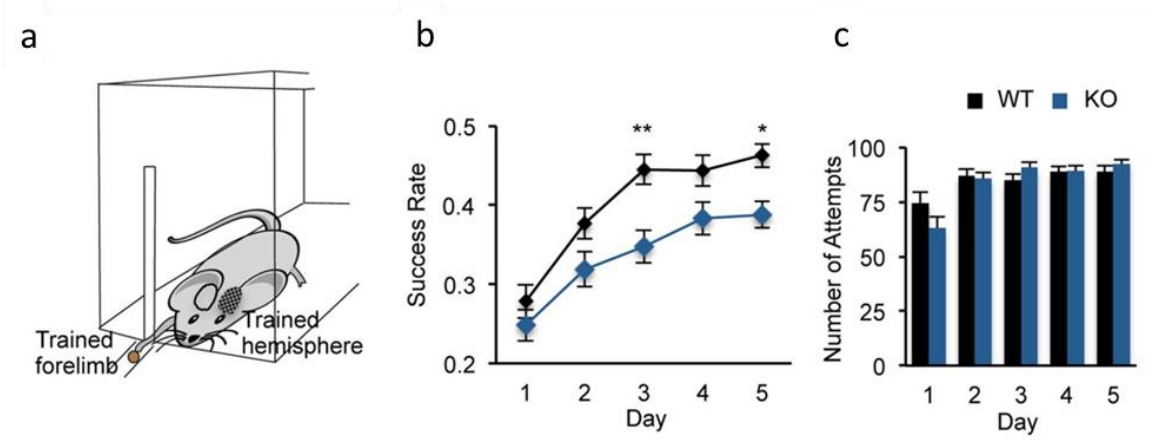

Figure 11: Impaired motor skill learning in the fmr1 KO mouse. (a) An illustration of the training box with a mouse reaching out for a food pellet through a narrow slit. The trained forelimb and the contralateral-trained hemisphere are marked. **(b)** Average success rates during training for WT controls (black, n = 36) and fmr1 KO (blue, n = 38) mice. Both genotype and days of training affect success rate ($p < 0.01$, two-way repeated-measures ANOVA). **(c)** There was no difference in the number of reaches performed by the KO and WT mice at any of the training days. mean ± SEM. *$p < 0.05$, **$p < 0.01$

Both genotype and days of training affect success rate ($p < 0.01$, two-way repeated-measures ANOVA). Significant differences were observed on day 3 (WT, 0.44 ± 0.02; KO, 0.35 ± 0.02, $p = 0.002$), and day 5 (WT, 0.46 ± 0.01; KO, 0.39 ± 0.02, $p = 0.034$; *Figure* 11b*)*. Additional training days did not lead to increased success rate in the KO mice (Day 6, 0.36 ± 0.03; Day 7, 0.38 ± 0.03; Day 8 KO, 0.39 ± 0.03, $n = 7$). The success rate on the first day of training (WT, 0.28 ± 0.02; KO, 0.25 ± 0.02, $p > 0.99$) as well as total number of reaching attempts made each day (Figure 11c), were not significantly different between the WT and KO mice. These data indicate that the fmr1 KO mice display a motor skill learning impairment that is not due to a basic motor function deficit.

3.3b *Motor skill training-induced synaptic delivery of GluA1 is impaired in fmr1 KO mice*

Synaptic delivery of AMPA-type glutamate receptors is thought to be a major contributor to LTP (Granger & Nicoll, 2014; Malinow & Malenka, 2002). We therefore tested whether motor skill training induces translocation of AMPA receptor subunit GluA1 into synapses in the trained hemisphere and if it is impaired in the fmr1 KO mouse. We first determined whether there was a difference in levels of synaptic GluA1 between the hemispheres before motor skill training. We determined paw preference without further training. Crude synaptosomal preparations were isolated from the preferred (pr) and unpreferred (upr) M1 forelimb regions of untrained mice and synaptic GluA1 levels were determined using Western blot analysis (Figure 12a). In the untrained WT mice (nonlittermate controls), there was no difference in synaptic GluA1 between the hemispheres (pr: 0.78 ± 0.1; upr: 0.94 ± 0.11; n = 8, unpaired t test, p = 0.3). This suggests that before training there is no increased synaptic GluA1 in the M1 forelimb region of the preferred hemisphere. This is consistent with no difference in synaptic strength between hemispheres before training (Padmashri et al 2013). We next trained the mice and isolated synaptosomes from the trained and untrained M1 forelimb regions at different times after training and determined the levels of synaptic GluA1. Although 2 hrs after training there was no difference in the interhemisphere ratio (trained/untrained) compared with untrained mice (Figure 12b, pr/unpr; utr: 1 ± 0.12, n = 10; 2 h tr: 1.29 ± 0.19, n = 7, p = 1, two-way ANOVA), 1 d after training the interhemisphere ratio of synaptic GluA1 was significantly higher (Figure 12b, 1 d tr: 2.19 ± 0.28, n = 14, p < 0.001, two-way ANOVA). No difference was found between littermate controls and WT mice (data not shown); therefore, we combined these groups. These data suggest that motor skill training drives GluA1 to synapses. Because GluA1 translocation into synapses is transient with LTP and experience (Matsuo et al., 2008; Shi et al., 1999) we next examined synaptic GluA1 after 2 and 5 d of training. There was a

gradual decrease in the interhemisphere ratio of synaptic levels of GluA1 (2 d tr: 1.9 ± 0.19, n = 7 mice, p= 0.028, two-way ANOVA) with no interhemisphere difference detected after five days of training (Figure 12b, 5 d tr: 1.01 ± 0.15 n = 8 mice, two-way ANOVA, p = 1,Figure 13b). Similar results were found when surface, rather than total synaptic levels of GluA1 were measured using a biotinylation method (utr: 1 ± 0.11, n = 7; 1 d tr: 2 ± 0.34, n = 7, t test, p = 0.02, Figure 13a). These results suggest that motor skill training leads to a transient translocation of GluA1 into synapses.

In cortical neuronal cultures from fmr1 KO mice, there is a deficit in GluA1 trafficking with LTP (Hu et al., 2008). Whether experience and learning in the fmr1 KO mouse result in impaired translocation of GluA1 into synapses *in vivo* is not known. We first compared basal synaptic levels of GluA1 in WT and KO untrained mice. No difference in levels of synaptic GluA1 were found between the genotypes of untrained mice (WT, 0.92 ± 0.15, n = 11; KO, 0.86 ± 0.09, n = 8; p = 0.78, unpaired t test). As in the WT, no increase in GluA1 was observed 2 h after motor skill training (utr KO, 1 ± 0.07, n = 15 mice; 2 h KO, 0.98 ± 0.14, n = 7 mice; p = 1, two-way ANOVA,). Surprisingly, unlike in the WT mice, 1 d of motor skill training did not lead to increased synaptic expression of GluA1 in the trained hemisphere of the fmr1 KO mice (1 d KO, 1.09 ± 0.2, n = 8, p = 1, 2-way ANOVA; Figure 12b). We next examined whether there was a delay in synaptic translocation of GluA1 in the fmr1 KO mice. In mice trained for 2 d, we observed an increase in levels of synaptic GluA1 in the trained hemisphere compared with untrained KO mice (2 d KO, 2.12 ± 0.35, n = 9, p < 0.001, two-way ANOVA). Similar to WT mice, the increase in synaptic GluA1, albeit delayed, was transient as no increase was observed in the trained hemisphere after 5 d of training (5 d KO, 1.21 ± 0.1, n = 7, p = 1, two-way ANOVA; Figure 12b). These results suggest that in the fmr1 KO mouse, there is a temporal impairment in the motor skill training-induced translocation of GluA1 into synapses that might contribute to the reduced learning in these mice.

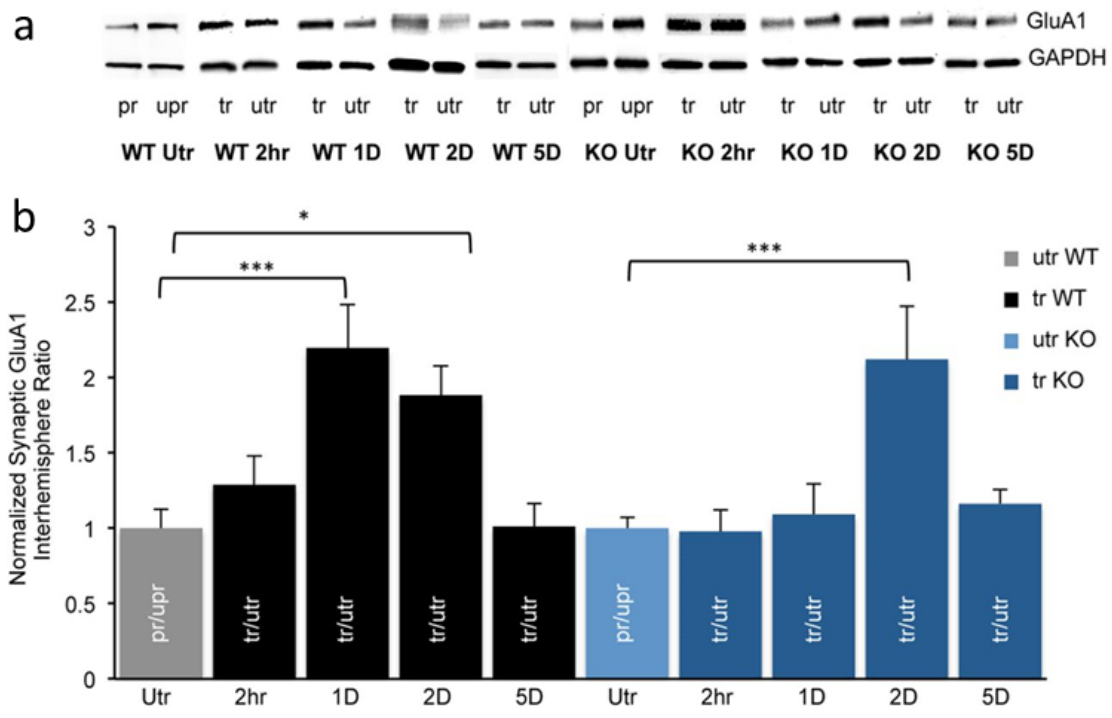

Figure 12: Learning induces a transient increase in synaptic GluA1 that is delayed in the *fmr1* KO mouse. (a) Western blots of synaptic GluA1 from forelimb M1 regions of preferred (pr) and unpreferred (upr) hemispheres from untrained (Utr) mice or from trained (tr) and untrained (utr) hemispheres of trained WT and *fmr1* KO mice.**(b)** Untrained WT mice (n = 10) were compared with trained WT mice after 2 h (n = 7), 1 d (n = 14), 2 d (n = 7), or 5 d (n = 8) of training. Untrained KO mice (n = 15) were compared with trained KO mice after 2 h (n = 7), 1 d (n = 8), 2 d (n = 9), or 5 d (n = 7) of training. For quantification, protein levels were normalized to GAPDH and interhemisphere ratios were normalized to untrained WT or KO mice. Mean ± SEM. The interaction between genotype and training on GluA1 interhemisphere ratio was significant (p = 0.013, two-way ANOVA); *p < 0.05, ***p < 0.001

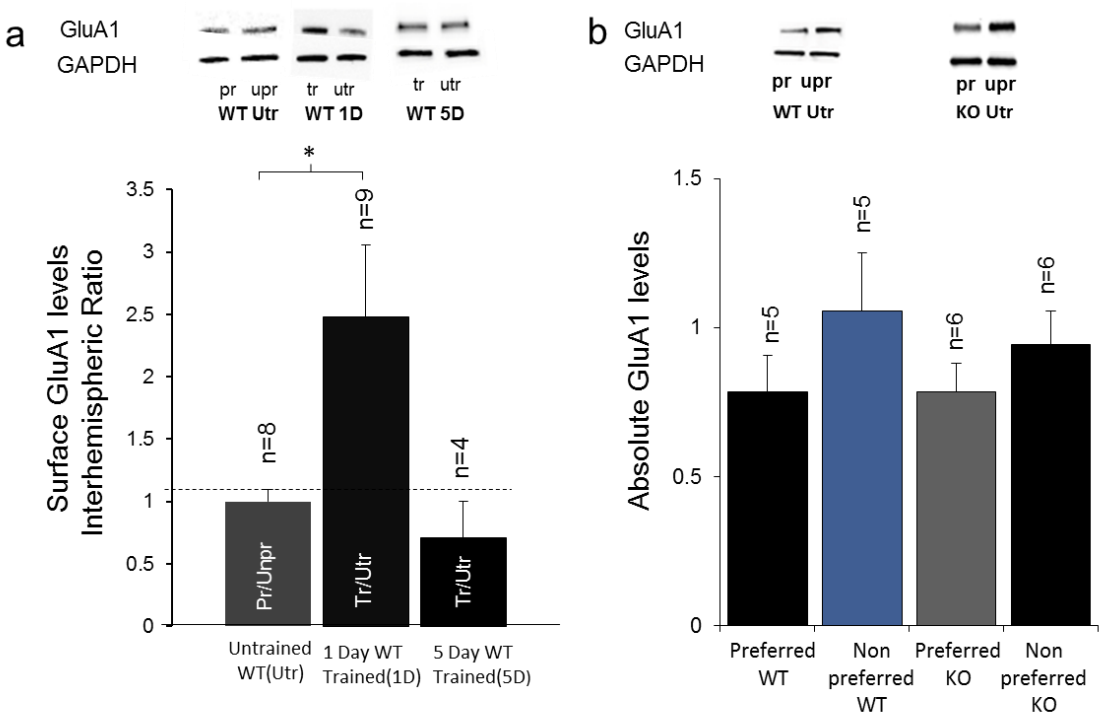

Figure 13: Learning induces a transient increase in surface GluA1 with no basal differences in synaptic GluA1 levels in the KO. (a) Above: Western blots of surface GluA1 from forelimb M1 regions of preferred (pr) and unpreferred (upr) hemispheres from untrained (Utr) mice or from trained (tr) and untrained (utr) hemispheres of trained WT. Below Untrained WT mice (*n* = 8mice) were compared with trained WT mice after 18 h (*n* = 9mice) or 5 d (*n* = 4mice) of training. For quantification, protein levels were normalized to GAPDH and interhemisphere ratios were normalized to untrained WT mice ($p = 0.023$, one way ANOVA with Bonferroni correction); *$p < 0.05$, Mean ± SEM. **(b)** Above**:** Western blots of synaptic GluA1 from forelimb M1 regions of preferred (pr) and unpreferred (upr) hemispheres from untrained (Utr) WT and KO mice: Below No difference in absolute synaptic levels of GluA1 between either preferred hemispheres and unpreferred hemispheres in both WT (n = 5mice) and KO (n = 6mice) genotypes (p>0.05, two way ANOVA with Bonferroni correction)

3.4 Discussion

Here we report that motor-skill training induces synaptic changes in the primary motor cortex and that in the fmr1 KO mice, there are deficits in both motor-skill learning and in synaptic AMPAR insertion.

In normal WT mice, analysis of motor-skill training-induced synaptic changes demonstrated increased synaptic GluA1 after just one day of training. Synaptic insertion of GluA1 is a characteristic of long term potentiation. Since there is evidence of LTP-like mechanisms in this learning paradigm (Rioult-Pedotti et al., 2000), the increased levels of synaptic GluA1 could be mirroring expression of LTP-like plasticity within M1 cortex. The increase in synaptic GluA1 was gradual, with a 20% increase immediately (2 hours) after training which subsequently increased two fold about 16hrs later. Considering the time scales involved in the learning paradigm, this points to a relatively rapid expression of LTP-like plasticity within the motor cortex. Interestingly, the increase in GluA1 was transient and started to wane by the second day of training and dropped back to baseline at the end of five days. Since extrinsic LTP expression is known to be occluded after 5 days of motor-skill training, one explanation for the occlusion is saturation of plasticity mechanisms to the earlier round of LTP.

Another feature of this learning paradigm is rapid structural plasticity with new spines observed as early as 2 hours following motor training (Xu et al., 2009a). Since, LTP expression is known to induce synaptogenesis (in slices) it has been thought that the structural plasticity is a consequence of LTP-like plasticity within neurons during learning. However, since GluA1 levels peak about 16 hours later this suggests the functional plasticity lags structural changes. One possible explanation is that LTP-like mechanism is being triggered in a few synapses in response to the behavior which then causes synaptogenesis in surrounding regions. Later on these newly formed synapses accumulate AMPAR leading to further increase in total synaptic GluA1 which is large

enough to be detected biochemically. Since LTP is known to selectively stabilize spines (Hill & Zito, 2013) and the learning-induced newly formed spines are preferentially stabilized, this lends further support to the hypothesis.

Additionally, we identified that the fmr1 KO mouse had deficits in motor-skill learning and a delay in learning induced GluA1 insertion. The motor-skill learning deficit reported here is consistent with mild behavioral impairments reported for the *fmr1* KO mice (Consortium, 1994; D'Hooge et al., 1997; Krueger et al., 2011; Vinueza Veloz et al., 2012). We cannot exclude the possibility that other impairments in the *fmr1* KO mice, such as altered anxiety and activity levels, might affect motor skill learning. Nevertheless, reduced motor skill learning is not likely to be due to reduced motor performance or motivation because we observed a similar initial success rate as well as total number of reaching attempts made by the KO and WT mice. The absence of impairments in basic motor function in the *fmr1* KO has also been previously reported (Vinueza Veloz et al., 2012; Wang et al., 2008) and the impairment in motor-skill learning we report here might be related to the motor-skill impairments reported in FXS patients (Van der Molen et al., 2010; Zingerevich et al., 2009).

In this same study we also identified deficits in LTP in the motor cortex of fmr1 KO mouse (Padmashri et al., 2013). This fits in well with the current finding of delay in GluA1 insertion with training and is line with studies suggesting that synapses in the fmr1 KO mice are less sensitive to potentiation (Meredith et al., 2007; Pan et al., 2010). Consistent with the above cited studies, motor-skill training did not induce rapid synaptic formation in the fmr1 KO as would be expected from deficient LTP induction following learning.

The described biochemical studies have limitations regarding the information they provide on the spatiotemporal dynamics of AMPAR insertion following motor training. Since, the biochemical assay samples the entire forelimb representation area with the primary motor cortex, any laminar differences would be lost in this analysis. Since spine properties vary

according to the layer of neurons (A. J. Holtmaat et al., 2005; Zuo et al., 2005), our results do not rule out laminar differences in synaptic plasticity following motor learning. Similarly, as discussed earlier dendritic spines are heterogeneous, with morphology correlated with long term synaptic fate. The exact population of spines undergoing AMPAR insertion could be important for understanding the mechanisms of memory storage. Furthermore, insight into how functional plasticity influences local micro-circuitry as discussed under the cluster memory storage hypothesis, are also unclear from these biochemical results. Finally, how basal alterations in AMPAR-spine relationship in the fmr1 KO mouse as discussed in Chapter 2 affect learning induced synaptic plasticity is also unclear. To answer these questions, one needs to combine *in vivo* two photon imaging techniques with motor training to monitor the AMPAR and spines. In ongoing experiments we are interested to examine the population and consequences of AMPAR insertion within spines during learning and how these are altered in the fmr1 KO mouse.

In this body of work we monitored different AMPAR subunits wherein GluA2 was tracked in the basal studies (chapter 2) and GluA1 with learning (chapter 3). When we started this project the overarching consensus in the field was that GluA1 was trafficked into synapses in an activity dependent manner (Shi et al., 1999) and was then replaced by GluA2 containing AMPAR in a constitutive regulatory mode (Derkach, Oh, Guire, & Soderling, 2007). Hence, overall strength of synapse was maintained by GluA2 trafficking but activity induced potentiation was through GluA1. However, more recent studies, have challenged this model of differential subunit based AMPAR trafficking (Nicoll & Roche, 2013). This was in part due to the finding that 95% of functional synaptic AMPAR were composed of GluA2 with the predominant composition being GluA2/GluA1 heteromers (W. Lu et al., 2009). Further, the Nicoll group demonstrated using a genetic deletion approach that GluA2 and GluA1 were equally likely to be inserted into synapses upon potentiation (Granger, Shi, Lu, Cerpas, & Nicoll, 2013). The only prerequisite to potentiation was

presence of a pool of extrasynaptic AMPAR. This model suggests that both GluA1 and GluA2 would have identical temporal dynamics with learning induced synaptic potentiation.

Chapter 4 Appendices

Appendix A: Abbreviations.

ACC: Anterior Cingulate cortex

ACSF: Artificial cerebrospinal fluid

AMPAR: α-amino-3-hydroxy-5-methyl-4-isoxazolepropionic acid receptor

AP: Action potential

ARC: Activity regulated cytoskeleton associated protein

BRCA1: Breast cancer gene 1

CAMKII: Ca2+/calmodulin-dependent protein kinase II

CD: Caudate nuclei

CNS: Central nervous system

ERK: Extracellular regulated kinase

FXS: Fragile X syndrome

FXTAS: Fragile X tremor/ataxia syndrome

GKAP: Guanylate kinase-associated protein

GPCR: G protein coupled receptor

HITS-CLIP: High-throughput sequencing of RNA isolated by crosslinking immunoprecipitation

ID: Intellectual disability

IQ: Intelligence quotient

LTD: Long term depression

LTP: Long term potentiation

MAPK: Mitogen activated protein kinase

mGluR: Metabotropic glutamate receptor

NES: Nuclear export signal

NLS: Nuclear localization signal

NMDA: N-methyl-D-aspartate receptor

PP1: Protein phosphatase 1

PSD: Post synaptic density

SER: Smooth endoplasmic reticulum

STEP: Striatal enriched protein tyrosine phosphotase

TARP: Transmembrane AMPAR receptor regulatory protein

TPLM- Two photon light microscopy

Appendix B: References.

Adams-Cioaba, M. A., Guo, Y., Bian, C., Amaya, M. F., Lam, R., Wasney, G. A., . . . Min, J. (2010). Structural studies of the tandem Tudor domains of fragile X mental retardation related proteins FXR1 and FXR2. *PLoS One, 5*(11), e13559. doi:10.1371/journal.pone.0013559

Adesnik, H., & Nicoll, R. A. (2007). Conservation of glutamate receptor 2-containing AMPA receptors during long-term potentiation. *J Neurosci, 27*(17), 4598-4602. doi:10.1523/JNEUROSCI.0325-07.2007

Adesnik, H., Nicoll, R. A., & England, P. M. (2005). Photoinactivation of native AMPA receptors reveals their real-time trafficking. *Neuron, 48*(6), 977-985. doi:10.1016/j.neuron.2005.11.030

Agulhon, C., Blanchet, P., Kobetz, A., Marchant, D., Faucon, N., Sarda, P., . . . Abitbol, M. (1999). Expression of FMR1, FXR1, and FXR2 genes in human prenatal tissues. *J Neuropathol Exp Neurol, 58*(8), 867-880.

Alpatov, R., Lesch, B. J., Nakamoto-Kinoshita, M., Blanco, A., Chen, S., Stutzer, A., . . . Shi, Y. (2014). A chromatin-dependent role of the fragile X mental retardation protein FMRP in the DNA damage response. *Cell, 157*(4), 869-881. doi:10.1016/j.cell.2014.03.040

Alvarez, V. A., & Sabatini, B. L. (2007). Anatomical and physiological plasticity of dendritic spines. *Annu Rev Neurosci, 30*, 79-97.

American.College.of.Medical.Genetics. (1994). *Fragile X syndrome: diagnostic and carrier testing. Working Group of the Genetic Screening Subcommittee of the Clinical Practice Committee. American College of Medical Genetics* (Vol. 53).

Anggono, V., & Huganir, R. L. (2012). Regulation of AMPA receptor trafficking and synaptic plasticity. *Curr Opin Neurobiol, 22*(3), 461-469. doi:10.1016/j.conb.2011.12.006

Ashley, C. T., Jr., Wilkinson, K. D., Reines, D., & Warren, S. T. (1993). FMR1 protein: conserved RNP family domains and selective RNA binding. *Science, 262*(5133), 563-566.

Ashley, C. T., Sutcliffe, J. S., Kunst, C. B., Leiner, H. A., Eichler, E. E., Nelson, D. L., & Warren, S. T. (1993). Human and murine FMR-1: alternative splicing and translational initiation downstream of the CGG-repeat. *Nat Genet, 4*(3), 244-251. doi:10.1038/ng0793-244

Bagni, C., Tassone, F., Neri, G., & Hagerman, R. (2012). Fragile X syndrome: causes, diagnosis, mechanisms, and therapeutics. *J Clin Invest, 122*(12), 4314-4322. doi:10.1172/JCI63141

Baker, K. B., Wray, S. P., Ritter, R., Mason, S., Lanthorn, T. H., & Savelieva, K. V. (2010). Male and female Fmr1 knockout mice on C57 albino background exhibit spatial learning and memory impairments. *Genes Brain Behav, 9*(6), 562-574. doi:10.1111/j.1601-183X.2010.00585.x

Bakker, C. E., & Oostra, B. A. (2003). Understanding fragile X syndrome: insights from animal models. *Cytogenet Genome Res, 100*(1-4), 111-123. doi:72845

Bastrikova, N., Gardner, G. A., Reece, J. M., Jeromin, A., & Dudek, S. M. (2008). Synapse elimination accompanies functional plasticity in hippocampal neurons. *Proc Natl Acad Sci U S A, 105*(8), 3123-3127. doi:10.1073/pnas.0800027105

Bear, M. F., Huber, K. M., & Warren, S. T. (2004). The mGluR theory of fragile X mental retardation. *Trends Neurosci, 27*(7), 370-377. doi:10.1016/j.tins.2004.04.009

Bellot, A., Guivernau, B., Tajes, M., Bosch-Morato, M., Valls-Comamala, V., & Munoz, F. J. (2014). The structure and function of actin cytoskeleton in mature glutamatergic dendritic spines. *Brain Res, 1573*, 1-16. doi:10.1016/j.brainres.2014.05.024

Beneyto, M., & Meador-Woodruff, J. H. (2004). Expression of transcripts encoding AMPA receptor subunits and associated postsynaptic proteins in the macaque brain. *J Comp Neurol, 468*(4), 530-554. doi:10.1002/cne.10981

Berman, R. F., Buijsen, R. A., Usdin, K., Pintado, E., Kooy, F., Pretto, D., . . . Hukema, R. K. (2014). Mouse models of the fragile X premutation and fragile X-associated tremor/ataxia syndrome. *J Neurodev Disord, 6*(1), 25. doi:10.1186/1866-1955-6-25

Berman, R. F., & Willemsen, R. (2009). Mouse models of fragile X-associated tremor ataxia. *J Investig Med, 57*(8), 837-841. doi:10.2310/JIM.0b013e3181af59d6

Bhattacharya, A., Kaphzan, H., Alvarez-Dieppa, A. C., Murphy, J. P., Pierre, P., & Klann, E. (2012). Genetic removal of p70 S6 kinase 1 corrects molecular, synaptic, and behavioral phenotypes in fragile X syndrome mice. *Neuron, 76*(2), 325-337. doi:10.1016/j.neuron.2012.07.022

Bingol, B., & Schuman, E. M. (2006). Activity-dependent dynamics and sequestration of proteasomes in dendritic spines. *Nature, 441*(7097), 1144-1148. doi:10.1038/nature04769

Bingol, B., & Sheng, M. (2011). Deconstruction for reconstruction: the role of proteolysis in neural plasticity and disease. *Neuron, 69*(1), 22-32. doi:10.1016/j.neuron.2010.11.006

Blackwell, E., Zhang, X., & Ceman, S. (2010). Arginines of the RGG box regulate FMRP association with polyribosomes and mRNA. *Hum Mol Genet, 19*(7), 1314-1323. doi:10.1093/hmg/ddq007

Bontekoe, C. J., Bakker, C. E., Nieuwenhuizen, I. M., van der Linde, H., Lans, H., de Lange, D., . . . Oostra, B. A. (2001). Instability of a (CGG)98 repeat in the Fmr1 promoter. *Hum Mol Genet, 10*(16), 1693-1699.

Bosch, M., & Hayashi, Y. (2012). Structural plasticity of dendritic spines. *Curr Opin Neurobiol, 22*(3), 383-388. doi:10.1016/j.conb.2011.09.002

Bourne, J., & Harris, K. M. (2007). Do thin spines learn to be mushroom spines that remember? *Curr Opin Neurobiol*.

Bourne, J. N., & Harris, K. M. (2008). Balancing structure and function at hippocampal dendritic spines. *Annu Rev Neurosci, 31*, 47-67. doi:10.1146/annurev.neuro.31.060407.125646

Buchs, P. A., & Muller, D. (1996). Induction of long-term potentiation is associated with major ultrastructural changes of activated synapses. *Proc Natl Acad Sci U S A, 93*(15), 8040-8045.

Busquets-Garcia, A., Gomis-Gonzalez, M., Guegan, T., Agustin-Pavon, C., Pastor, A., Mato, S., . . . Ozaita, A. (2013). Targeting the endocannabinoid system

in the treatment of fragile X syndrome. *Nat Med, 19*(5), 603-607. doi:10.1038/nm.3127

Cajal, R. y. (1888). Estructura de los centros nerviosos de las aves. *Rev. Trim. Histol. Norm. Pat., 1*, 1-10.

Cane, M., Maco, B., Knott, G., & Holtmaat, A. (2014). The relationship between PSD-95 clustering and spine stability in vivo. *J Neurosci, 34*(6), 2075-2086. doi:10.1523/JNEUROSCI.3353-13.2014

Carroll, R. C., Beattie, E. C., von Zastrow, M., & Malenka, R. C. (2001). Role of AMPA receptor endocytosis in synaptic plasticity. *Nat Rev Neurosci, 2*(5), 315-324. doi:10.1038/35072500

Chen, S. X., Kim, A. N., Peters, A. J., & Komiyama, T. (2015). Subtype-specific plasticity of inhibitory circuits in motor cortex during motor learning. *Nat Neurosci, 18*(8), 1109-1115. doi:10.1038/nn.4049

Chen, T., Lu, J. S., Song, Q., Liu, M. G., Koga, K., Descalzi, G., . . . Zhuo, M. (2014). Pharmacological rescue of cortical synaptic and network potentiation in a mouse model for fragile X syndrome. *Neuropsychopharmacology, 39*(8), 1955-1967. doi:10.1038/npp.2014.44

Cho, R. W., Park, J. M., Wolff, S. B., Xu, D., Hopf, C., Kim, J. A., . . . Worley, P. F. (2008). mGluR1/5-dependent long-term depression requires the regulated ectodomain cleavage of neuronal pentraxin NPR by TACE. *Neuron, 57*(6), 858-871. doi:10.1016/j.neuron.2008.01.010

Chowdhury, S., Shepherd, J. D., Okuno, H., Lyford, G., Petralia, R. S., Plath, N., . . . Worley, P. F. (2006). Arc/Arg3.1 interacts with the endocytic machinery to regulate AMPA receptor trafficking. *Neuron, 52*(3), 445-459. doi:10.1016/j.neuron.2006.08.033

Cohen, J. D., Nichols, T., Brignone, L., Hall, S. S., & Reiss, A. L. (2011). Insular volume reduction in fragile X syndrome. *Int J Dev Neurosci, 29*(4), 489-494. doi:10.1016/j.ijdevneu.2011.01.003

Coiro, P., Padmashri, R., Suresh, A., Spartz, E., Pendyala, G., Chou, S., . . . Dunaevsky, A. (2015). Impaired synaptic development in a maternal

immune activation mouse model of neurodevelopmental disorders. *Brain Behav Immun, 50*, 249-258. doi:10.1016/j.bbi.2015.07.022

Collingridge, G. L., Peineau, S., Howland, J. G., & Wang, Y. T. (2010). Long-term depression in the CNS. *Nat Rev Neurosci, 11*(7), 459-473. doi:10.1038/nrn2867

Comery, T. A., Harris, J. B., Willems, P. J., Oostra, B. A., Irwin, S. A., Weiler, I. J., & Greenough, W. T. (1997). Abnormal dendritic spines in fragile X knockout mice: maturation and pruning deficits. *Proc. Natl. Acad. Sci. U S A, 94*, 5401-5404.

Consortium, T. D.-B. F. X. (1994). Fmr1 knockout mice: a model to study fragile X mental retardation. The Dutch-Belgian Fragile X Consortium. *Cell, 78*(1), 23-33.

Contractor, A., Klyachko, V. A., & Portera-Cailliau, C. (2015). Altered Neuronal and Circuit Excitability in Fragile X Syndrome. *Neuron, 87*(4), 699-715. doi:10.1016/j.neuron.2015.06.017

Cordeiro, L., Abucayan, F., Hagerman, R., Tassone, F., & Hessl, D. (2015). Anxiety disorders in fragile X premutation carriers: Preliminary characterization of probands and non-probands. *Intractable Rare Dis Res, 4*(3), 123-130. doi:10.5582/irdr.2015.01029

Cruz-Martin, A., Crespo, M., & Portera-Cailliau, C. (2010). Delayed stabilization of dendritic spines in fragile X mice. *J Neurosci, 30*(23), 7793-7803.

Czarnecki, K., Haas, C. A., Bas Orth, C., Deller, T., & Frotscher, M. (2005). Postnatal development of synaptopodin expression in the rodent hippocampus. *J Comp Neurol, 490*(2), 133-144. doi:10.1002/cne.20651

D'Hooge, R., Nagels, G., Franck, F., Bakker, C. E., Reyniers, E., Storm, K., . . . De Deyn, P. P. (1997). Mildly impaired water maze performance in male Fmr1 knockout mice. *Neuroscience, 76*(2), 367-376.

Darnell, J. C., & Klann, E. (2013). The translation of translational control by FMRP: therapeutic targets for FXS. *Nat Neurosci, 16*(11), 1530-1536. doi:10.1038/nn.3379

Darnell, J. C., Van Driesche, S. J., Zhang, C., Hung, K. Y., Mele, A., Fraser, C. E., . . . Darnell, R. B. (2011). FMRP stalls ribosomal translocation on mRNAs linked to synaptic function and autism. *Cell, 146*(2), 247-261. doi:S0092-8674(11)00655-6 [pii]

10.1016/j.cell.2011.06.013

Davidkova, G., & Carroll, R. C. (2007). Characterization of the role of microtubule-associated protein 1B in metabotropic glutamate receptor-mediated endocytosis of AMPA receptors in hippocampus. *J Neurosci, 27*(48), 13273-13278. doi:10.1523/JNEUROSCI.3334-07.2007

De Boulle, K., Verkerk, A. J., Reyniers, E., Vits, L., Hendrickx, J., Van Roy, B., . . . Willems, P. J. (1993). A point mutation in the FMR-1 gene associated with fragile X mental retardation. *Nat Genet, 3*(1), 31-35. doi:10.1038/ng0193-31

De Roo, M., Klauser, P., & Muller, D. (2008). LTP promotes a selective long-term stabilization and clustering of dendritic spines. *PLoS Biol, 6*(9), e219. doi:10.1371/journal.pbio.0060219

DeFelipe, J., Alonso-Nanclares, L., & Arellano, J. I. (2002). Microstructure of the neocortex: comparative aspects. *J Neurocytol, 31*(3-5), 299-316.

Derkach, V. A., Oh, M. C., Guire, E. S., & Soderling, T. R. (2007). Regulatory mechanisms of AMPA receptors in synaptic plasticity. *Nat Rev Neurosci, 8*(2), 101-113. doi:10.1038/nrn2055

Dolen, G., Osterweil, E., Rao, B. S., Smith, G. B., Auerbach, B. D., Chattarji, S., & Bear, M. F. (2007). Correction of fragile X syndrome in mice. *Neuron, 56*(6), 955-962.

Dolzhanskaya, N., Sung, Y. J., Conti, J., Currie, J. R., & Denman, R. B. (2003). The fragile X mental retardation protein interacts with U-rich RNAs in a yeast three-hybrid system. *Biochem Biophys Res Commun, 305*(2), 434-441.

Druckmann, S., Feng, L., Lee, B., Yook, C., Zhao, T., Magee, J. C., & Kim, J. (2014). Structured synaptic connectivity between hippocampal regions. *Neuron, 81*(3), 629-640. doi:10.1016/j.neuron.2013.11.026

Dunaevsky, A., Tashiro, A., Majewska, A., Mason, C., & Yuste, R. (1999). Developmental regulation of spine motility in the mammalian central nervous system. *Proc Natl Acad Sci USA, 96*, 13438-13443.

Eberhart, D. E., Malter, H. E., Feng, Y., & Warren, S. T. (1996). The fragile X mental retardation protein is a ribonucleoprotein containing both nuclear localization and nuclear export signals. *Hum Mol Genet, 5*(8), 1083-1091.

Ehlers, M. D., Heine, M., Groc, L., Lee, M. C., & Choquet, D. (2007). Diffusional trapping of GluR1 AMPA receptors by input-specific synaptic activity. *Neuron, 54*(3), 447-460. doi:10.1016/j.neuron.2007.04.010

Eliez, S., Blasey, C. M., Freund, L. S., Hastie, T., & Reiss, A. L. (2001). Brain anatomy, gender and IQ in children and adolescents with fragile X syndrome. *Brain, 124*(Pt 8), 1610-1618.

Engert, F., & Bonhoeffer, T. (1999a). Dendritic spine changes associated with hippocampal long-term synaptic plasticity. *Nature, 399*(6731), 66-70. doi:10.1038/19978

Engert, F., & Bonhoeffer, T. (1999b). Dendritic spine changes associated with hippocampal long-term synaptic plasticity. *Nature, 399*, 66-70.

Entezam, A., Biacsi, R., Orrison, B., Saha, T., Hoffman, G. E., Grabczyk, E., . . . Usdin, K. (2007). Regional FMRP deficits and large repeat expansions into the full mutation range in a new Fragile X premutation mouse model. *Gene, 395*(1-2), 125-134. doi:10.1016/j.gene.2007.02.026

Feng, G., Mellor, R. H., Bernstein, M., Keller-Peck, C., Nguyen, Q. T., Wallace, M., . . . Sanes, J. R. (2000). Imaging neuronal subsets in transgenic mice expressing multiple spectral variants of GFP. *Neuron, 28*(1), 41-51.

Feng, Y., Gutekunst, C. A., Eberhart, D. E., Yi, H., Warren, S. T., & Hersch, S. M. (1997). Fragile X mental retardation protein: nucleocytoplasmic shuttling and association with somatodendritic ribosomes. *J. Neursoci., 17*, 1539-1547.

Fiala, J. C., Allwardt, B., & Harris, K. M. (2002). Dendritic spines do not split during hippocampal LTP or maturation. *Nat Neurosci, 5*(4), 297-298.

Fonseca, R., Nagerl, U. V., & Bonhoeffer, T. (2006). Neuronal activity determines the protein synthesis dependence of long-term potentiation. *Nat Neurosci, 9*(4), 478-480. doi:10.1038/nn1667

Fonseca, R., Nagerl, U. V., Morris, R. G., & Bonhoeffer, T. (2004). Competing for memory: hippocampal LTP under regimes of reduced protein synthesis. *Neuron, 44*(6), 1011-1020. doi:10.1016/j.neuron.2004.10.033

Frankland, P. W., Wang, Y., Rosner, B., Shimizu, T., Balleine, B. W., Dykens, E. M., . . . Silva, A. J. (2004). Sensorimotor gating abnormalities in young males with fragile X syndrome and Fmr1-knockout mice. *Mol Psychiatry, 9*(4), 417-425.

Fu, M., Yu, X., Lu, J., & Zuo, Y. (2012). Repetitive motor learning induces coordinated formation of clustered dendritic spines in vivo. *Nature, 483*(7387), 92-95. doi:10.1038/nature10844

Fu, M., & Zuo, Y. (2011). Experience-dependent structural plasticity in the cortex. *Trends Neurosci, 34*(4), 177-187. doi:10.1016/j.tins.2011.02.001

Fu, Y. H., Kuhl, D. P., Pizzuti, A., Pieretti, M., Sutcliffe, J. S., Richards, S., . . . et al. (1991). Variation of the CGG repeat at the fragile X site results in genetic instability: resolution of the Sherman paradox. *Cell, 67*(6), 1047-1058.

Galvez, R., & Greenough, W. T. (2005). Sequence of abnormal dendritic spine development in primary somatosensory cortex of a mouse model of the fragile X mental retardation syndrome. *Am J Med Genet A, 135*(2), 155-160. doi:10.1002/ajmg.a.30709

Gernsbacher, M. A., Sauer, E. A., Geye, H. M., Schweigert, E. K., & Hill Goldsmith, H. (2008). Infant and toddler oral- and manual-motor skills predict later speech fluency in autism. *J Child Psychol Psychiatry, 49*(1), 43-50.

Gocel, J., & Larson, J. (2012). Synaptic NMDA receptor-mediated currents in anterior piriform cortex are reduced in the adult fragile X mouse. *Neuroscience, 221*, 170-181. doi:10.1016/j.neuroscience.2012.06.052

Godfraind, J. M., Reyniers, E., De Boulle, K., D'Hooge, R., De Deyn, P. P., Bakker, C. E., . . . Willems, P. J. (1996). Long-term potentiation in the hippocampus of fragile X knockout mice. *Am J Med Genet, 64*(2), 246-251.

doi:10.1002/(SICI)1096-8628(19960809)64:2<246::AID-AJMG2>3.0.CO;2-S

Govindarajan, A., Kelleher, R. J., & Tonegawa, S. (2006). A clustered plasticity model of long-term memory engrams. *Nat Rev Neurosci, 7*(7), 575-583. doi:10.1038/nrn1937

Grahn, J. A., Parkinson, J. A., & Owen, A. M. (2008). The cognitive functions of the caudate nucleus. *Prog Neurobiol, 86*(3), 141-155. doi:10.1016/j.pneurobio.2008.09.004

Granger, A. J., & Nicoll, R. A. (2014). Expression mechanisms underlying long-term potentiation: a postsynaptic view, 10 years on. *Philos Trans R Soc Lond B Biol Sci, 369*(1633), 20130136. doi:10.1098/rstb.2013.0136

Granger, A. J., Shi, Y., Lu, W., Cerpas, M., & Nicoll, R. A. (2013). LTP requires a reserve pool of glutamate receptors independent of subunit type. *Nature, 493*(7433), 495-500. doi:10.1038/nature11775

Gray, E. G. (1959). Axo-somatic and axo-dendritic synapses of the cerebral cortex: an electron microscopic study. *J. Anat., 83*, 420-433.

Gray, E. G. (1959). Axo-somatic and axo-dendritic synapses of the cerebral cortex: an electron microscope study. *J Anat, 93*, 420-433.

Gray, N. W., Weimer, R. M., Bureau, I., & Svoboda, K. (2006). Rapid redistribution of synaptic PSD-95 in the neocortex in vivo. *PLoS Biol, 4*(11), e370. doi:10.1371/journal.pbio.0040370

Gross, C., Berry-Kravis, E. M., & Bassell, G. J. (2012). Therapeutic strategies in fragile X syndrome: dysregulated mGluR signaling and beyond. *Neuropsychopharmacology, 37*(1), 178-195. doi:10.1038/npp.2011.137

Grutzendler, J., Kasthuri, N., & Gan, W. B. (2002). Long-term dendritic spine stability in the adult cortex. *Nature, 420*(6917), 812-816.

Guo, W., Murthy, A. C., Zhang, L., Johnson, E. B., Schaller, E. G., Allan, A. M., & Zhao, X. (2012). Inhibition of GSK3beta improves hippocampus-dependent learning and rescues neurogenesis in a mouse model of fragile X syndrome. *Hum Mol Genet, 21*(3), 681-691. doi:10.1093/hmg/ddr501

Guo, W., Polich, E. D., Su, J., Gao, Y., Christopher, D. M., Allan, A. M., . . . Zhao, X. (2015). Fragile X Proteins FMRP and FXR2P Control Synaptic GluA1 Expression and Neuronal Maturation via Distinct Mechanisms. *Cell Rep, 11*(10), 1651-1666. doi:10.1016/j.celrep.2015.05.013

Gustafsson, B., & Wigstrom, H. (1990). Long-term potentiation in the hippocampal CA1 region: its induction and early temporal development. *Prog Brain Res, 83*, 223-232.

Hagerman, R., & Hagerman, P. (2013). Advances in clinical and molecular understanding of the FMR1 premutation and fragile X-associated tremor/ataxia syndrome. *Lancet Neurol, 12*(8), 786-798. doi:10.1016/S1474-4422(13)70125-X

Hagerman, R., Lauterborn, J., Au, J., & Berry-Kravis, E. (2012). Fragile X syndrome and targeted treatment trials. *Results Probl Cell Differ, 54*, 297-335. doi:10.1007/978-3-642-21649-7_17

Hagerman, R. J., Berry-Kravis, E., Kaufmann, W. E., Ono, M. Y., Tartaglia, N., Lachiewicz, A., . . . Tranfaglia, M. (2009). Advances in the treatment of fragile X syndrome. *Pediatrics, 123*(1), 378-390. doi:10.1542/peds.2008-0317

Harms, K. J., Rioult-Pedotti, M. S., Carter, D. R., & Dunaevsky, A. (2008). Transient spine expansion and learning-induced plasticity in layer 1 primary motor cortex. *J Neurosci, 28*(22), 5686-5690.

Harris, K. M., Fiala, J. C., & Ostroff, L. (2003). Structural changes at dendritic spine synapses during long-term potentiation. *Philos Trans R Soc Lond B Biol Sci, 358*(1432), 745-748.

Harris, K. M., Jensen, F. E., & Tsao, B. (1992). Three-dimensional structure of dendritic spines and synapses in rat hippocampus (CA1) at postnatal day 15 and adult ages: implications for the maturation of synaptic physiology and long-term potentiation. *J. Neurosci., 12*, 2685-2705.

Harris, K. M., & Stevens, J. K. (1989). Dendritic spines of CA1 pyramidal cells in the rat hippocampus: serial electron microscopy with reference to their biophysical characteristics. *J. Neurosci., 9*, 2982-2997.

Harvey, C. D., Yasuda, R., Zhong, H., & Svoboda, K. (2008). The spread of Ras activity triggered by activation of a single dendritic spine. *Science, 321*(5885), 136-140. doi:10.1126/science.1159675

Hasegawa, S., Sakuragi, S., Tominaga-Yoshino, K., & Ogura, A. (2015). Dendritic spine dynamics leading to spine elimination after repeated inductions of LTD. *Sci Rep, 5*, 7707. doi:10.1038/srep07707

Hayashi-Takagi, A., Yagishita, S., Nakamura, M., Shirai, F., Wu, Y. I., Loshbaugh, A. L., . . . Kasai, H. (2015). Labelling and optical erasure of synaptic memory traces in the motor cortex. *Nature, 525*(7569), 333-338. doi:10.1038/nature15257

Hayashi, M. L., Rao, B. S., Seo, J. S., Choi, H. S., Dolan, B. M., Choi, S. Y., . . . Tonegawa, S. (2007). Inhibition of p21-activated kinase rescues symptoms of fragile X syndrome in mice. *Proc Natl Acad Sci U S A, 104*(27), 11489-11494. doi:10.1073/pnas.0705003104

He, C. X., & Portera-Cailliau, C. (2013). The trouble with spines in fragile X syndrome: density, maturity and plasticity. *Neuroscience, 251*, 120-128. doi:10.1016/j.neuroscience.2012.03.049

He, Q., Nomura, T., Xu, J., & Contractor, A. (2014). The developmental switch in GABA polarity is delayed in fragile X mice. *J Neurosci, 34*(2), 446-450. doi:10.1523/JNEUROSCI.4447-13.2014

Hill, T. C., & Zito, K. (2013). LTP-induced long-term stabilization of individual nascent dendritic spines. *J Neurosci, 33*(2), 678-686. doi:10.1523/JNEUROSCI.1404-12.2013

Hinds, H. L., Ashley, C. T., Sutcliffe, J. S., Nelson, D. L., Warren, S. T., Housman, D. E., & Schalling, M. (1993). Tissue specific expression of FMR-1 provides evidence for a functional role in fragile X syndrome. *Nat Genet, 3*(1), 36-43. doi:10.1038/ng0193-36

Hinton, V. J., Brown, W. T., Wisniewski, K., & Rudelli, R. D. (1991). Analysis of neocortex in three males with the fragile X syndrome. *Am. J. Med. Genet., 41*, 289-294.

Hirst, M. C., Knight, S. J., Christodoulou, Z., Grewal, P. K., Fryns, J. P., & Davies, K. E. (1993). Origins of the fragile X syndrome mutation. *J Med Genet, 30*(8), 647-650.

Hodgson, R. A., Ji, Z., Standish, S., Boyd-Hodgson, T. E., Henderson, A. K., & Racine, R. J. (2005). Training-induced and electrically induced potentiation in the neocortex. *Neurobiol Learn Mem, 83*(1), 22-32.

Hoeft, F., Carter, J. C., Lightbody, A. A., Cody Hazlett, H., Piven, J., & Reiss, A. L. (2010). Region-specific alterations in brain development in one- to three-year-old boys with fragile X syndrome. *Proc Natl Acad Sci U S A, 107*(20), 9335-9339. doi:10.1073/pnas.1002762107

Hofer, S. B., & Bonhoeffer, T. (2010). Dendritic spines: the stuff that memories are made of? *Curr Biol, 20*(4), R157-159. doi:10.1016/j.cub.2009.12.040

Hollmann, M., & Heinemann, S. (1994). Cloned glutamate receptors. *Annu Rev Neurosci, 17*, 31-108. doi:10.1146/annurev.ne.17.030194.000335

Holtmaat, A., Bonhoeffer, T., Chow, D. K., Chuckowree, J., De Paola, V., Hofer, S. B., . . . Wilbrecht, L. (2009). Long-term, high-resolution imaging in the mouse neocortex through a chronic cranial window. *Nat Protoc, 4*(8), 1128-1144. doi:10.1038/nprot.2009.89

Holtmaat, A., & Svoboda, K. (2009). Experience-dependent structural synaptic plasticity in the mammalian brain. *Nat Rev Neurosci, 10*(9), 647-658. doi:10.1038/nrn2699

Holtmaat, A., Wilbrecht, L., Knott, G. W., Welker, E., & Svoboda, K. (2006). Experience-dependent and cell-type-specific spine growth in the neocortex. *Nature, 441*(7096), 979-983.

Holtmaat, A. J., Trachtenberg, J. T., Wilbrecht, L., Shepherd, G. M., Zhang, X., Knott, G. W., & Svoboda, K. (2005). Transient and persistent dendritic spines in the neocortex in vivo. *Neuron, 45*(2), 279-291.

Hopfield, J. J. (1982). Neural networks and physical systems with emergent collective computational abilities. *Proc Natl Acad Sci U S A, 79*(8), 2554-2558.

Hou, L., Antion, M. D., Hu, D., Spencer, C. M., Paylor, R., & Klann, E. (2006). Dynamic translational and proteasomal regulation of fragile X mental retardation protein controls mGluR-dependent long-term depression. *Neuron, 51*(4), 441-454. doi:10.1016/j.neuron.2006.07.005

Hu, H., Qin, Y., Bochorishvili, G., Zhu, Y., van Aelst, L., & Zhu, J. J. (2008). Ras signaling mechanisms underlying impaired GluR1-dependent plasticity associated with fragile X syndrome. *J Neurosci, 28*(31), 7847-7862.

Huber, K. M., Gallagher, S. M., Warren, S. T., & Bear, M. F. (2002). Altered synaptic plasticity in a mouse model of fragile X mental retardation. *Proc Natl Acad Sci U S A, 99*(11), 7746-7750.

Huber, K. M., Kayser, M. S., & Bear, M. F. (2000). Role for rapid dendritic protein synthesis in hippocampal mGluR-dependent long-term depression. *Science, 288*(5469), 1254-1257.

Huber, K. M., Roder, J. C., & Bear, M. F. (2001). Chemical induction of mGluR5- and protein synthesis--dependent long-term depression in hippocampal area CA1. *J Neurophysiol, 86*(1), 321-325.

Huganir, R. L., & Nicoll, R. A. (2013). AMPARs and synaptic plasticity: the last 25 years. *Neuron, 80*(3), 704-717. doi:10.1016/j.neuron.2013.10.025

Irwin, S. A., Galvez, R., & Greenough, W. T. (2000). Dendritic spine structural anomalies in fragile-X mental retardation syndrome. *Cereb. Cortex, 10*, 1038-1044.

Irwin, S. A., Patel, B., Idupulapati, M., Harris, J. B., Crisostomo, R. A., Larsen, B. P., . . . Greenough, W. T. (2001). Abnormal dendritic spine characteristics in the temporal and visual cortices of patients with fragile-X syndrome: a quantitative examination. *Am J Med Genet, 98*(2), 161-167.

Ito, M., Sakurai, M., & Tongroach, P. (1982). Climbing fibre induced depression of both mossy fibre responsiveness and glutamate sensitivity of cerebellar Purkinje cells. *J Physiol, 324*, 113-134.

Jennifer L. Hodges, X. Y., Anthony Gilmore, Hannah Bennett, Michelle Tjia, James F. Perna, Chia-Chien Chen, Xiang Li, Ju Lu, Yi Zuo. (2016). Astrocytic

Contributions to Synaptic and Learning Abnormalities in a Mouse Model of Fragile X Syndrome. *Biological Psychiatry*.

Jeon, S. J., Han, S. H., Yang, S. I., Choi, J. W., Kwon, K. J., Park, S. H., . . . Shin, C. Y. (2012). Positive feedback regulation of Akt-FMRP pathway protects neurons from cell death. *J Neurochem, 123*(2), 226-238. doi:10.1111/j.1471-4159.2012.07886.x

Jeon, S. J., Seo, J. E., Yang, S. I., Choi, J. W., Wells, D., Shin, C. Y., & Ko, K. H. (2011). Cellular stress-induced up-regulation of FMRP promotes cell survival by modulating PI3K-Akt phosphorylation cascades. *J Biomed Sci, 18*, 17. doi:10.1186/1423-0127-18-17

Kaplan, D. M., Liu, A. M., Abrams, M. T., Warsofsky, I. S., Kates, W. R., White, C. D., . . . Reiss, A. L. (1997). Application of an automated parcellation method to the analysis of pediatric brain volumes. *Psychiatry Res, 76*(1), 15-27.

Kasai, H., Matsuzaki, M., Noguchi, J., Yasumatsu, N., & Nakahara, H. (2003). Structure-stability-function relationships of dendritic spines. *Trends Neurosci, 26*(7), 360-368.

Kastellakis, G., Cai, D. J., Mednick, S. C., Silva, A. J., & Poirazi, P. (2015). Synaptic clustering within dendrites: an emerging theory of memory formation. *Prog Neurobiol, 126*, 19-35. doi:10.1016/j.pneurobio.2014.12.002

Kates, W. R., Abrams, M. T., Kaufmann, W. E., Breiter, S. N., & Reiss, A. L. (1997). Reliability and validity of MRI measurement of the amygdala and hippocampus in children with fragile X syndrome. *Psychiatry Res, 75*(1), 31-48.

Kessels, H. W., Kopec, C. D., Klein, M. E., & Malinow, R. (2009). Roles of stargazin and phosphorylation in the control of AMPA receptor subcellular distribution. *Nat Neurosci, 12*(7), 888-896. doi:10.1038/nn.2340

Khandjian, E. W., Corbin, F., Woerly, S., & Rousseau, F. (1996). The fragile X mental retardation protein is associated with ribosomes. *Nat Genet, 12*(1), 91-93. doi:10.1038/ng0196-91

Kim, H., Gibboni, R., Kirkhart, C., & Bao, S. (2013). Impaired critical period plasticity in primary auditory cortex of fragile X model mice. *J Neurosci, 33*(40), 15686-15692. doi:10.1523/JNEUROSCI.3246-12.2013

Kim, M., Bellini, M., & Ceman, S. (2009). Fragile X mental retardation protein FMRP binds mRNAs in the nucleus. *Mol Cell Biol, 29*(1), 214-228. doi:10.1128/MCB.01377-08

Kleim, J. A., Lussnig, E., Schwarz, E. R., Comery, T. A., & Greenough, W. T. (1996). Synaptogenesis and Fos expression in the motor cortex of the adult rat after motor skill learning. *J Neurosci, 16*(14), 4529-4535.

Kleindienst, T., Winnubst, J., Roth-Alpermann, C., Bonhoeffer, T., & Lohmann, C. (2011). Activity-dependent clustering of functional synaptic inputs on developing hippocampal dendrites. *Neuron, 72*(6), 1012-1024. doi:10.1016/j.neuron.2011.10.015

Koekkoek, S. K., Yamaguchi, K., Milojkovic, B. A., Dortland, B. R., Ruigrok, T. J., Maex, R., . . . De Zeeuw, C. I. (2005). Deletion of FMR1 in Purkinje cells enhances parallel fiber LTD, enlarges spines, and attenuates cerebellar eyelid conditioning in Fragile X syndrome. *Neuron, 47*(3), 339-352.

Koga, K., Liu, M. G., Qiu, S., Song, Q., O'Den, G., Chen, T., & Zhuo, M. (2015). Impaired presynaptic long-term potentiation in the anterior cingulate cortex of Fmr1 knock-out mice. *J Neurosci, 35*(5), 2033-2043. doi:10.1523/JNEUROSCI.2644-14.2015

Kooy, R. F., D'Hooge, R., Reyniers, E., Bakker, C. E., Nagels, G., De Boulle, K., . . . Willems, P. J. (1996). Transgenic mouse model for the fragile X syndrome. *Am J Med Genet, 64*(2), 241-245. doi:10.1002/(SICI)1096-8628(19960809)64:2<241::AID-AJMG1>3.0.CO;2-X

Kopec, C. D., Li, B., Wei, W., Boehm, J., & Malinow, R. (2006). Glutamate receptor exocytosis and spine enlargement during chemically induced long-term potentiation. *J Neurosci, 26*(7), 2000-2009.

Kopec, C. D., Real, E., Kessels, H. W., & Malinow, R. (2007). GluR1 links structural and functional plasticity at excitatory synapses. *J Neurosci, 27*(50), 13706-13718.

Krueger, D. D., & Bear, M. F. Toward Fulfilling the Promise of Molecular Medicine in Fragile X Syndrome. *Annu Rev Med*.

Krueger, D. D., Osterweil, E. K., Chen, S. P., Tye, L. D., & Bear, M. F. (2011). Cognitive dysfunction and prefrontal synaptic abnormalities in a mouse model of fragile X syndrome. *Proc Natl Acad Sci U S A*.

Kuhlman, S. J., O'Connor, D. H., Fox, K., & Svoboda, K. (2014). Structural plasticity within the barrel cortex during initial phases of whisker-dependent learning. *J Neurosci, 34*(17), 6078-6083. doi:10.1523/JNEUROSCI.4919-12.2014

Lachiewicz, A., Dawson, D., Spiridigliozzi, G., Cuccaro, M., Lachiewicz, M., & McConkie-Rosell, A. (2010). Indicators of anxiety and depression in women with the fragile X premutation: assessment of a clinical sample. *J Intellect Disabil Res, 54*(7), 597-610. doi:10.1111/j.1365-2788.2010.01290.x

Lai, C. S., Franke, T. F., & Gan, W. B. (2012). Opposite effects of fear conditioning and extinction on dendritic spine remodelling. *Nature, 483*(7387), 87-91. doi:10.1038/nature10792

Lee, K. F., Soares, C., & Beique, J. C. (2012). Examining form and function of dendritic spines. *Neural Plast, 2012*, 704103. doi:10.1155/2012/704103

Li, Z., Jo, J., Jia, J. M., Lo, S. C., Whitcomb, D. J., Jiao, S., . . . Sheng, M. (2010). Caspase-3 activation via mitochondria is required for long-term depression and AMPA receptor internalization. *Cell, 141*(5), 859-871. doi:10.1016/j.cell.2010.03.053

Link, W., Konietzko, U., Kauselmann, G., Krug, M., Schwanke, B., Frey, U., & Kuhl, D. (1995). Somatodendritic expression of an immediate early gene is regulated by synaptic activity. *Proc Natl Acad Sci U S A, 92*(12), 5734-5738.

Lisman, J. (1989). A mechanism for the Hebb and the anti-Hebb processes underlying learning and memory. *Proc Natl Acad Sci U S A, 86*(23), 9574-9578.

Liu, Z. H., Chuang, D. M., & Smith, C. B. (2011). Lithium ameliorates phenotypic deficits in a mouse model of fragile X syndrome. *Int J*

Neuropsychopharmacol, 14(5), 618-630. doi:10.1017/S1461145710000520

Losonczy, A., & Magee, J. C. (2006). Integrative properties of radial oblique dendrites in hippocampal CA1 pyramidal neurons. *Neuron, 50*(2), 291-307. doi:10.1016/j.neuron.2006.03.016

Lu, R., Wang, H., Liang, Z., Ku, L., O'Donnell W, T., Li, W., . . . Feng, Y. (2004). The fragile X protein controls microtubule-associated protein 1B translation and microtubule stability in brain neuron development. *Proc Natl Acad Sci U S A, 101*(42), 15201-15206. doi:10.1073/pnas.0404995101

Lu, W., Shi, Y., Jackson, A. C., Bjorgan, K., During, M. J., Sprengel, R., . . . Nicoll, R. A. (2009). Subunit composition of synaptic AMPA receptors revealed by a single-cell genetic approach. *Neuron, 62*(2), 254-268. doi:10.1016/j.neuron.2009.02.027

Luo, S. Y., Wu, L. Q., & Duan, R. H. (2016). Molecular medicine of fragile X syndrome: based on known molecular mechanisms. *World J Pediatr, 12*(1), 19-27. doi:10.1007/s12519-015-0052-0

Luscher, C., & Malenka, R. C. (2012). NMDA receptor-dependent long-term potentiation and long-term depression (LTP/LTD). *Cold Spring Harb Perspect Biol, 4*(6). doi:10.1101/cshperspect.a005710

Luscher, C., Nicoll, R. A., Malenka, R. C., & Muller, D. (2000). Synaptic plasticity and dynamic modulation of the postsynaptic membrane. *Nat Neurosci, 3*(6), 545-550.

Lyford, G. L., Yamagata, K., Kaufmann, W. E., Barnes, C. A., Sanders, L. K., Copeland, N. G., . . . Worley, P. F. (1995). Arc, a growth factor and activity-regulated gene, encodes a novel cytoskeleton-associated protein that is enriched in neuronal dendrites. *Neuron, 14*(2), 433-445.

Ma, L., Qiao, Q., Tsai, J. W., Yang, G., Li, W., & Gan, W. B. (2016). Experience-dependent plasticity of dendritic spines of layer 2/3 pyramidal neurons in the mouse cortex. *Dev Neurobiol, 76*(3), 277-286. doi:10.1002/dneu.22313

Makino, H., & Malinow, R. (2009). AMPA receptor incorporation into synapses during LTP: the role of lateral movement and exocytosis. *Neuron, 64*(3), 381-390. doi:10.1016/j.neuron.2009.08.035

Makino, H., & Malinow, R. (2011). Compartmentalized versus Global Synaptic Plasticity on Dendrites Controlled by Experience. *Neuron, 72*(6), 1001-1011. doi:S0896-6273(11)00993-7 [pii]

10.1016/j.neuron.2011.09.036

Malenka, R. C., & Bear, M. F. (2004). LTP and LTD: an embarrassment of riches. *Neuron, 44*(1), 5-21.

Malinow, R., & Malenka, R. C. (2002). AMPA receptor trafficking and synaptic plasticity. *Annu Rev Neurosci, 25*, 103-126.

Martin, H. G., Lassalle, O., Brown, J. T., & Manzoni, O. J. (2016). Age-Dependent Long-Term Potentiation Deficits in the Prefrontal Cortex of the Fmr1 Knockout Mouse Model of Fragile X Syndrome. *Cereb Cortex, 26*(5), 2084-2092. doi:10.1093/cercor/bhv031

Martin, J. P., & Bell, J. (1943). A Pedigree of Mental Defect Showing Sex-Linkage. *J Neurol Psychiatry, 6*(3-4), 154-157.

Matsuo, N., Reijmers, L., & Mayford, M. (2008). Spine-type-specific recruitment of newly synthesized AMPA receptors with learning. *Science, 319*(5866), 1104-1107.

Matsuzaki, M., Ellis-Davies, G. C., Nemoto, T., Miyashita, Y., Iino, M., & Kasai, H. (2001). Dendritic spine geometry is critical for AMPA receptor expression in hippocampal CA1 pyramidal neurons. *Nat Neurosci, 4*(11), 1086-1092.

Matsuzaki, M., Honkura, N., Ellis-Davies, G. C., & Kasai, H. (2004). Structural basis of long-term potentiation in single dendritic spines. *Nature, 429*(6993), 761-766.

McBride, T. J., Rodriguez-Contreras, A., Trinh, A., Bailey, R., & Debello, W. M. (2008). Learning drives differential clustering of axodendritic contacts in the barn owl auditory system. *J Neurosci, 28*(27), 6960-6973. doi:10.1523/JNEUROSCI.1352-08.2008

McKinney, B. C., Grossman, A. W., Elisseou, N. M., & Greenough, W. T. (2005). Dendritic spine abnormalities in the occipital cortex of C57BL/6 Fmr1 knockout mice. *Am J Med Genet B Neuropsychiatr Genet, 136*(1), 98-102.

McNaughton, B. L. (2003). Long-term potentiation, cooperativity and Hebb's cell assemblies: a personal history. *Philos Trans R Soc Lond B Biol Sci, 358*(1432), 629-634. doi:10.1098/rstb.2002.1231

Meredith, R. M., Holmgren, C. D., Weidum, M., Burnashev, N., & Mansvelder, H. D. (2007). Increased threshold for spike-timing-dependent plasticity is caused by unreliable calcium signaling in mice lacking fragile X gene FMR1. *Neuron, 54*(4), 627-638. doi:10.1016/j.neuron.2007.04.028

Miesenbock, G., De Angelis, D. A., & Rothman, J. E. (1998). Visualizing secretion and synaptic transmission with pH-sensitive green fluorescent proteins. *Nature, 394*(6689), 192-195. doi:10.1038/28190

Mines, M. A., Yuskaitis, C. J., King, M. K., Beurel, E., & Jope, R. S. (2010). GSK3 influences social preference and anxiety-related behaviors during social interaction in a mouse model of fragile X syndrome and autism. *PLoS One, 5*(3), e9706. doi:10.1371/journal.pone.0009706

Mineur, Y. S., Huynh, L. X., & Crusio, W. E. (2006). Social behavior deficits in the Fmr1 mutant mouse. *Behav Brain Res, 168*(1), 172-175. doi:10.1016/j.bbr.2005.11.004

Miyashiro, K. Y., Beckel-Mitchener, A., Purk, T. P., Becker, K. G., Barret, T., Liu, L., . . . Eberwine, J. (2003). RNA cargoes associating with FMRP reveal deficits in cellular functioning in Fmr1 null mice. *Neuron, 37*(3), 417-431.

Moczulska, K. E., Tinter-Thiede, J., Peter, M., Ushakova, L., Wernle, T., Bathellier, B., & Rumpel, S. (2013). Dynamics of dendritic spines in the mouse auditory cortex during memory formation and memory recall. *Proc Natl Acad Sci U S A, 110*(45), 18315-18320. doi:10.1073/pnas.1312508110

Mostofsky, S. H., Mazzocco, M. M., Aakalu, G., Warsofsky, I. S., Denckla, M. B., & Reiss, A. L. (1998). Decreased cerebellar posterior vermis size in fragile X syndrome: correlation with neurocognitive performance. *Neurology, 50*(1), 121-130.

Mostofsky, S. H., Mazzocco, M. M., Aakalu, G., Warsofsky, I. S., Denckla, M. B., & Reiss, A. L. (1998). Decreased cerebellar posterior vermis size in fragile X syndrome: correlation with neurocognitive performance. *Neurology, 50*, 121-130.

Moult, P. R., Gladding, C. M., Sanderson, T. M., Fitzjohn, S. M., Bashir, Z. I., Molnar, E., & Collingridge, G. L. (2006). Tyrosine phosphatases regulate AMPA receptor trafficking during metabotropic glutamate receptor-mediated long-term depression. *J Neurosci, 26*(9), 2544-2554. doi:10.1523/JNEUROSCI.4322-05.2006

Moult, P. R., Schnabel, R., Kilpatrick, I. C., Bashir, Z. I., & Collingridge, G. L. (2002). Tyrosine dephosphorylation underlies DHPG-induced LTD. *Neuropharmacology, 43*(2), 175-180.

Moy, S. S., Nadler, J. J., Perez, A., Barbaro, R. P., Johns, J. M., Magnuson, T. R., . . . Crawley, J. N. (2004). Sociability and preference for social novelty in five inbred strains: an approach to assess autistic-like behavior in mice. *Genes Brain Behav, 3*(5), 287-302. doi:10.1111/j.1601-1848.2004.00076.x

Mulkey, R. M., Endo, S., Shenolikar, S., & Malenka, R. C. (1994). Involvement of a calcineurin/inhibitor-1 phosphatase cascade in hippocampal long-term depression. *Nature, 369*(6480), 486-488. doi:10.1038/369486a0

Mulkey, R. M., Herron, C. E., & Malenka, R. C. (1993). An essential role for protein phosphatases in hippocampal long-term depression. *Science, 261*(5124), 1051-1055.

Murakoshi, H., Wang, H., & Yasuda, R. (2011). Local, persistent activation of Rho GTPases during plasticity of single dendritic spines. *Nature, 472*(7341), 100-104. doi:10.1038/nature09823

Nagaoka, A., Takehara, H., Hayashi-Takagi, A., Noguchi, J., Ishii, K., Shirai, F., . . . Kasai, H. (2016). Abnormal intrinsic dynamics of dendritic spines in a fragile X syndrome mouse model in vivo. *Sci Rep, 6*, 26651. doi:10.1038/srep26651

Nagerl, U. V., Eberhorn, N., Cambridge, S. B., & Bonhoeffer, T. (2004). Bidirectional activity-dependent morphological plasticity in hippocampal neurons. *Neuron, 44*(5), 759-767.

Nicoll, R. A., & Roche, K. W. (2013). Long-term potentiation: peeling the onion. *Neuropharmacology, 74*, 18-22. doi:10.1016/j.neuropharm.2013.02.010

Niere, F., Wilkerson, J. R., & Huber, K. M. (2012). Evidence for a fragile X mental retardation protein-mediated translational switch in metabotropic glutamate receptor-triggered Arc translation and long-term depression. *J Neurosci, 32*(17), 5924-5936. doi:10.1523/JNEUROSCI.4650-11.2012

Nimchinsky, E. A., Oberlander, A. M., & Svoboda, K. (2001). Abnormal development of dendritic spines in FMR1 knock-out mice. *J Neurosci, 21*(14), 5139-5146.

Nimchinsky, E. A., Sabatini, B. L., & Svoboda, K. (2002). Structure and function of dendritic spines. *Annu Rev Physiol, 64*, 313-353.

Nishiyama, J., & Yasuda, R. (2015). Biochemical Computation for Spine Structural Plasticity. *Neuron, 87*(1), 63-75. doi:10.1016/j.neuron.2015.05.043

Noguchi, J., Nagaoka, A., Watanabe, S., Ellis-Davies, G. C., Kitamura, K., Kano, M., . . . Kasai, H. (2011). In vivo two-photon uncaging of glutamate revealing the structure-function relationships of dendritic spines in the neocortex of adult mice. *J Physiol, 589*(Pt 10), 2447-2457. doi:jphysiol.2011.207100 [pii]

10.1113/jphysiol.2011.207100

O'Donnell, W. T., & Warren, S. T. (2002). A decade of molecular studies of fragile X syndrome. *Annu Rev Neurosci, 25*, 315-338. doi:10.1146/annurev.neuro.25.112701.142909

Oh, W. C., Parajuli, L. K., & Zito, K. (2015). Heterosynaptic structural plasticity on local dendritic segments of hippocampal CA1 neurons. *Cell Rep, 10*(2), 162-169. doi:10.1016/j.celrep.2014.12.016

Oliet, S. H., Malenka, R. C., & Nicoll, R. A. (1997). Two distinct forms of long-term depression coexist in CA1 hippocampal pyramidal cells. *Neuron, 18*(6), 969-982.

Olmos-Serrano, J. L., Corbin, J. G., & Burns, M. P. (2011). The GABA(A) receptor agonist THIP ameliorates specific behavioral deficits in the mouse model of fragile X syndrome. *Dev Neurosci, 33*(5), 395-403. doi:10.1159/000332884

Opazo, P., & Choquet, D. (2011). A three-step model for the synaptic recruitment of AMPA receptors. *Mol Cell Neurosci, 46*(1), 1-8. doi:10.1016/j.mcn.2010.08.014

Oray, S., Majewska, A., & Sur, M. (2004). Dendritic spine dynamics are regulated by monocular deprivation and extracellular matrix degradation. *Neuron, 44*(6), 1021-1030.

Ostroff, L. E., Fiala, J. C., Allwardt, B., & Harris, K. M. (2002). Polyribosomes redistribute from dendritic shafts into spines with enlarged synapses during LTP in developing rat hippocampal slices. *Neuron, 35*(3), 535-545.

Padmashri, R., Reiner, B. C., Suresh, A., Spartz, E., & Dunaevsky, A. (2013). Altered structural and functional synaptic plasticity with motor skill learning in a mouse model of fragile x syndrome. *J Neurosci, 33*(50), 19715-19723. doi:10.1523/JNEUROSCI.2514-13.2013

Palmer, M. J., Irving, A. J., Seabrook, G. R., Jane, D. E., & Collingridge, G. L. (1997). The group I mGlu receptor agonist DHPG induces a novel form of LTD in the CA1 region of the hippocampus. *Neuropharmacology, 36*(11-12), 1517-1532.

Pan, F., Aldridge, G. M., Greenough, W. T., & Gan, W. B. (2010). Dendritic spine instability and insensitivity to modulation by sensory experience in a mouse model of fragile X syndrome. *Proc Natl Acad Sci U S A, 107*(41), 17768-17773. doi:1012496107 [pii]

10.1073/pnas.1012496107

Paradee, W., Melikian, H. E., Rasmussen, D. L., Kenneson, A., Conn, P. J., & Warren, S. T. (1999). Fragile X mouse: strain effects of knockout phenotype and evidence suggesting deficient amygdala function. *Neuroscience, 94*(1), 185-192.

Park, S., Park, J. M., Kim, S., Kim, J. A., Shepherd, J. D., Smith-Hicks, C. L., . . . Worley, P. F. (2008). Elongation factor 2 and fragile X mental retardation

protein control the dynamic translation of Arc/Arg3.1 essential for mGluR-LTD. *Neuron, 59*(1), 70-83. doi:10.1016/j.neuron.2008.05.023

Patterson, M., & Yasuda, R. (2011). Signalling pathways underlying structural plasticity of dendritic spines. *Br J Pharmacol, 163*(8), 1626-1638. doi:10.1111/j.1476-5381.2011.01328.x

Patterson, M. A., Szatmari, E. M., & Yasuda, R. (2010). AMPA receptors are exocytosed in stimulated spines and adjacent dendrites in a Ras-ERK-dependent manner during long-term potentiation. *Proc Natl Acad Sci U S A, 107*(36), 15951-15956. doi:10.1073/pnas.0913875107

Peier, A. M., McIlwain, K. L., Kenneson, A., Warren, S. T., Paylor, R., & Nelson, D. L. (2000). (Over)correction of FMR1 deficiency with YAC transgenics: behavioral and physical features. *Hum Mol Genet, 9*(8), 1145-1159.

Penagarikano, O., Mulle, J. G., & Warren, S. T. (2007). The pathophysiology of fragile x syndrome. *Annu Rev Genomics Hum Genet, 8*, 109-129.

Penfield, W. B., E. (1937). SOMATIC MOTOR AND SENSORY REPRESENTATION IN THE CEREBRAL CORTEX OF MAN AS STUDIED BY ELECTRICAL STIMULATION *Brain: A Journal of Neurology*.

Peng, D. X., Kelley, R. G., Quintin, E. M., Raman, M., Thompson, P. M., & Reiss, A. L. (2014). Cognitive and behavioral correlates of caudate subregion shape variation in fragile X syndrome. *Hum Brain Mapp, 35*(6), 2861-2868. doi:10.1002/hbm.22376

Peng, J., Kim, M. J., Cheng, D., Duong, D. M., Gygi, S. P., & Sheng, M. (2004). Semiquantitative proteomic analysis of rat forebrain postsynaptic density fractions by mass spectrometry. *J Biol Chem, 279*(20), 21003-21011. doi:10.1074/jbc.M400103200

Penzes, P., Cahill, M. E., Jones, K. A., VanLeeuwen, J. E., & Woolfrey, K. M. (2011). Dendritic spine pathology in neuropsychiatric disorders. *Nat Neurosci, 14*(3), 285-293.

Peter Westfall, R. D. T., and Russell D. Wolfinger. (2011). Multiple Comparisons and Multiple Tests Using SAS@R. *Cary, NC, SAS Institute, Second Edition*.

Peters, A., & Kaiserman-Abramhof, I. R. (1970). The small pyramidal neuron of the rat cerebral cortex. The perikaryon, dendrites and spines. *Am. J. Anat., 127*, 321-356.

Peters, A., & Kaiserman-Abramof, I. R. (1970). The small pyramidal neuron of the rat cerebral cortex. The perikaryon, dendrites and spines. *Am J Anat, 127*(4), 321-355. doi:10.1002/aja.1001270402

Peters, A. J., Chen, S. X., & Komiyama, T. (2014). Emergence of reproducible spatiotemporal activity during motor learning. *Nature, 510*(7504), 263-267. doi:10.1038/nature13235

Pfeiffer, B. E., & Huber, K. M. (2009). The state of synapses in fragile X syndrome. *Neuroscientist, 15*(5), 549-567. doi:10.1177/1073858409333075

Phillips, M. J., & Voeltz, G. K. (2016). Structure and function of ER membrane contact sites with other organelles. *Nat Rev Mol Cell Biol, 17*(2), 69-82. doi:10.1038/nrm.2015.8

Poirazi, P., Brannon, T., & Mel, B. W. (2003a). Arithmetic of subthreshold synaptic summation in a model CA1 pyramidal cell. *Neuron, 37*(6), 977-987.

Poirazi, P., Brannon, T., & Mel, B. W. (2003b). Pyramidal neuron as two-layer neural network. *Neuron, 37*(6), 989-999.

Pologruto, T. A., Sabatini, B. L., & Svoboda, K. (2003). ScanImage: flexible software for operating laser scanning microscopes. *Biomed Eng Online, 2*, 13. doi:10.1186/1475-925X-2-13

Polsky, A., Mel, B. W., & Schiller, J. (2004). Computational subunits in thin dendrites of pyramidal cells. *Nat Neurosci, 7*(6), 621-627. doi:10.1038/nn1253

Purves, D., Augustine GJ, Fitzpatrick D. (2008). *Neuroscience 4th edition*: Sinauer Associated.

Ramon y Cajal, S. (1888). Estructura de los centros nervioso de las aves,. *Rev Trim Hitol norm Pat, 1*, 1-10.

Redondo, R. L., & Morris, R. G. (2011). Making memories last: the synaptic tagging and capture hypothesis. *Nat Rev Neurosci, 12*(1), 17-30. doi:10.1038/nrn2963

Reiner, B. C., & Dunaevsky, A. (2015). Deficit in motor training-induced clustering, but not stabilization, of new dendritic spines in FMR1 knock-out mice. *PLoS One, 10*(5), e0126572. doi:10.1371/journal.pone.0126572

Reiss, A. L., Lee, J., & Freund, L. (1994). Neuroanatomy of fragile X syndrome: the temporal lobe. *Neurology, 44*(7), 1317-1324.

Restivo, L., Ferrari, F., Passino, E., Sgobio, C., Bock, J., Oostra, B. A., . . . Ammassari-Teule, M. (2005). Enriched environment promotes behavioral and morphological recovery in a mouse model for the fragile X syndrome. *Proc Natl Acad Sci U S A, 102*(32), 11557-11562. doi:10.1073/pnas.0504984102

Rioult-Pedotti, M. S., Donoghue, J. P., & Dunaevsky, A. (2007). Plasticity of the synaptic modification range. *J Neurophysiol, 98*(6), 3688-3695.

Rioult-Pedotti, M. S., Friedman, D., & Donoghue, J. P. (2000). Learning-induced LTP in neocortex. *Science, 290*(5491), 533-536.

Rioult-Pedotti, M. S., Friedman, D., Hess, G., & Donoghue, J. P. (1998). Strengthening of horizontal cortical connections following skill learning. *Nat Neurosci, 1*(3), 230-234.

Roberts, T. F., Tschida, K. A., Klein, M. E., & Mooney, R. (2010). Rapid spine stabilization and synaptic enhancement at the onset of behavioural learning. *Nature, 463*(7283), 948-952. doi:10.1038/nature08759

Rodriguez-Revenga, L., Madrigal, I., Alegret, M., Santos, M., & Mila, M. (2008). Evidence of depressive symptoms in fragile-X syndrome premutated females. *Psychiatr Genet, 18*(4), 153-155. doi:10.1097/YPG.0b013e3282f97e0b

Roggenhofer, E., Fidzinski, P., Shor, O., & Behr, J. (2013). Reduced threshold for induction of LTP by activation of dopamine D1/D5 receptors at hippocampal CA1-subiculum synapses. *PLoS One, 8*(4), e62520. doi:10.1371/journal.pone.0062520

Ronesi, J. A., & Huber, K. M. (2008). Homer interactions are necessary for metabotropic glutamate receptor-induced long-term depression and

translational activation. *J Neurosci, 28*(2), 543-547. doi:10.1523/JNEUROSCI.5019-07.2008

Rotschafer, S. E., Trujillo, M. S., Dansie, L. E., Ethell, I. M., & Razak, K. A. (2012). Minocycline treatment reverses ultrasonic vocalization production deficit in a mouse model of Fragile X Syndrome. *Brain Res, 1439*, 7-14. doi:10.1016/j.brainres.2011.12.041

Roy, S., Watkins, N., & Heck, D. (2012). Comprehensive analysis of ultrasonic vocalizations in a mouse model of fragile X syndrome reveals limited, call type specific deficits. *PLoS One, 7*(9), e44816. doi:10.1371/journal.pone.0044816

Rudelli, R. D., Brown, W. T., Wisniewski, K., Jenkins, E. C., Laure-Kamionowska, M., Connel, W., & Wisniewski, H. M. (1985). Adult fragile X syndrome cliniconeuropathologic findings. *Acta Neuropathol., 67*, 289-295.

Rumpel, S., LeDoux, J., Zador, A., & Malinow, R. (2005). Postsynaptic receptor trafficking underlying a form of associative learning. *Science, 308*(5718), 83-88.

Sabaratnam, M., Murthy, N. V., Wijeratne, A., Buckingham, A., & Payne, S. (2003). Autistic-like behaviour profile and psychiatric morbidity in Fragile X Syndrome: a prospective ten-year follow-up study. *Eur Child Adolesc Psychiatry, 12*(4), 172-177. doi:10.1007/s00787-003-0333-3

Saito, T., & Nakatsuji, N. (2001). Efficient gene transfer into the embryonic mouse brain using in vivo electroporation. *Dev Biol, 240*(1), 237-246. doi:10.1006/dbio.2001.0439

Sala, C., & Segal, M. (2014). Dendritic spines: the locus of structural and functional plasticity. *Physiol Rev, 94*(1), 141-188. doi:10.1152/physrev.00012.2013

Santoro, M. R., Bray, S. M., & Warren, S. T. (2012). Molecular mechanisms of fragile X syndrome: a twenty-year perspective. *Annu Rev Pathol, 7*, 219-245. doi:10.1146/annurev-pathol-011811-132457

Santos, A. R., Kanellopoulos, A. K., & Bagni, C. (2014). Learning and behavioral deficits associated with the absence of the fragile X mental retardation

protein: what a fly and mouse model can teach us. *Learn Mem, 21*(10), 543-555. doi:10.1101/lm.035956.114

Segal, M., Vlachos, A., & Korkotian, E. (2010). The spine apparatus, synaptopodin, and dendritic spine plasticity. *Neuroscientist, 16*(2), 125-131. doi:10.1177/1073858409355829

Seog, D. H. (2004). Glutamate receptor-interacting protein 1 protein binds to the microtubule-associated protein. *Biosci Biotechnol Biochem, 68*(8), 1808-1810. doi:10.1271/bbb.68.1808

Shang, Y., Wang, H., Mercaldo, V., Li, X., Chen, T., & Zhuo, M. (2009). Fragile X mental retardation protein is required for chemically-induced long-term potentiation of the hippocampus in adult mice. *J Neurochem, 111*(3), 635-646. doi:10.1111/j.1471-4159.2009.06314.x

Sheng, M., & Hoogenraad, C. C. (2007). The postsynaptic architecture of excitatory synapses: a more quantitative view. *Annu Rev Biochem, 76*, 823-847. doi:10.1146/annurev.biochem.76.060805.160029

Shepherd, J. D., & Huganir, R. L. (2007). The cell biology of synaptic plasticity: AMPA receptor trafficking. *Annu Rev Cell Dev Biol, 23*, 613-643. doi:10.1146/annurev.cellbio.23.090506.123516

Sherman, S., Pletcher, B. A., & Driscoll, D. A. (2005). Fragile X syndrome: diagnostic and carrier testing. *Genet Med, 7*(8), 584-587. doi:10.109701.GIM.0000182468.22666.dd

Shi, S. H., Hayashi, Y., Petralia, R. S., Zaman, S. H., Wenthold, R. J., Svoboda, K., & Malinow, R. (1999). Rapid spine delivery and redistribution of AMPA receptors after synaptic NMDA receptor activation. *Science, 284*(5421), 1811-1816.

Shmuelof, L., & Krakauer, J. W. (2011). Are we ready for a natural history of motor learning? *Neuron, 72*(3), 469-476. doi:10.1016/j.neuron.2011.10.017

Snyder, E. M., Philpot, B. D., Huber, K. M., Dong, X., Fallon, J. R., & Bear, M. F. (2001). Internalization of ionotropic glutamate receptors in response to mGluR activation. *Nat Neurosci, 4*(11), 1079-1085. doi:10.1038/nn746

nn746 [pii]

Spacek, J. (1985). Three-dimensional analysis of dendritic spines. II. Spine apparatus and other cytoplasmic components. *Anat Embryol (Berl), 171*(2), 235-243.

Spacek, J., & Harris, K. M. (1997). Three-dimensional organization of smooth endoplasmic reticulum in hippocampal CA1 dendrites and dendritic spines of the immature and mature rat. *J Neurosci, 17*(1), 190-203.

Spencer, C. M., Alekseyenko, O., Serysheva, E., Yuva-Paylor, L. A., & Paylor, R. (2005). Altered anxiety-related and social behaviors in the Fmr1 knockout mouse model of fragile X syndrome. *Genes Brain Behav, 4*(7), 420-430. doi:10.1111/j.1601-183X.2005.00123.x

Stevens, F. L., Hurley, R. A., & Taber, K. H. (2011). Anterior cingulate cortex: unique role in cognition and emotion. *J Neuropsychiatry Clin Neurosci, 23*(2), 121-125. doi:10.1176/appi.neuropsych.23.2.121

10.1176/jnp.23.2.jnp121

Steward, O., & Levy, W. B. (1982). Preferential localization of polyribosomes under the base of dendritic spines in granule cells of the dentate gyrus. *J Neurosci, 2*(3), 284-291.

Su, T., Fan, H. X., Jiang, T., Sun, W. W., Den, W. Y., Gao, M. M., . . . Yi, Y. H. (2011). Early continuous inhibition of group 1 mGlu signaling partially rescues dendritic spine abnormalities in the Fmr1 knockout mouse model for fragile X syndrome. *Psychopharmacology (Berl), 215*(2), 291-300. doi:10.1007/s00213-010-2130-2

Suresh, A., & Dunaevsky, A. (2015). Preparation of Synaptosomes from the Motor Cortex of Motor Skill Trained Mice. *Bio Protoc, 5*(4).

Suvrathan, A., Hoeffer, C. A., Wong, H., Klann, E., & Chattarji, S. (2010). Characterization and reversal of synaptic defects in the amygdala in a mouse model of fragile X syndrome. *Proc Natl Acad Sci U S A, 107*(25), 11591-11596.

Svitkina, T., Lin, W. H., Webb, D. J., Yasuda, R., Wayman, G. A., Van Aelst, L., & Soderling, S. H. (2010). Regulation of the postsynaptic cytoskeleton: roles

in development, plasticity, and disorders. *J Neurosci, 30*(45), 14937-14942. doi:10.1523/JNEUROSCI.4276-10.2010

Tabolacci, E., Moscato, U., Zalfa, F., Bagni, C., Chiurazzi, P., & Neri, G. (2008). Epigenetic analysis reveals a euchromatic configuration in the FMR1 unmethylated full mutations. *Eur J Hum Genet, 16*(12), 1487-1498. doi:10.1038/ejhg.2008.130

Takahashi, N., Kitamura, K., Matsuo, N., Mayford, M., Kano, M., Matsuki, N., & Ikegaya, Y. (2012). Locally synchronized synaptic inputs. *Science, 335*(6066), 353-356. doi:10.1126/science.1210362

Takahashi, T., Svoboda, K., & Malinow, R. (2003). Experience strengthening transmission by driving AMPA receptors into synapses. *Science, 299*(5612), 1585-1588.

Tamanini, F., Willemsen, R., van Unen, L., Bontekoe, C., Galjaard, H., Oostra, B. A., & Hoogeveen, A. T. (1997). Differential expression of FMR1, FXR1 and FXR2 proteins in human brain and testis. *Hum Mol Genet, 6*(8), 1315-1322.

Tennant, K. A., Adkins, D. L., Donlan, N. A., Asay, A. L., Thomas, N., Kleim, J. A., & Jones, T. A. (2011). The Organization of the Forelimb Representation of the C57BL/6 Mouse Motor Cortex as Defined by Intracortical Microstimulation and Cytoarchitecture. *Cereb Cortex*.

Todd, P. K., Mack, K. J., & Malter, J. S. (2003). The fragile X mental retardation protein is required for type-I metabotropic glutamate receptor-dependent translation of PSD-95. *Proc Natl Acad Sci U S A, 100*(24), 14374-14378. doi:10.1073/pnas.2336265100

Tonnesen, J., Katona, G., Rozsa, B., & Nagerl, U. V. (2014). Spine neck plasticity regulates compartmentalization of synapses. *Nat Neurosci, 17*(5), 678-685. doi:10.1038/nn.3682

Tonnesen, J., & Nagerl, U. V. (2016). Dendritic Spines as Tunable Regulators of Synaptic Signals. *Front Psychiatry, 7*, 101. doi:10.3389/fpsyt.2016.00101

Trachtenberg, J. T., Chen, B. E., Knott, G. W., Feng, G., Sanes, J. R., Welker, E., & Svoboda, K. (2002). Long-term in vivo imaging of experience-dependent synaptic plasticity in adult cortex. *Nature, 420*(6917), 788-794.

Traynelis, S. F., Wollmuth, L. P., McBain, C. J., Menniti, F. S., Vance, K. M., Ogden, K. K., . . . Dingledine, R. (2010). Glutamate receptor ion channels: structure, regulation, and function. *Pharmacol Rev, 62*(3), 405-496. doi:10.1124/pr.109.002451

Tsai, N. P., Wilkerson, J. R., Guo, W., Maksimova, M. A., DeMartino, G. N., Cowan, C. W., & Huber, K. M. (2012). Multiple autism-linked genes mediate synapse elimination via proteasomal degradation of a synaptic scaffold PSD-95. *Cell, 151*(7), 1581-1594. doi:10.1016/j.cell.2012.11.040

Turrigiano, G. (2012). Homeostatic synaptic plasticity: local and global mechanisms for stabilizing neuronal function. *Cold Spring Harb Perspect Biol, 4*(1), a005736. doi:10.1101/cshperspect.a005736

Van der Molen, M. J., Huizinga, M., Huizenga, H. M., Ridderinkhof, K. R., Van der Molen, M. W., Hamel, B. J., . . . Ramakers, G. J. (2010). Profiling Fragile X Syndrome in males: strengths and weaknesses in cognitive abilities. *Res Dev Disabil, 31*(2), 426-439. doi:10.1016/j.ridd.2009.10.013

Vanvuchelen, M., Roeyers, H., & De Weerdt, W. (2007). Nature of motor imitation problems in school-aged boys with autism: a motor or a cognitive problem? *Autism, 11*(3), 225-240.

Veeraragavan, S., Graham, D., Bui, N., Yuva-Paylor, L. A., Wess, J., & Paylor, R. (2012). Genetic reduction of muscarinic M4 receptor modulates analgesic response and acoustic startle response in a mouse model of fragile X syndrome (FXS). *Behav Brain Res, 228*(1), 1-8. doi:10.1016/j.bbr.2011.11.018

Ventura, R., Pascucci, T., Catania, M. V., Musumeci, S. A., & Puglisi-Allegra, S. (2004). Object recognition impairment in Fmr1 knockout mice is reversed by amphetamine: involvement of dopamine in the medial prefrontal cortex. *Behav Pharmacol, 15*(5-6), 433-442.

Verkerk, A. J., Pieretti, M., Sutcliffe, J. S., Fu, Y. H., Kuhl, D. P., Pizzuti, A., . . . et al. (1991). Identification of a gene (FMR-1) containing a CGG repeat coincident with a breakpoint cluster region exhibiting length variation in fragile X syndrome. *Cell, 65*(5), 905-914.

Villa, K. L., Berry, K. P., Subramanian, J., Cha, J. W., Oh, W. C., Kwon, H. B., . . . Nedivi, E. (2016). Inhibitory Synapses Are Repeatedly Assembled and Removed at Persistent Sites In Vivo. *Neuron, 89*(4), 756-769. doi:10.1016/j.neuron.2016.01.010

Villablanca, J. R. (2010). Why do we have a caudate nucleus? *Acta Neurobiol Exp (Wars), 70*(1), 95-105.

Vinueza Veloz, M. F., Buijsen, R. A., Willemsen, R., Cupido, A., Bosman, L. W., Koekkoek, S. K., . . . De Zeeuw, C. I. (2012). The effect of an mGluR5 inhibitor on procedural memory and avoidance discrimination impairments in Fmr1 KO mice. *Genes Brain Behav, 11*(3), 325-331. doi:10.1111/j.1601-183X.2011.00763.x

Vlachos, A., Korkotian, E., Schonfeld, E., Copanaki, E., Deller, T., & Segal, M. (2009). Synaptopodin regulates plasticity of dendritic spines in hippocampal neurons. *J Neurosci, 29*(4), 1017-1033. doi:10.1523/JNEUROSCI.5528-08.2009

Walikonis, R. S., Jensen, O. N., Mann, M., Provance, D. W., Jr., Mercer, J. A., & Kennedy, M. B. (2000). Identification of proteins in the postsynaptic density fraction by mass spectrometry. *J Neurosci, 20*(11), 4069-4080.

Wang, H., Wu, L. J., Kim, S. S., Lee, F. J., Gong, B., Toyoda, H., . . . Zhuo, M. (2008). FMRP acts as a key messenger for dopamine modulation in the forebrain. *Neuron, 59*(4), 634-647. doi:10.1016/j.neuron.2008.06.027

Warren, S. T., & Nelson, D. L. (1994). Advances in molecular analysis of fragile X syndrome. *JAMA, 271*(7), 536-542.

Waung, M. W., & Huber, K. M. (2009). Protein translation in synaptic plasticity: mGluR-LTD, Fragile X. *Curr Opin Neurobiol, 19*(3), 319-326. doi:10.1016/j.conb.2009.03.011

Waung, M. W., Pfeiffer, B. E., Nosyreva, E. D., Ronesi, J. A., & Huber, K. M. (2008). Rapid translation of Arc/Arg3.1 selectively mediates mGluR-dependent LTD through persistent increases in AMPAR endocytosis rate. *Neuron, 59*(1), 84-97. doi:10.1016/j.neuron.2008.05.014

Wenthold, R. J., Petralia, R. S., Blahos, J., II, & Niedzielski, A. S. (1996). Evidence for multiple AMPA receptor complexes in hippocampal CA1/CA2 neurons. *J Neurosci, 16*(6), 1982-1989.

Westmark, C. J., & Malter, J. S. (2007). FMRP mediates mGluR5-dependent translation of amyloid precursor protein. *PLoS Biol, 5*(3), e52. doi:10.1371/journal.pbio.0050052

Wilbrecht, L., Holtmaat, A., Wright, N., Fox, K., & Svoboda, K. (2010). Structural plasticity underlies experience-dependent functional plasticity of cortical circuits. *J Neurosci, 30*(14), 4927-4932. doi:10.1523/JNEUROSCI.6403-09.2010

Wisniewski, K. E., French, J. H., Fernando, S., Brown, W. T., Jenkins, E. C., Friedman, E., . . . Miezejeski, C. M. (1985). Fragile X syndrome: associated neurological abnormalities and developmental disabilities. *Ann Neurol, 18*(6), 665-669.

Wu, G. Y., Deisseroth, K., & Tsien, R. W. (2001). Spaced stimuli stabilize MAPK pathway activation and its effects on dendritic morphology. *Nat Neurosci, 4*(2), 151-158. doi:10.1038/83976

Xu, T., Yu, X., Perlik, A. J., Tobin, W. F., Zweig, J. A., Tennant, K., . . . Zuo, Y. (2009a). Rapid formation and selective stabilization of synapses for enduring motor memories. *Nature, 462*(7275), 915-919. doi:10.1038/nature08389

Xu, T., Yu, X., Perlik, A. J., Tobin, W. F., Zweig, J. A., Tennant, K., . . . Zuo, Y. (2009b). Rapid formation and selective stabilization of synapses for enduring motor memories. *Nature, 462*(7275), 915-919.

Yadav, A., Gao, Y. Z., Rodriguez, A., Dickstein, D. L., Wearne, S. L., Luebke, J. I., . . . Weaver, C. M. (2012). Morphologic evidence for spatially clustered spines in apical dendrites of monkey neocortical pyramidal cells. *J Comp Neurol, 520*(13), 2888-2902. doi:10.1002/cne.23070

Yan, Q. J., Asafo-Adjei, P. K., Arnold, H. M., Brown, R. E., & Bauchwitz, R. P. (2004). A phenotypic and molecular characterization of the fmr1-tm1Cgr

fragile X mouse. *Genes Brain Behav, 3*(6), 337-359. doi:10.1111/j.1601-183X.2004.00087.x

Yan, Q. J., Rammal, M., Tranfaglia, M., & Bauchwitz, R. P. (2005). Suppression of two major Fragile X Syndrome mouse model phenotypes by the mGluR5 antagonist MPEP. *Neuropharmacology, 49*(7), 1053-1066. doi:10.1016/j.neuropharm.2005.06.004

Yang, G., Pan, F., & Gan, W. B. (2009). Stably maintained dendritic spines are associated with lifelong memories. *Nature, 462*(7275), 920-924. doi:10.1038/nature08577

Yang, S., Yang, S., Park, J. S., Kirkwood, A., & Bao, S. (2014). Failed stabilization for long-term potentiation in the auditory cortex of FMR1 knockout mice. *PLoS One, 9*(8), e104691. doi:10.1371/journal.pone.0104691

Yang, Y., Wang, X. B., Frerking, M., & Zhou, Q. (2008). Spine expansion and stabilization associated with long-term potentiation. *J Neurosci, 28*(22), 5740-5751.

Yuskaitis, C. J., Mines, M. A., King, M. K., Sweatt, J. D., Miller, C. A., & Jope, R. S. (2010). Lithium ameliorates altered glycogen synthase kinase-3 and behavior in a mouse model of fragile X syndrome. *Biochem Pharmacol, 79*(4), 632-646. doi:10.1016/j.bcp.2009.09.023

Yuste, R. (2011). Dendritic spines and distributed circuits. *Neuron, 71*(5), 772-781. doi:10.1016/j.neuron.2011.07.024

Yuste, R. (2013). Electrical compartmentalization in dendritic spines. *Annu Rev Neurosci, 36*, 429-449. doi:10.1146/annurev-neuro-062111-150455

Yuste, R., & Bonhoeffer, T. (2001). Morphological changes in dendritic spines associated with long-term synaptic plasticity. *Annu Rev Neurosci, 24*, 1071-1089.

Yuste, R., & Denk, W. (1995). Dendritic spines as basic functional units of neuronal integration. *Nature, 375*, 682-684.

Yuste, R., & Urban, R. (2004). Dendritic spines and linear networks. *J Physiol Paris, 98*(4-6), 479-486. doi:10.1016/j.jphysparis.2005.09.014

Zeidan, A., & Ziv, N. E. (2012). Neuroligin-1 loss is associated with reduced tenacity of excitatory synapses. *PLoS One, 7*(7), e42314. doi:10.1371/journal.pone.0042314

Zhang, Y., Brown, M. R., Hyland, C., Chen, Y., Kronengold, J., Fleming, M. R., . . . Kaczmarek, L. K. (2012). Regulation of neuronal excitability by interaction of fragile X mental retardation protein with slack potassium channels. *J Neurosci, 32*(44), 15318-15327. doi:10.1523/JNEUROSCI.2162-12.2012

Zhang, Y., Cudmore, R. H., Lin, D. T., Linden, D. J., & Huganir, R. L. (2015). Visualization of NMDA receptor-dependent AMPA receptor synaptic plasticity in vivo. *Nat Neurosci, 18*(3), 402-407. doi:10.1038/nn.3936

Zhang, Y., Venkitaramani, D. V., Gladding, C. M., Zhang, Y., Kurup, P., Molnar, E., . . . Lombroso, P. J. (2008). The tyrosine phosphatase STEP mediates AMPA receptor endocytosis after metabotropic glutamate receptor stimulation. *J Neurosci, 28*(42), 10561-10566. doi:10.1523/JNEUROSCI.2666-08.2008

Zhou, Q., Homma, K. J., & Poo, M. M. (2004). Shrinkage of dendritic spines associated with long-term depression of hippocampal synapses. *Neuron, 44*(5), 749-757.

Zingerevich, C., Greiss-Hess, L., Lemons-Chitwood, K., Harris, S. W., Hessl, D., Cook, K., & Hagerman, R. J. (2009). Motor abilities of children diagnosed with fragile X syndrome with and without autism. *J Intellect Disabil Res, 53*(1), 11-18.

Zito, K., Scheuss, V., Knott, G., Hill, T., & Svoboda, K. (2009). Rapid functional maturation of nascent dendritic spines. *Neuron, 61*(2), 247-258. doi:10.1016/j.neuron.2008.10.054

Zou, K., Liu, J., Zhu, N., Lin, J., Liang, Q., Brown, W. T., . . . Zhong, N. (2008). Identification of FMRP-associated mRNAs using yeast three-hybrid system. *Am J Med Genet B Neuropsychiatr Genet, 147B*(6), 769-777. doi:10.1002/ajmg.b.30678

Zuo, Y., Lin, A., Chang, P., & Gan, W. B. (2005). Development of long-term dendritic spine stability in diverse regions of cerebral cortex. *Neuron, 46*(2), 181-189. doi:10.1016/j.neuron.2005.04.001